DEPARTMENT OF MECHANICAL ENGINEERING
COLLEGE OF ENGINEERING AND TECHNOLOGY
OLD DOMINION UNIVERSITY
NORFOLK, VIRGINIA 23529

NUMBERICAL INVESTIGATION OF DUAL-MODE SCRAMJET COMBUSTOR WITH LARGE UPSTREAM INTERACTION

By
T. O. Mohieldin, Co-Principal Investigator
and
S. N. Tiwari, Principal Investigator

Final Report
For the period ending June 30, 2004

Prepared for
National Aeronautics and Space Administration
Langley Research Center
Hampton, VA 23681-2199

Under
NASA Grant NAG-1-2266
David E. Reubush, Technical Officer
OCB/SAEPO-Hyper-X Program Office
ODURF #194141

Submitted by
Old Dominion University Research Foundation
Norfolk, VA 23509

December 2004

FOREWARD

This is a final report on the research work completed on the project "Numerical Simulation of Mixing and Combustion in Scramjet Engines." This work was done under the subcategory "Numerical Investigation of Dual-Mode Scramjet Combustor with Large Upstream Interaction."

This work was supported by NASA Langley Research Center through the Grant NAG-1-2266. The grant was monitored by Mr. David E. Reubush, OCB/SAEPO-Hyper-X Program Office, Mail Stop 353X, NASA Langley Research Center, Hampton, Virginia 23681-2199.

NUMERICAL INVESTIGATION OF DUAL-MODE SCRAMJET COMBUSTOR WITH LARGE UPSTREAM INTERACTION

SUMMARY

Dual-mode scramjet combustor configuration with significant upstream interaction is investigated numerically. The possibility of scaling the domain to accelerate the convergence and reduce the computational time is explored. The supersonic combustor configuration was selected to provide an understanding of key features of upstream interaction and to identify physical and numerical issues relating to modeling of dual-mode configurations. The numerical analysis was performed with vitiated air at freestream Mach number of 2.5 using hydrogen as the sonic injectant. Results are presented for two-dimensional models and a three-dimensional jet-to-jet symmetric geometry. Comparisons are made with experimental results. Two-dimensional and three-dimensional results show substantial oblique shock train reaching upstream of the fuel injectors. Flow characteristics slow numerical convergence, while the upstream interaction slowly increases with further iterations. As the flow field develops, the symmetric assumption breaks down. A large separation zone develops and extends further upstream of the step. This asymmetric flow structure is not seen in the experimental data. Results obtained using a sub-scale domain (both two-dimensional and three-dimensional) qualitatively recover the flow physics obtained from full-scale simulations. All results show that numerical modeling using a scaled geometry provides good agreement with full-scale numerical results and experimental results for this configuration. This study supports the argument that numerical scaling is useful in simulating dual-mode scramjet combustor flowfields and could provide an excellent convergence acceleration technique for dual-mode simulations.

TABLE OF CONTENTS

LIST OF TABLES

LIST OF FIGURES

1. INTRODUCTION

Essential to the design of the dual-mode scramjet engine is a detailed understanding of the complex physics present in different regions of the flowfield for various operating conditions. While much research have been conducted for both ramjet and scramjet (supersonic combustion ramjet) engines, few studies have been directed towards the design of the mid-speed range of the dual-mode scramjet combustion chamber.

A dual mode ramjet can combine both subsonic and supersonic combustion operations to cover a wide flight domain, from potentially M=2 to M>15. For high-speed flow (flight Mach number over 8), the combustion chamber flowfield is dominated by supersonic combustion. The pressure increase due to combustion is confined to the combustion chamber, thus influencing only the downstream flow. As the flight Mach number is decreased, efficient power production becomes complex. At these relatively low Mach numbers, subsonic combustion occurs. To achieve this, the supersonic flow is allowed to shock down to subsonic speeds. With flow expansion and additional heat from combustion the flow accelerates to supersonic speeds; the needed energy is attained. This transitional regime, between scram and ram-mode operation, is termed dual-mode. It is typically between flight Mach numbers 5-8.

The complex physics of dual mode combustion poses interesting problems for research and design. In a supersonic combustor the residence time of the gases becomes on the order of a millisecond. Reduced mixing due to compressibility effects at high

Mach numbers have further complicated progress towards an effective fuel injection design.[1,2] Thus, mixing augmentation techniques are an essential requirement for the development of this engine. The pressure rise due to combustion heat generation separates the boundary layer and creates large recirculation regions upstream of the injection. These regions may extend into the isolator, which is designed to assure the pressure disturbance does not reach the inlet. Here, the core flow may become subsonic, remain supersonic, or result in inlet unstart. The extent of this upstream interaction may be affected by several factors: ratio of inflow-enthalpy to combustion heat generation, inflow distortion, non-adiabatic conditions, step-changes in flow, aspect ratio, or downstream expansion ratio. The length of the isolator is of great importance. While a long isolator is necessary to maintain a stable flowfield, a short isolator is advantageous for weight constraints.

Most dual-mode combustors are complicated. One design, for example, consists of transverse sonic fuel injection, rearward facing steps, dual-mode combustion, a long isolator, and the presence of large subsonic and supersonic pockets. This isolator region is characterized by large separated regions along the walls and a slowing supersonic core flow. Generally the average Mach number becomes subsonic (M~0.8-0.9), but the core flow just reaches sonic conditions. Experimental measurements within such a flow are difficult due to disturbance propagations in the low Mach flow and high static temperature regions. Unfortunately this complex flowfield is also very difficult to simulate numerically. More studies about the dual mode combustion must be conducted to understand the complicated physics of such flows.

Constraints on system size and weight have created a need to improve technology for designing and analyzing complex systems. Faster processors and efficient numerical techniques are essential. However, often it is the physical dimensions of the problem that, in requiring a fine mesh, consume a great deal of computational time. In such cases, it is the responsibility of CFD modelers to understand how physical problems can be scaled to utilize computational space more efficiently. It is well known that for many systems it is possible to scale physical dimensions and governing equations to give non-dimensional results. As a minimum, the results from scaled geometry could be used to

accelerate the convergence of full-scale geometry simulations. The complexities of the turbulence, mixing, and chemical reaction make scaling of this problem an interesting task.

The motivation of this study is twofold. First, essential to the design of the supersonic combustion ramjet (scramjet) engine is a detailed understanding of the complex flowfield in different regions of the combustion system. Second, in a fiercely competitive market, it is necessary to research means of simplifying computer simulations to utilize space more efficiently. Geometrical scaling can be used in some cases to cut costs of computational analysis.

The defining characteristic of dual mode combustion flowfield is the upstream interaction. Many studies have been conducted in response to the increased interest in the development of dual mode combustion systems.[2-16] Some of these recent studies have been concentrated around an experiment performed in Japan.[6-9] Matsuo et al.[10] and Mizobuchi et al.[11] conducted numerical-experimental studies to investigate turbulence temperature fluctuations in a scramjet combustion chamber. They concluded that the treatment of turbulence modeling was the key to an accurate computational scheme. Riggins[12] explained some of the shortcomings in current modeling capability. He concluded that the extent of upstream interaction and the details of the pressure distribution in the combustion chamber could not be accurately represented at this time. Rodriguez et al.[13-16] also investigated this three-dimensional dual mode system. Numerical modeling with and without anti-symmetry assumptions was compared. The anti-symmetric assumption results showed good comparison with experimental data. However, after removing the anti-symmetry constraint, the experimental results were not accurately reproduced. Rodriguez concluded that the expected anti-symmetry was missing and the numerical results were unstable.

Dutton and Carroll[17] found asymmetric phenomena in their numerical and experimental study of supersonic duct flow. They concluded that shock train interaction with boundary layer may have caused a highly non-uniform and possibly unsteady flow at

the duct exit. In two recent publications, Rodriguez et al.[15] and Rodriguez[16] discussed the interaction of the separated flow regions interacting with shock-train as a possible source of the asymmetric perturbation. Mohieldin et al.[18] presented some of the results of this present study, and discussed the apparent breakdown of the symmetry condition.

There have been occurrences of asymmetric and possibly transient behavior in flowfield of supersonic air over a backward facing step. However, very few studies have addressed this issue.

In a two-dimensional numerical simulation, Uenishi et al.[19] modeled laminar Mach 3.5 flow over a small backward-facing step. This simulation did not reach a steady state and it appeared to be periodic. They also noticed that the degree of unsteadiness of the flow was directly related to the thickness of the boundary layer approaching the step.

In a recent paper, Matsuo and Mizomoto[20] performed two-dimensional numerical simulations of Mach 2.5 flow over a backward-facing step with normal sonic jet penetration downstream of the step. For a 6mm step, they found unsteady oscillations in the flowfield downstream of the step for a dynamic pressure ratio range from 0.2-0.6; outside that ratio range the flow was steady. They observed that the mechanism of oscillation and its frequency were dependent on the static jet-to-back pressure ratio.

There has been an abundance of research, both experimental and numerical, into separated flow in a symmetric geometry where asymmetric/unsteady flow is observed. A popular geometry is the axisymmetric sudden expansion duct. This flow is essentially the same as flow over dual backward-facing steps. However, to qualify as a sudden expansion, the step height to domain height ratio has to be at least 1:2. Both two-dimensional and three-dimensional models of sudden expansion geometry have been investigated. Asymmetries in the flow have been observed as different reattachment lengths or uneven velocity distributions. Classic papers on this subject include Abbott and Kline[21], Durst et al.[22], Cherdron et al.[23], and Restivo and Whitelaw[24]. More recent papers include Cole and Glauser[25], Kudela[26], Aloui and Souhar[27], and Lee and Sung[28].

In an often-cited paper by Abbott and Kline[21], experimental results for turbulent flow in a symmetric sudden expansion duct are presented. They demonstrated that Prandtl's classical model of stall, which implies a steady two-dimensional flow, was only

an approximation to the real phenomenon of stall. They explained that even for simple two-dimensional geometries, there exist three-dimensional and time-dependent effects. From their experimental results, they were able to divide the turbulent separation region into three parts: (I) a three-dimensional zone directly downstream of the steps and characterized by two or more counter-rotating vortices rotating about axis parallel to though flow direction, (II) a two-dimensional region adjacent to zone (I) that is the classical recirculation region, and (III) a time dependent tail region downstream of zone (II) that is periodically changing in size. For ducts with expansion area ratios over two they found asymmetric results. As turbulent intensity was varied from 1% to 18%, there was no appreciable change in lengths of the zones. They also observed little change in flow model and reattachment length with changes in the inlet boundary layer. These findings led to their conclusion that turbulence is extremely important in that the self-generated mixing dominates any turbulence normally existing in the inlet flow. Although the test range, Re=20,000-50,000, was small, they concluded that these turbulent results could be extended to all turbulent flows, as long as the Re number is high enough to provide turbulent boundary layers at the inlet.

Recently, Cole and Glauser[25] performed an experiment at Re=41,000 to investigate possible causes of the unsteady flow. Careful attention was paid to not disturb the flowfield with measurement equipment. Flow asymmetry was obvious by the unsteady reattachment length. They concluded that coherent structures from the near field shear layer may propagate downstream into the reattachment region and cause asymmetries. Kudela[26] used a vortex method to numerically model two-dimensional channel flow. At Re=56 he found a symmetric result. At about Re=114, the symmetric solution was lost. Finally, for a Re=100,000 he recorded asymmetric behavior. While the focus of his paper was to investigate the vortex method, it showed another computational method that provides results in asymmetric behavior. A recent experiment of symmetric turbulent water flow with sudden expansion was provided by Aloui and Souhar[27]. For a Re of 32,000, this symmetric two-dimensional experiment showed an asymmetric result. Lee and Sung[28], also performed an experiment, using multi-point measurements, to investigate wall pressure fluctuations over a backward-facing step.

They concluded that shed vortices play an important role in the mechanism of the breakdown of symmetry and the pressure fluctuations.

Since unsteady behavior is commonly associated with turbulence (vortex shedding), it is completely unexpected to find asymmetries in flow where one would innocently assume symmetry, with Reynolds numbers as low as 155. However, this is exactly where the asymmetry begins. For this reason, there has been much research into laminar flow and asymmetric behavior.

Possibly the first experiment in laminar sudden expansion in plane flow was conducted by Durst et al[22]. At Re=56, they observed generally symmetric flow. At Re=114 and 252, they found asymmetric yet stable results.

A paper by Chedron et al.[23] provided detailed data from a laminar experiment of a symmetric two-dimensional sudden expansion geometry. This paper provided an excellent review of asymmetric and unstable behavior in symmetric problems and offered explanations for the asymmetric experimental results. The source of the asymmetry is a disturbance generated at the leading edge of the expansion step. The shear layers amplify this perturbation. This report concluded that the length of the recirculation regions is dependent on maximum velocity, step height, and initial mean velocity profile and not on the expansion ratio.

Restivo and Whitelaw[24] further investigated the flow regime from initially becoming asymmetric with vortex structures to turbulent flow at about Re=2000. Their findings lent further support to the ideas of Cherdron et al[23].

Sobey and Drazin[29] examined laminar flow in a sudden expansion duct. As the Reynolds number increased, a symmetric result changed to a possibly periodic solution; the flow attached preferentially to one wall. Once the velocity increased on that wall, the pressure decreased. This pressure difference maintained the asymmetry of the flow.

Recent experimental and numerical data are found in Fearn et al[30]. This paper showed that critical Re is dependent on expansion ratio, and, at critical Re, the solution bifurcates losing stability into a pair of stable asymmetric solutions. It also provides experimental evidence that the time-dependent solution at higher Re is associated with three-dimensional effects not Hopf bifurcation.

Most studies into combustion chambers or simple geometries with dual/opposite steps make the assumption of symmetry along the chamber centerline, modeling half the domain. This seems obvious, since the geometry is symmetric. However, it appears that this is not a safe assumption. While the critical Reynolds number (where transition from symmetric solution to asymmetric solution occurs) is still unknown, it is commonly accepted that flow with a large sudden expansion results in asymmetric flow. The differences between these past studies and the present study are acknowledged. The effects of compressibility, high temperatures, and supersonic flow on symmetric/asymmetric sudden expansion flow have not been studied.

Scaling is frequently used to achieve non-dimensional results. Unfortunately, only a few studies have been conducted on the scaling of mixing and reacting flows. Diskin and Northam[31] conducted an experimental study on the effects of scale on dual mode combustor performance. They concluded that the calculated combustion efficiency appears to be independent of scale for the same geometry, yet more tests are required to verify this. For a combustion chamber with constant area region downstream of the jet, their results show amazing similarity between the small and large scale cases. The efficiencies of mixing and combustion are independent of the scale. Also, prediction of pressure seems unchanged with scaling. Some results from the present study were presented by Mohieldin et al[32]. This paper concluded that scaling could be a useful convergence technique.

The objective of this study is to numerically investigate a dual-mode scramjet combustor configuration with significant upstream interaction. First, an investigation is made into geometrical scaling. The complex flowfield of the dual-mode engine is dominated by heat release from combustion and the resulting pressure increase. When modeling such a situation it is possible to obtain a fairly accurate solution using a scaled model. Both two-dimensional and three-dimensional models of the scramjet engine are studied. Results from ¼ scale, ½ scale, and full scale are compared to assess the effect of scaling.

While investigating the possibility of scaling a dual-mode engine, asymmetric behavior was encountered where symmetric behavior was expected. As a result more

studies are conducted to provide an understanding of key features of dual-mode combustion. Progression of the flow solution, particularly upstream interaction is studied using two-dimensional and three-dimensional models. Numerical results are compared with experimental data.

2. THEORETICAL FORMULATIONS

2.1 Physical Domain and Conditions

Experiments were performed on a laboratory model for the scramjet, in a blow-down type wind tunnel. The tests were conducted at the National Aerospace Laboratory (NAL) in Japan[6-9].

The rectangular combustor was directly connected to the facility nozzle. Between the nozzle and the combustor, a constant cross-sectional area isolator was inserted (Fig. 2.1). It was insulated to mitigate combustor-facility interaction and to prevent the combustion induced pressure wave from propagating upstream into the nozzle. The isolator height was 32 mm and extends 200 mm downstream. There were 3.2 mm backward-facing steps on the upper and lower sidewalls of the chamber. A constant cross-sectional area was attached downstream of the step for 96 mm. Then the sidewalls diverged at 1.7 degree angle. The width remained constant throughout the chamber at 147.3 mm. A hydrogen vitiation air heater was used for simulating high temperature air entering the supersonic combustor. The freestream vitiated air Mach number of 2.5 represents a flight Mach of 7.5. It had O_2, N_2, and H_2O mole fractions of 20%, 55%, and 25% respectively. The total temperature was 2000 K and total pressure was 10 atm.

Fuel jets were located 12.8 mm downstream of the steps on the upper and lower sidewalls. On the lower wall, there were five fuel injection holes and four on the upper wall. These fuel injection jets were equally spaced with 32 mm between the injectors. The injectors on the upper wall and the three center jets on the lower wall were of 4.0 mm diameter. The remaining 2 lower jets, closest to the walls, were of 2.8 mm diameter. Gaseous hydrogen was injected perpendicularly through these circular orifices at sonic condition with a total temperature of 280 K.

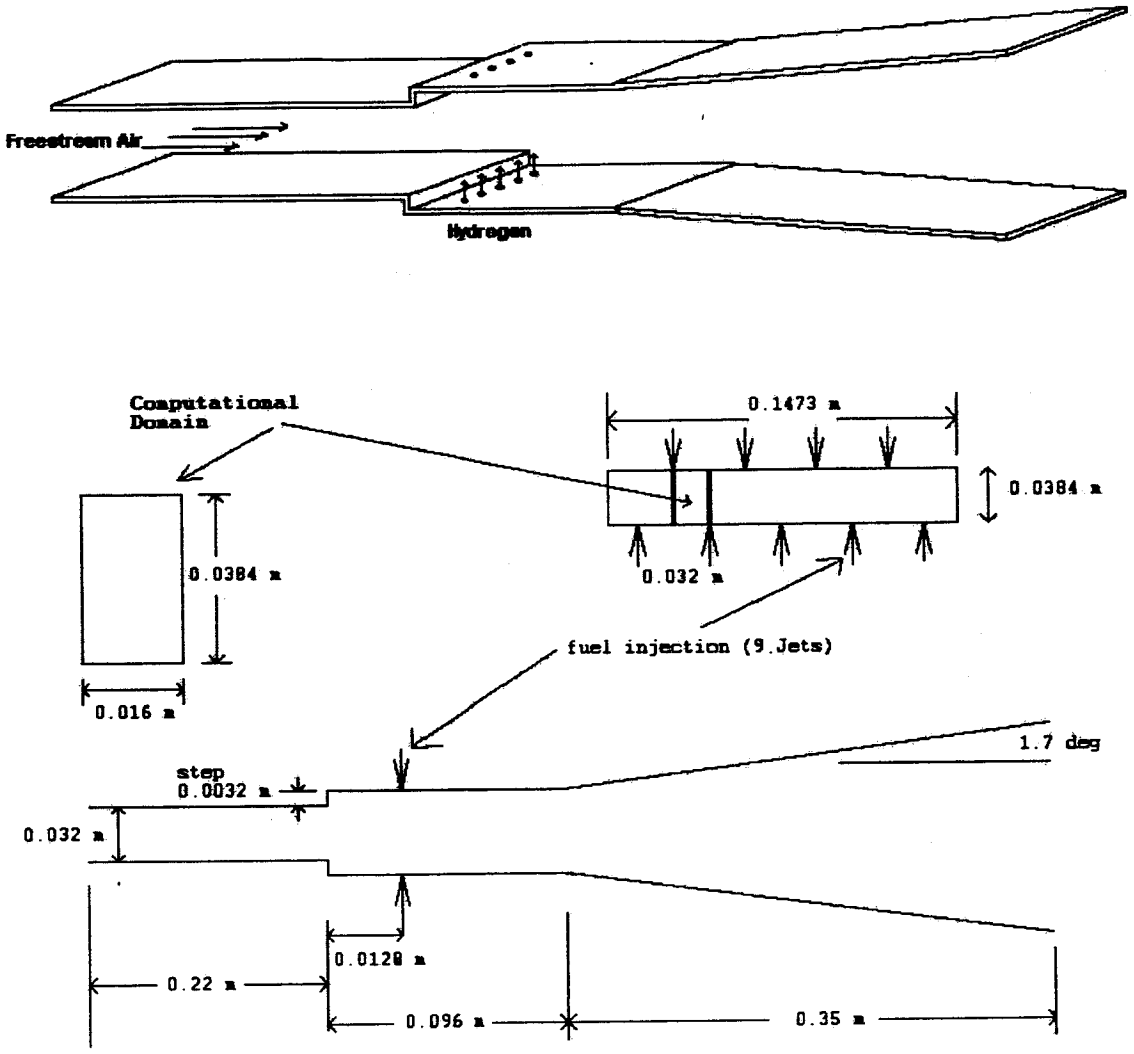

Figure 2.1 Schematic of experimental combustor.

2.2 Numerical Model

Before modeling the entire experimental domain, it was necessary to simplify the model to investigate certain aspects of the code. To simplify the three-dimensional case, jet-to-jet symmetry was assumed. As shown in Fig. 2.1, the computational domain was simplified to encompass half of the upper and half of the lower jet (using the symmetry condition for these planes). To conserve computational time the possibility of scaling the problem was also investigated. An analysis of a ¼ scale jet-to-jet three-dimensional model of the combustion chamber was performed.

A hydrogen jet was injected transversely into supersonic flow in a scramjet engine. The free-stream inlet height was 32 mm and the inlet channel was 220 mm long. There were 3.2 mm steps on the upper and lower walls of the chamber. The walls were then parallel over 96 mm. Finally, the chamber expanded at 1.7 degree angle. The jets were located 12.8 mm downstream of the steps on the upper and lower walls. For the three-dimensional jet-to-jet case, there were two half jet injection holes, one each on the upper wall and lower wall. The jets were of 4.0 mm diameter. The distance between the injection hole centers was 32 mm.

To reduce computational difficulties, the problem can be considered as two-dimensional. To simplify the geometry, one slot was placed on both the upper and lower walls. A slot width of 0.34 mm was calculated to maintain the mass flow rate ratio of free-stream air to hydrogen.

Table 2.1 provides the boundary conditions. The free-stream vitiated air Mach number was 2.5, with O_2, N_2, and H_2O mole fraction of 20%, 55%, and 25% respectively, with a total temperature of 2000 K and total pressure of 10 atm. However, to encourage upstream interaction in a two-dimensional case, the total pressure was cut to 5 atm. The hydrogen jets Mach number was 1.0 with a total temperature of 280 K and a total pressure of 6.64 atm.

Table 2.1 Boundary conditions

	Free-stream Viatiated Air	Jet Injection
M	2.5	1.0
Pt (atm)	10 *	6.64
Ps (atm)	0.55 *	3.51
Tt (K)	2000	280
Ts (K)	1055	233
Velocity (m/s)	1654	1160

* In the two-dimensional symmetry investigation the pressure is reduced by half.

2.3 Flow Characteristics

In this problem, the freestream Mach number is supersonic, but combustion cannot necessarily be considered high-speed scramjet combustion (flight Mach above 8). At the transition between ram-mode and scram-mode, flight Mach number between 5 and 8, the combustor flow is often "dual-mode." In a dual-mode system the flow field is not entirely subsonic or supersonic. It is characterized by regions of both subsonic and supersonic flow behaviors, which create a complex transitional fluid dynamics problem. In this section dual-mode scramjet flow characteristics are discussed.

2.4 Geometry

Essential to the design of a dual-mode scramjet engine is the geometry. Common features are backward facing steps and an isolator region upstream of the combustion chamber. The step serves several purposes. It separates the isolator boundary layer from the large pressure rise of combustion. It creates a recirculation region, downstream of the step, which increases fuel–air mixing and sustains combustion. This recirculation region is subsonic and helps to ignite and sustain combustion.[33] The isolator used in this study is a constant area section added as a buffer between the inlet and the combustor to diffuse the supersonic flow to subsonic condition and to prevent unstart. This region is particularly important for dual mode flow because of the occurrence of significant upstream interaction, which may extend a long distance upstream, possibly resulting in engine unstart. However, weight/cost issues prevent the introduction of a long isolator region. Understanding the length requirement of the isolator is of extreme importance in scramjet design.

2.5 Flow Dynamics

Characteristic features of the flow field can be seen in Fig. 2.2. The flow enters the combustion chamber over upper and lower backward-facing steps. As it passes over the steps the flow expands though a Prandtl-Meyer fan. Just downstream of the step a

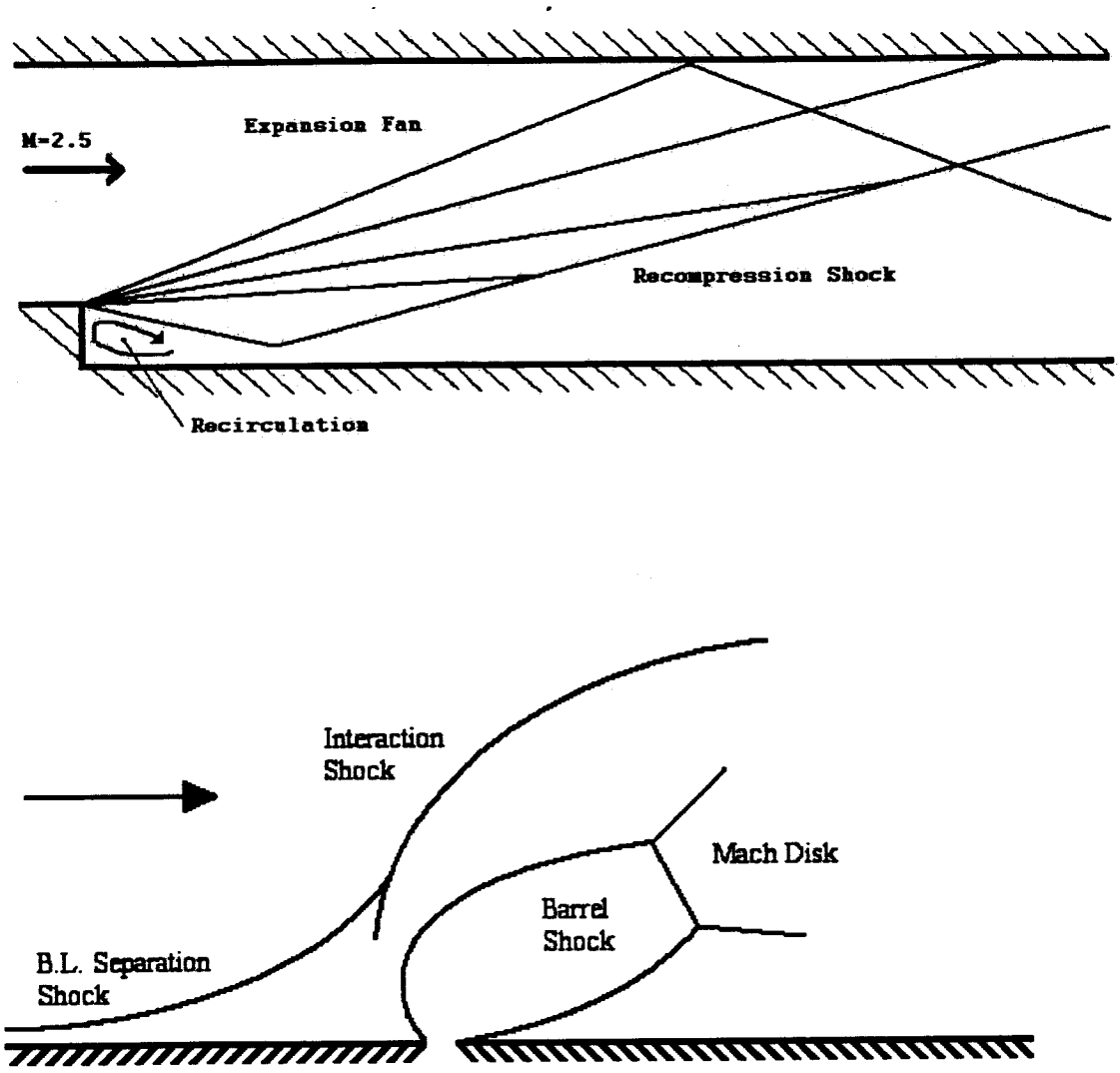

Figure 2.2 Flowfield characteristics.

subsonic recirculation region is created.[33] The flow continues though the reflected shock. Then it encounters the hydrogen jet. Under-expanded sonic hydrogen is discharged normal to the flow, creating a barrel shock structure, which includes a classical Mach disk. These features are seen by the supersonic crossflow as an obstruction to the flow, which results in the creation of a bow shock upstream of the jet. The bow shock turns the flow, deflecting the barrel shock and Mach disk over and keeping the injectant parallel to the wall.[34]

A shear layer forms between the injectant and crossflow air, due to differences in their velocities. Interaction of the bow shock with the boundary layer forces the flow to separate from the wall, creating a recirculation region upstream of the jet injection. Downstream of the jet, a boundary layer reattachment shock occurs.[35] The flow passes through the constant area combustion chamber and then accelerates in the downstream expansion region.

Injectant cross-section appears kidney-shaped caused by pressure and viscous forces acting on the fuel injection. The crossflow creates a pair of vortices much the same way as any obstruction placed in crossflow. Further downstream the presence of a vortex pair dominates the flow, although the original jet injection has dissipated.[36]

2.6 Dual-Mode Combustion

As previously discussed dual-mode is the transitional regime between a pure subsonic flow field, ramjet operation, and a completely supersonic field, scramjet operation. In a supersonic combustor, the upstream region is not affected by combustion. However, dual-mode combustion is characterized by extensive interaction with the flow upstream of the combustion chamber.

Due to the enormous heat release of combustion, the combustion chamber pressure rises. The ratio of this heat generation to incoming enthalpy is very large. This results in choked flow downstream (nozzle-throat). Hence, the upstream region may be affected by the downstream flow. An increased chamber pressure forces the upstream

shock further upstream, producing a normal shock downstream of the inlet and upstream of the combustor. Large recirculation bubbles are formed on the isolator walls. Also a series of oblique shocks form in the isolator between the recirculation bubbles.

The flow field in the isolator region is highly complex and variable. The core flow may be entirely supersonic. Incoming boundary layer can inherently have a large effect on such a complex flowfield. The recirculation bubbles are very significant and the three-dimensional characteristics of the wall and corners can also have a large effect on the flowfield.[13,15]

2.7 Governing Equations

The governing equations for this problem are continuity, momentum transport, energy, and species continuity equations. These equations are given below:

$$\frac{\partial}{\partial t}\rho = -\left(\nabla \cdot \rho \mathbf{v}\right) \tag{2.1a}$$

$$\frac{\partial}{\partial t}\rho \mathbf{v} = -\left(\nabla \cdot \left\{\rho \mathbf{v}\mathbf{v} + \pi\right\}\right) + \sum_{i=1}^{n}\rho_i \mathbf{g}_i \tag{2.1b}$$

$$\frac{\partial}{\partial t}\rho\left\{\hat{U} + \frac{1}{2}v^2\right\} = -\left(\nabla \cdot \left\{\rho\left(\hat{U} + \frac{1}{2}v^2\right)\mathbf{v} + \mathbf{q} + \left[\pi \cdot \mathbf{v}\right]\right\}\right) + \sum_{i=1}^{n}\left(\mathbf{n}_i \cdot \mathbf{g}_i\right) \tag{2.1c}$$

$$\frac{\partial}{\partial t}\rho_i = -\left(\nabla \cdot \left\{\rho_i \mathbf{v} + \mathbf{j}_i\right\}\right) + r_i \qquad i = 1, 2, \cdots, n \tag{2.1d}$$

In Eq. (2.1a)-(2.1d), ρ is density, t is time, $\mathbf{v}$ is the mass average velocity vector, $\pi = \tau + p\delta$, in which τ is the shear stress tensor, p is the pressure, δ is the unit tensor, $\mathbf{g}_i$ is the external force per unit mass, $\hat{U}$ is the internal energy per unit mass, v is the magnitude of the velocity, $\mathbf{q}$ is the multi-component energy flux, $\mathbf{n}$ is the mass flux

relative to stationary coordinates, **j** is the mass flux relative to the mass-average velocity, and r_i is the rate of production of species i. The set of equations is solved by using an appropriate numerical procedure.

2.8 Grid Generation

The program Gambit was used to generate the grids used in this study. GAMBIT (Ref. 37) is a software package designed to build and mesh models for computational fluid dynamics and other scientific applications. GAMBIT is capable of creating unstructured and structured grids. The user may specify that the mesh is composed primarily of tetrahedral mesh elements but it may also include hexahedral, pyramidal, and wedge elements where appropriate. For a regular structured grid, the user may specify that the mesh includes only hexahedral mesh elements.

In this study both two-dimensional and three-dimensional grids were created. The two-dimensional cases utilized unstructured grids with triangular cells. For three-dimensional cases unstructured grids with hexahedral were used.

2.9 Computer Code

For the present study, the compressible, unstructured code, FLUENT 5.2, was used to investigate the flow characteristics of the scramjet combustion chamber. The motivation for using FLUENT 5 code is its ability to handle high speed as well as low speed flows. The code solves steady and unsteady 3-D Reynolds-Averaged Navier-Stokes equations. It contains a large database of chemical properties for many species and reactions. It is also capable of using structured and unstructured grids. In the following sections, theoretical formulations of Fluent are described. Further details of the numerical methods used in FLUENT 5.2 can be found in Ref. 38.

The coupled solver in FLUENT solves the governing equations of continuity, momentum, energy, and species transport simultaneously (i.e., coupled together) as a set, or vector, of equations. Governing equations for additional scalars are solved sequentially (i.e., segregated from one another and from the coupled set). Because the

governing equations are non-linear (and coupled), several iterations of the solution loop must be performed before a converged solution is obtained. Each iteration consists of the steps outlined below:

1. Fluid properties are updated, based on the current solution.
2. The continuity, momentum, energy, and species equations are solved simultaneously, using either explicit or implicit scheme.
3. Turbulence equations are solved using the previously updated values of the other variables.
4. A check for convergence of the equation set is made.

These steps are continued until the convergence criteria are met.

2.10 Discretization Scheme

FLUENT uses a control-volume method to convert the governing equations to algebraic equations. The discrete values are stored at the cell centers. However, face values are required for the convection terms and must be interpolated from the cell center values. This is accomplished using an upwind scheme. FLUENT allows a choice of several upwind schemes: first-order upwind, second-order upwind, power law, or QUICK. Second-order accuracy is automatically used for the viscous terms.

2.11 Explicit v. Implicit Scheme

Implicit - For a given variable, the unknown value in each cell is computed using a relation that includes both existing and unknown values from neighboring cells. Therefore each unknown appears in more than one equation in the system, and these equations must be solved simultaneously to give the unknown quantities.

Explicit - For a given variable, the unknown value in each cell is computed using a relation that includes only existing values. Therefore each unknown appears in only one equation in the system and the equations for the unknown value in each cell can be solved one at a time to give the unknown quantities.

2.12 Turbulence Model

FLUENT is capable of using many turbulence models. For this study the RNG-based k-ε turbulence model with standard wall functions was used. It is derived from the instantaneous Navier-Stokes equations, using a mathematical technique called "renormalization group" (RNG) methods. The analytical derivation results in a model with constants different from those in the standard k-ε model, and additional terms and functions in the transport equations for k and ε. The default value of Schmidt number is 0.7. A more comprehensive description of RNG theory and its application to turbulence can be found in Ref. 38.

2.13 Chemistry Modeling

An eddy-dissipation model was used to relate the rate of reaction to the rate of dissipation of the reactant-and product-containing eddies. In turbulent reacting flows, FLUENT calculates both the Arrhenius reaction rate and the eddy-dissipation-model reaction rates employing the Magnussen and Hjertager model. The limiting (slowest) rate is used as the reaction rate and the contributions to the source terms in the species conservation and energy equations are calculated from this reaction rate.

2.14 Solution Procedure

The Navier-Stokes equations were solved using a second-order finite-volume integration scheme, the coupled (Block Gauss-Seidel) solver FLUENT. Both implicit and explicit solvers were used. Courant number was varied from 0.05 to 1 for the explicit solver. For the implicit solver, CFL values ranged from 1 to 2. Turbulence was modeled using the RNG k-ε model with standard wall functions. Steady state was assumed. A simple one step chemical reaction, using the eddy-dissipation model, was also assumed.

2.15 Boundary Conditions

The test gas was vitiated air set at a Mach number of 2.5, with O_2, N_2, and H_2O mole fractions of 20%, 55%, and 25% respectively. The total temperature was 2000 K

and the total pressure was 10 atm. The sonic hydrogen jets had a total temperature of 280 K and a total pressure of 6.64 atm.

No-slip boundary conditions were used along the combustor wall. All walls were assumed adiabatic requiring the normal derivative of temperature to vanish. Along the supersonic inflow boundaries, uniform conditions were used for both the freestream and jets. At the supersonic outflow boundary, non-reflective boundary conditions were used where the boundary values were found by linear extrapolation from the interior points. Initial conditions were obtained by specifying freestream conditions throughout the flowfield.

2.16 Convergence Techniques

To investigate convergence techniques the physical domain of the combustion system was scaled. The same grid was used for each scaled simulation. However, in each case, the turbulent length scale was also scaled to represent the length of the scaled model. Full-scale results were compared to ½ and ¼ scale results. As a minimum, the results from scaled geometry may be used to accelerate the convergence of full-scale geometry simulations. The complexities of the turbulence, mixing and chemical reaction make scaling of this problem an interesting task.

3. COMPUTATIONAL CODE VALIDATION

In this section, the validity of the commercial computation fluid dynamics code (Fluent 5.2) is investigated for the present study. A two-dimensional slot combustion chamber is used as the validation case. The results are compared with the data from the literature to determine the validity of the code for systems with significant upstream interaction.

3.1 Introduction

Two-dimensional CFD analysis of transverse slot injection was performed to investigate the upstream interaction caused by the sonic injection into the supersonic flow. Nitrogen was transversely injected at sonic speed into Mach 3.5 free-stream airflow over a flat plate. The flow field resulting from the interaction of this transverse gaseous jet with a supersonic free-stream flow was determined experimentally by Spaid and Zukoski[39]. Recent research into this geometry was conducted by Hosangadi et al.[40] and Rodriquez[41]. A simplified analytic model of the flow field was also constructed. The CFD results are compared with these experimental results and previous computational studies to validate the use of FLUENT for numerical studies, which are dual mode and have significant upstream interaction.

3.2 Experimental Arrangement

At the Jet Propulsion Laboratory, California Institute of Technology, a series of tests were completed in the 20-inch supersonic wind tunnel. Free-stream air flow over a flat plate with Mach numbers of 2.61, 3.50, and 4.54 was investigated. An underexpanded sonic jet of N_2 or He was injected transversely through a slot in the plate at various reservoir pressures. To maintain a two-dimensional result, end plates were mounted at either end of the slot for most of the experiments. Test-section flow

parameters, jet-reservoir flow parameters, and wall pressure distributions were measured. Details on the model configuration and experimental results are given in Ref. 39. The case investigated in this study (13 in Table 1, Ref. 39) was for transverse injection of sonic N_2 into Mach 3.5 air with a pressure ratio of 63.5 (p_{jet}/p_{fs}). Experimental results show that the flow became fully turbulent well before the slot injection.

3.3 Numerical Model

Figure 3.1 provides a schematic of the computational domain, which began at the leading edge of the flat plate ending 9 inches downstream of the slot injection. The slot of diameter 0.0105 inches was located 9 inches downstream from the leading edge. The height of the domain was 4.5 inches. The computational mesh is shown in Fig. 3.2. The structured grid was clustered in the regions of the jet and the wall.

The boundary conditions for this case are given in Table 3.1. These conditions were assumed to be uniform inflow conditions. No-slip boundary conditions were used for the flat plate, which was assumed to be adiabatic. At the supersonic outflow, non-reflective boundary conditions were used where the boundary values were found by linear extrapolation from the interior points. Initial conditions were obtained by applying free-stream inlet conditions throughout the flow field. Since the flow temperatures were below room temperature, no dissociation was assumed of the gases, which were also assumed to be calorically perfect. The flow was assumed to be turbulent; turbulent intensities of 1%, 5%, and 10% were investigated. The RNG k-epsilon turbulence model was used. Flow field results were obtained with Fluent 5.2 [Ref. 38].

3.4 Results of Validation

The two-dimensional flowfield of transverse sonic injection into supersonic flow was investigated and comparisons were made with the wall pressures. Computational results for a structured grid with different turbulence intensities were compared with experimental results.

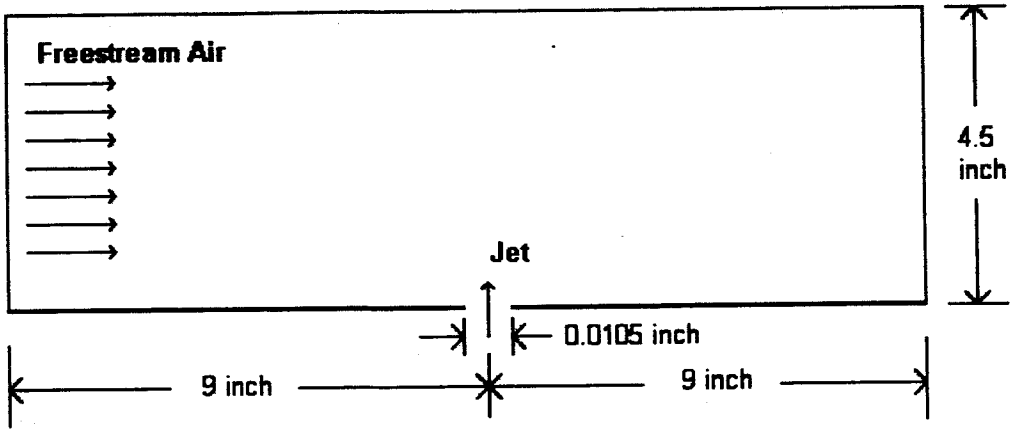

Figure 3.1 Computational domain of code validation case.

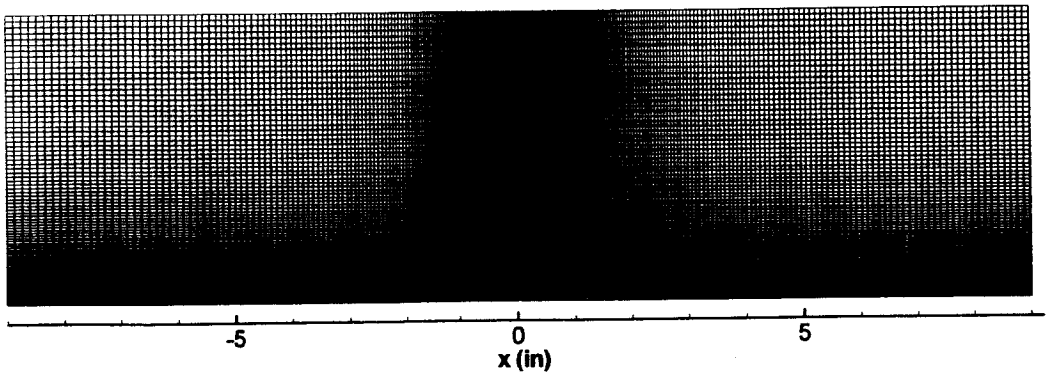

Figure 3.2 Two-dimensional slot injection mesh.

Table 3.1. Boundary conditions

	Free-stream Air	Jet Injection N_2
M	3.5	1.0
P_t (psi)	34.9	55.1
P_s (psi)	0.458	29.1
T_t (R)	566	525
T_s (R)	165	438
Velocity (ft/s)	2200	1043

Wall static pressure distribution is shown in Fig. 3.3. Static pressure is normalized by the free-stream flow static pressure. All results show fairly good agreement with experimental results of Ref. 39. However, results using turbulent intensity of 5% show the best agreement. In all cases, the magnitude of the pressure rise and the downstream effects are well predicted. It is in predicting the length of the upstream interaction that is highly dependent of the turbulent intensity. Some discrepancies are noted due to the fact that the boundary conditions are assumed to be uniform, with turbulent flow throughout the entire flow field and that calorically perfect gases are assumed.

Figure 3.4 shows the static pressure contours for each of the 3 cases: 1%, 5%, and 10% turbulent intensity. The slot jet expands into the flow field creating a barrel shock. This injection penetrates the flow field causing the free-stream flow to be blocked. Therefore, the flow must turn, which generates a shock in front of the jet injection. The existence of an upstream separation region causes the wall pressure to increase in the re-circulation region as shown. Figure 3.5 shows the velocity vector and streamline plots. The upstream re-circulation zone is readily apparent, as are the vortices in the region of the slot injection.

Figures 3.6 and 3.7 show the Mach number and N_2 mole fraction contours, respectively. Again the existence of the barrel shock and an upstream subsonic re-circulation zone is apparent. Also, it can be seen that the re-circulation region ahead of the jet convects nitrogen upstream, while most of the nitrogen remains close to the wall.

A numerical study of the two-dimensional transverse sonic injection into supersonic flow over a flat plate was conducted to provide understanding of the key features of upstream interaction, physical and numerical issues, and to validate use of the commercial code FLUENT for such numerical cases. Supersonic flow over a flat plate with normal jet injection was numerically modeled using a simplified two-dimensional slot injection model. This injection of under-expanded gas produced a large amount of upstream interaction. The results of the computational investigation were compared with

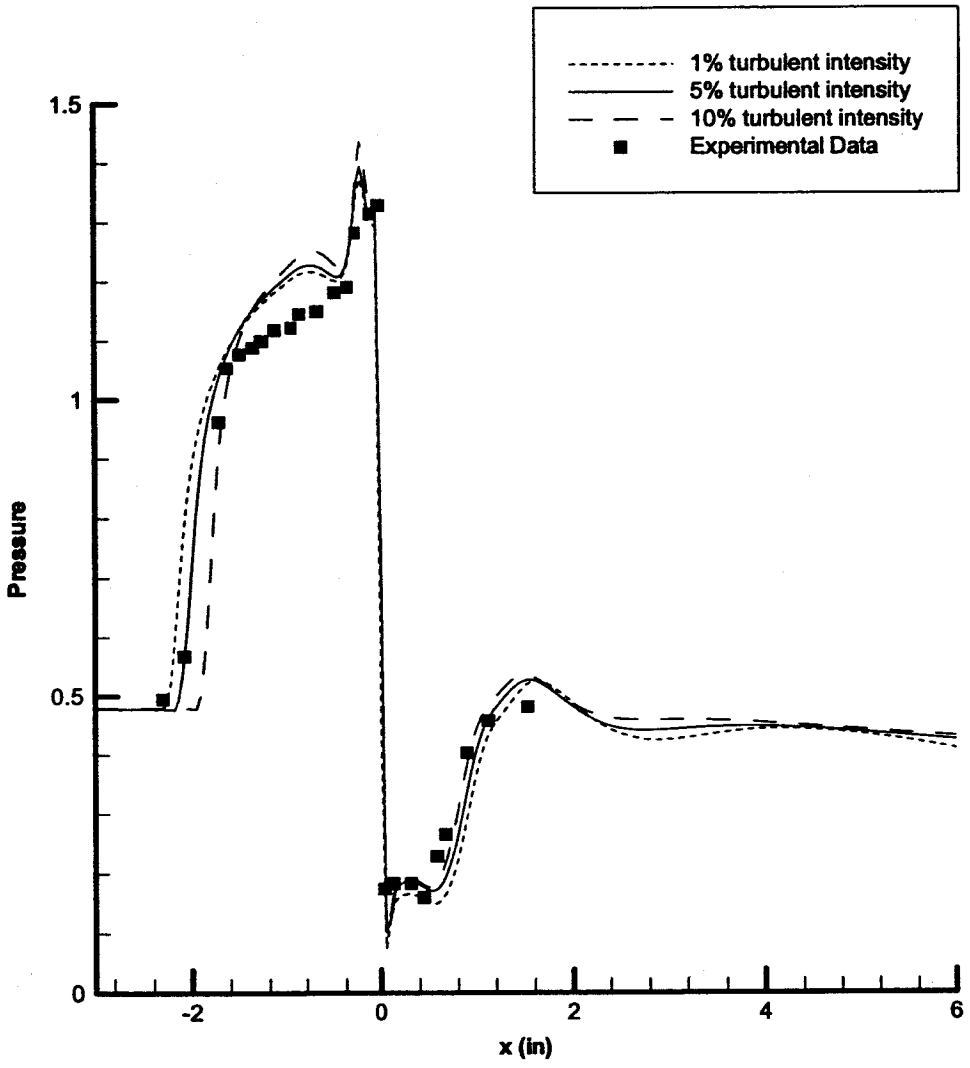

Figure 3.3 Wall static pressure distribution.

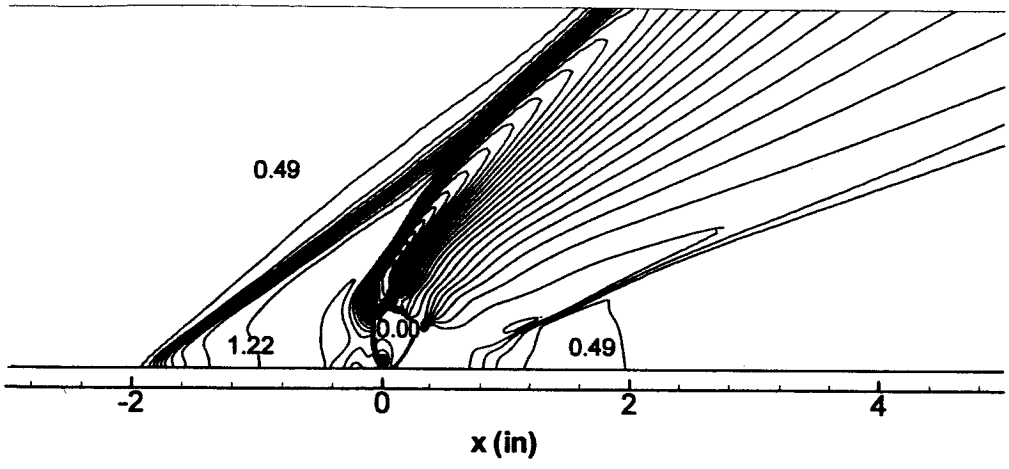

(a) 10% intensity

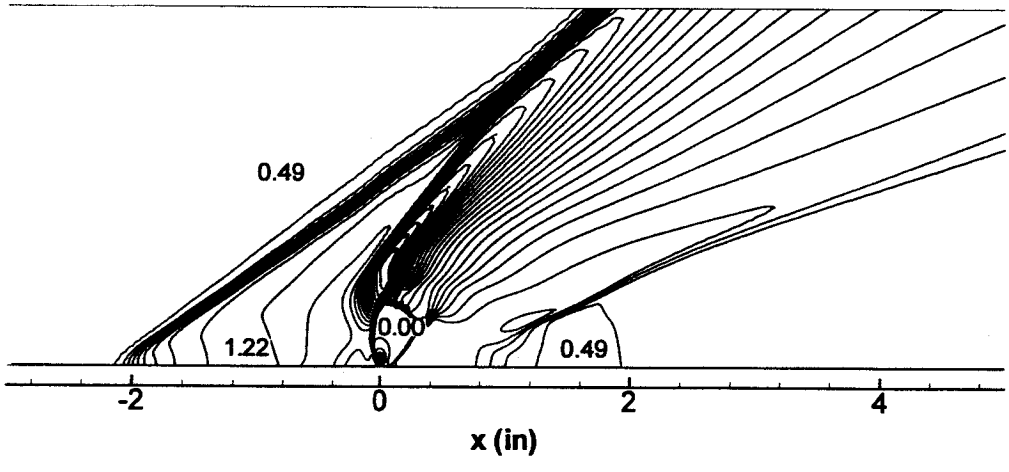

(b) 5% intensity

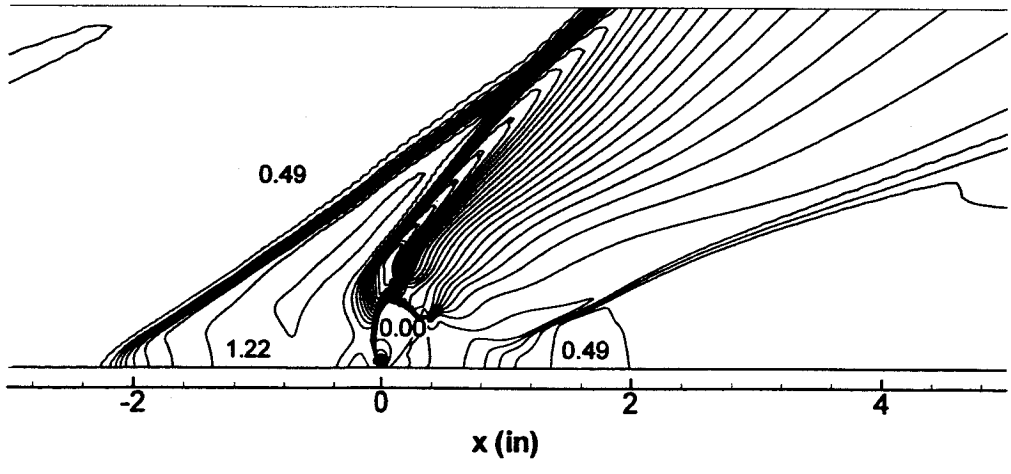

(c) 1% intensity

Figure 3.4 Static pressure contour plots.

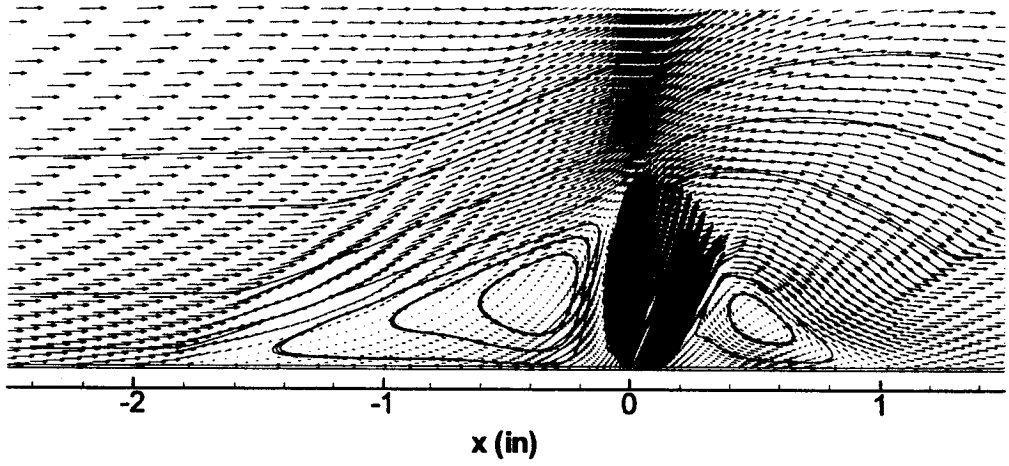

(a) 10% intensity

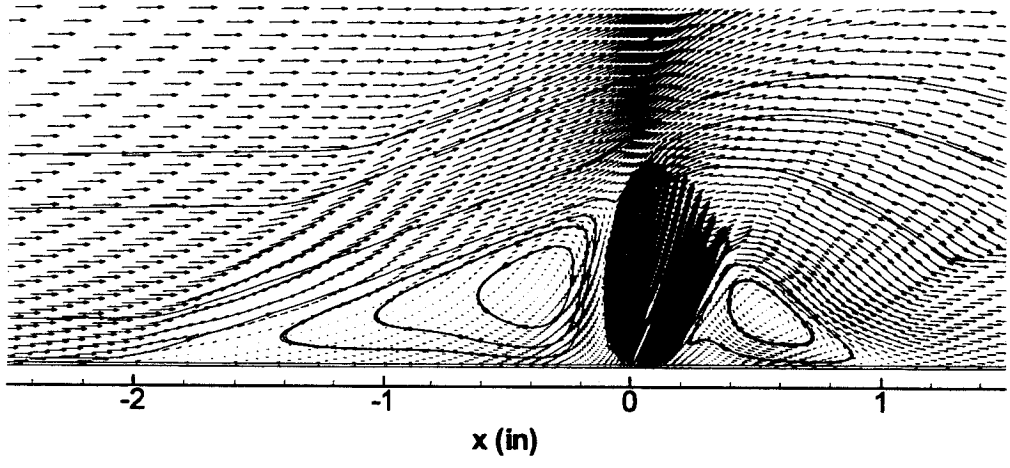

(b) 5% intensity

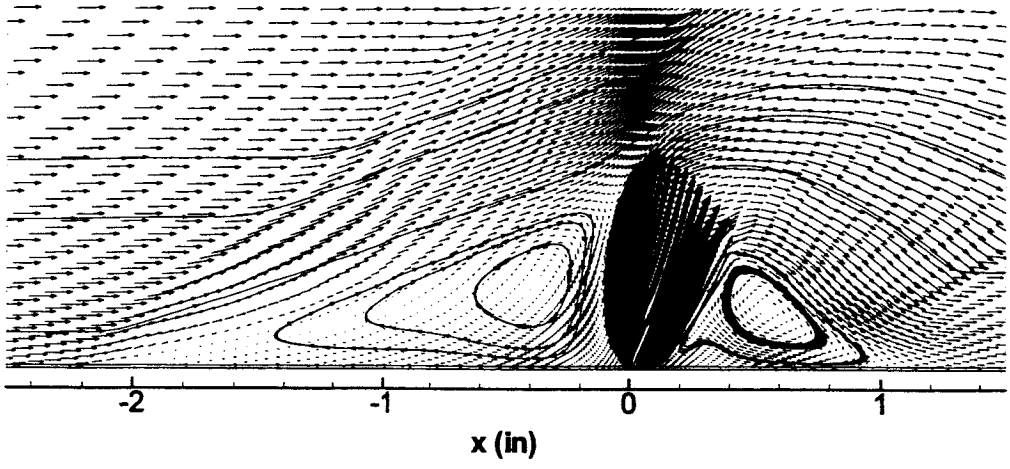

c. 1% intensity

Figure 3.5 Velocity vector and streamline plots.

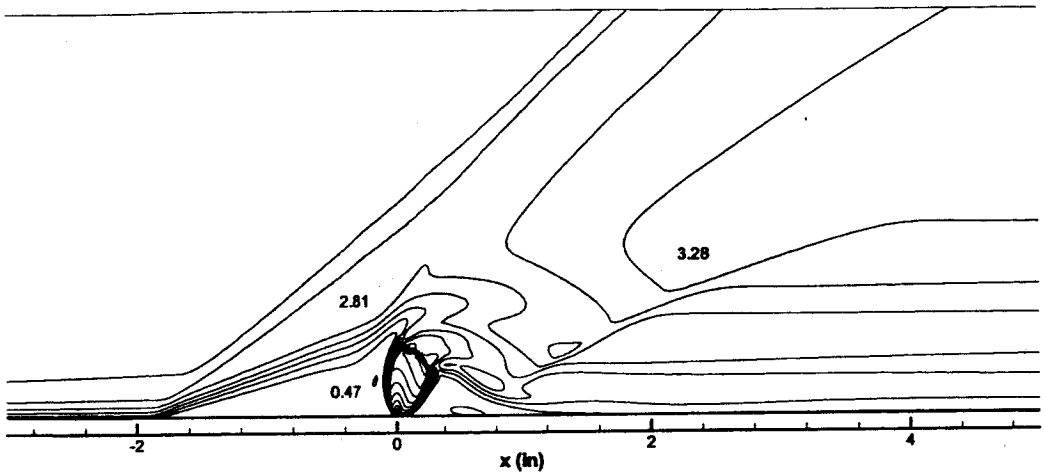

a. 10% intensity

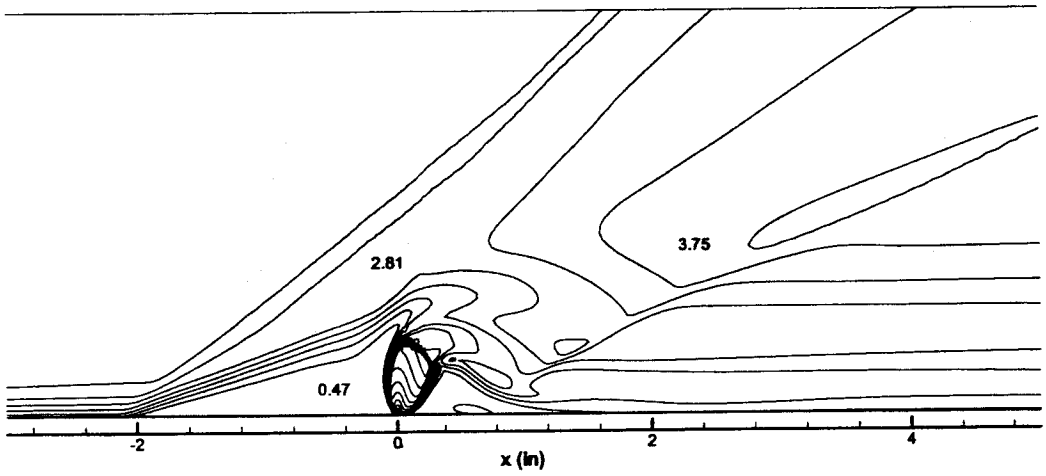

b. 5% intensity

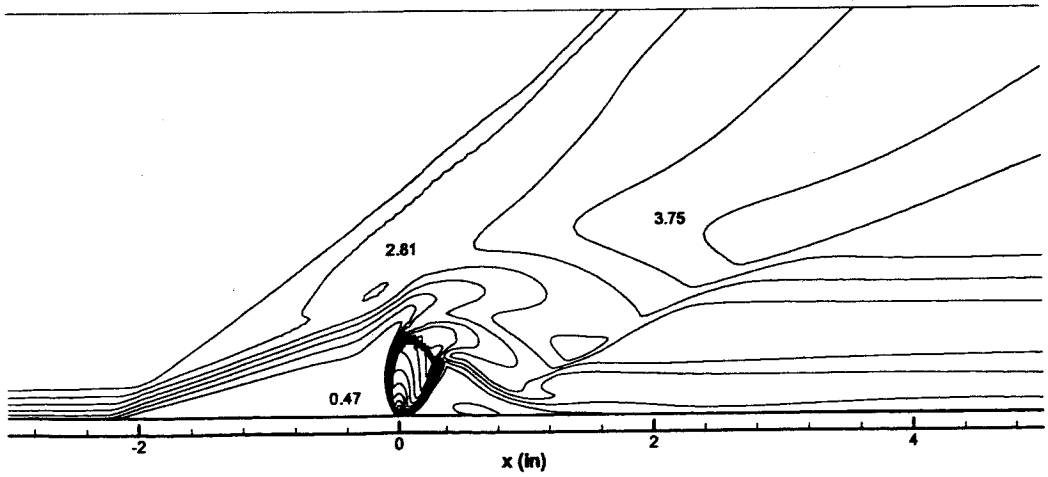

c. 1% intensity

Figure 3.6 Mach number contour plots.

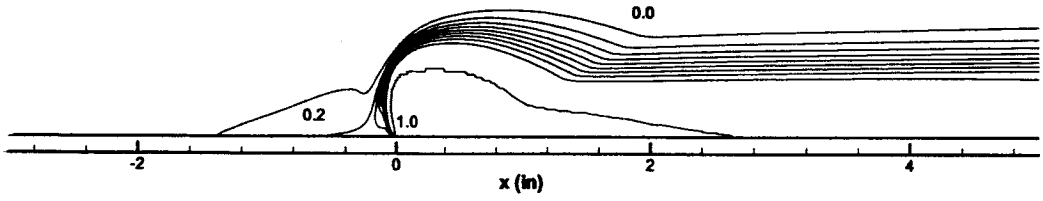

a. 10% intensity

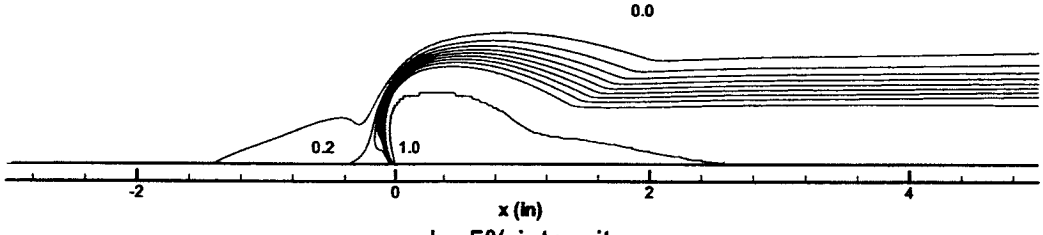

b. 5% intensity

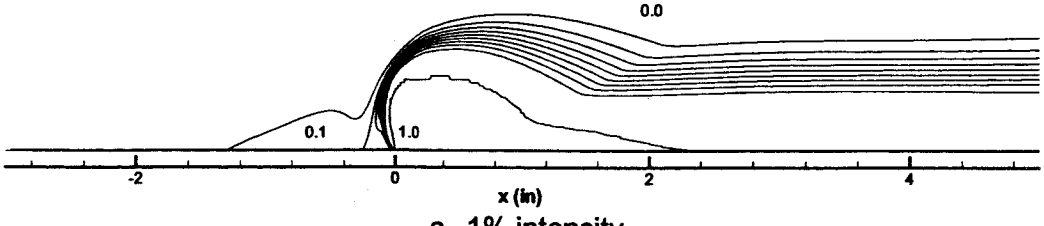

c. 1% intensity

Figure 3.7 Nitrogen mole fraction contour plots.

experimental results from tests performed at the Jet Propulsion Laboratory at the California Institute of Technology. It was found that using the commercial code FLUENT provided excellent computational results for this case. The computed flow field showed the correct physical characteristics. The calculated wall pressure profiles compared well with the experimental data. While all cases showed accurate prediction of the magnitude of the upstream pressure increase and accurate portrayal of the downstream wall pressure, use of 5% turbulent intensity provided the best computational results, most accurately predicting the length of the upstream separation region.

4. RESULTS AND DISCUSSION

In this section numerical results are presented and discussed for two-dimensional and three-dimensional models of the Japan National Aerospace Laboratory combustion chamber experimental model (JNAL), a dual-mode scramjet combustor configuration. In each subsection the specific cases are explained.

4.1 Two-Dimensional - Half-Height Domain

This two-dimensional model was based on the JNAL scramjet combustor (Fig. 2.1). The geometry was simplified to have one upper and one lower jet. Slot diameter was calculated to maintain the fuel to air ratio of the original three-dimensional combustor. The boundary conditions are given in Table 4.1. To further simplify the computational model, only half of the domain was created (Fig. 4.1). A symmetry plane was assumed at the centerline between the upper and lower jets. The results presented in this section were obtained using an unstructured grid consisting of 76,000 triangular cells, shown in Fig. 4.2. Results obtained using ¼ and ½ scale models are compared with those obtained using full-scale model.

The Mach number contour plots are given in Fig. 4.3. Main characteristics of the flow are well developed and are quite similar for each scaled model. Hydrogen injection expands from sonic and then recompresses forming the Mach disk. The bow shock is formed as the supersonic air interacts with the subsonic injectant. Leeward of the Mach disk a recompression shock is observed. Figure 4.4 shows a blowup of the Mach number contours around the injection port. A closer view of this figure indicates that the ½ scale and ¼ scale results are quite similar although some deviation from the full-scale results is clearly seen in this figure. Figure 4.5 shows a direct comparison of the shock systems (at M=2.5) While the results are similar, deviations are seen leeward of the barrel shock.

Table 4.1 Boundary conditions for half-height domain

	Free-stream Viatiated Air	Jet Injection
M	2.5	1.0
Pt (atm)	10	6.64
Ps (atm)	0.55	3.51
Tt (K)	2000	280
Ts (K)	1055	233
Velocity (m/s)	1654	1160

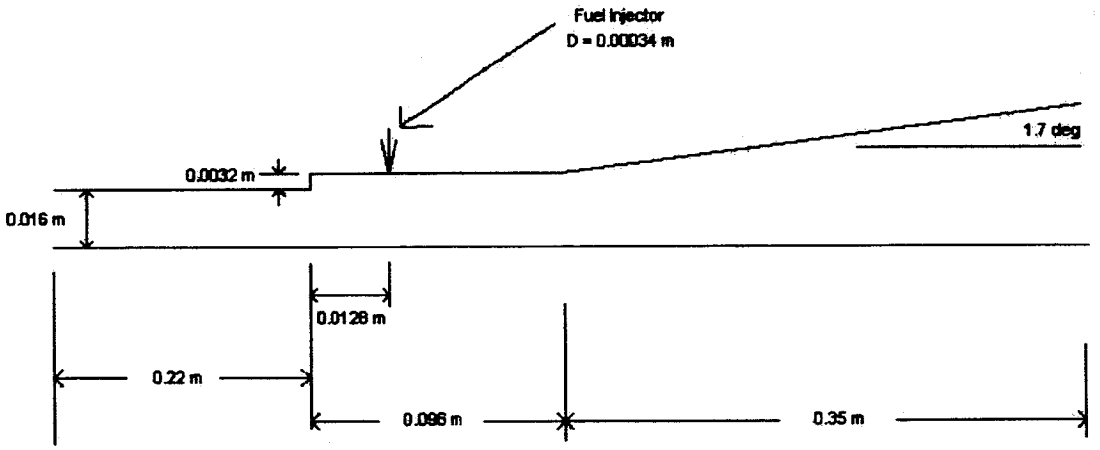

Figure 4.1 Schematic of half-height combustion chamber model.

Figure 4.2 Unstructured grid.

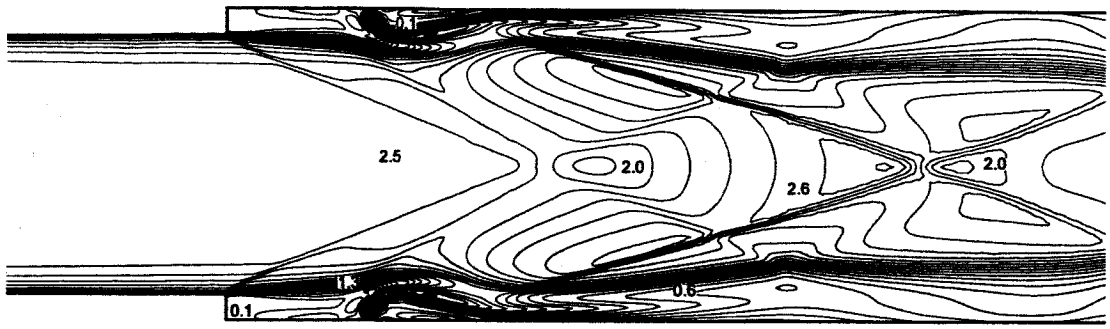

a. 1/4 Scale

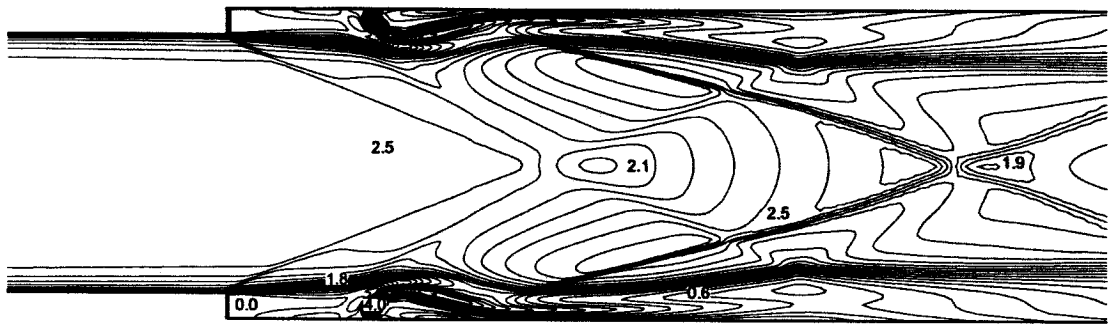

b. 1/2 Scale

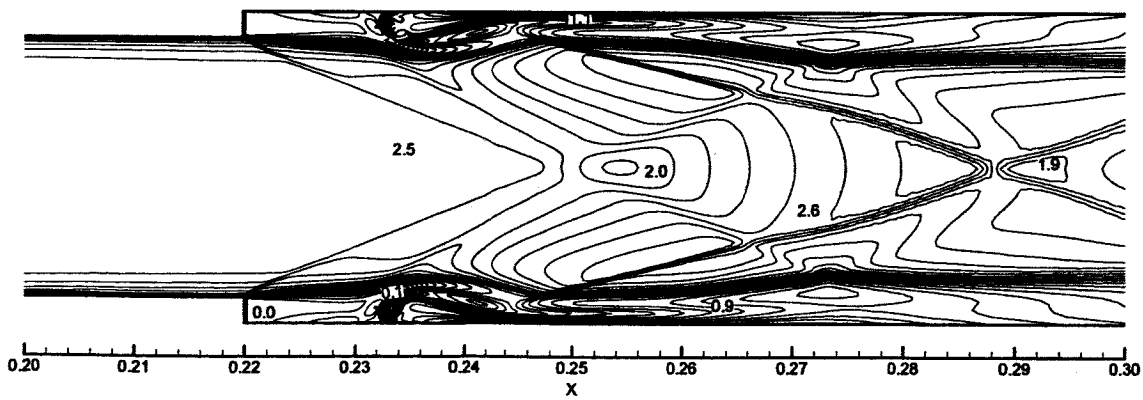

c. Full scale

Figure 4.3 Mach number contours.

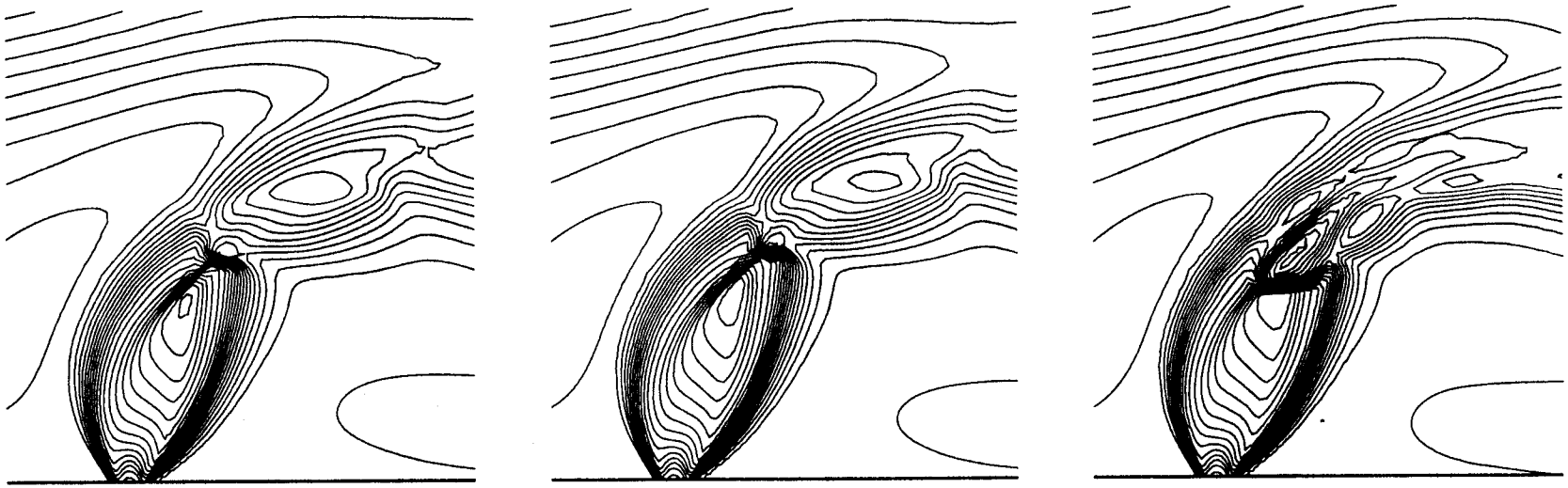

Figure 4.4 Mach number contours at jet injection.

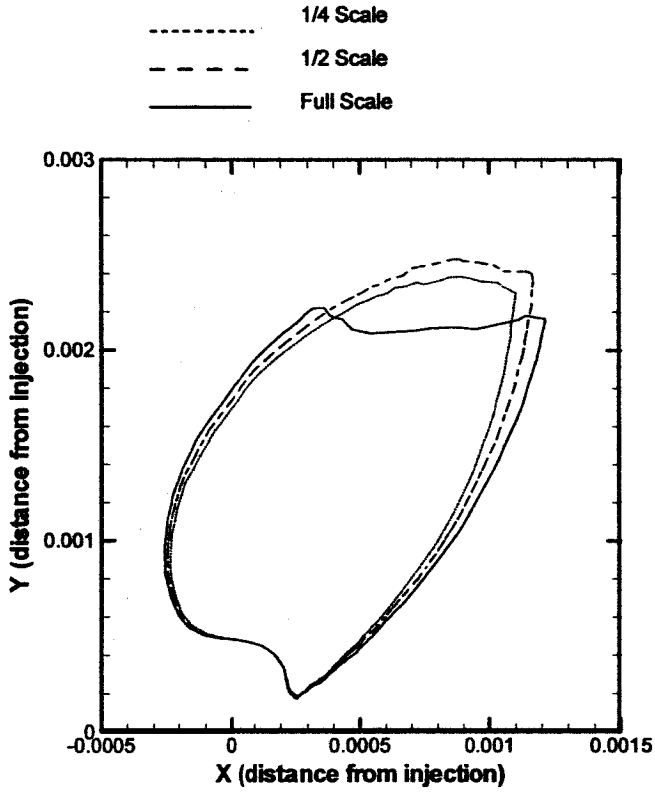

Figure 4.5 Comparison of shock systems, M=2.5.

Static pressure contours are shown in Fig. 4.6. Characteristic flow features, including expansion fan at steps, barrel shock, and Mach disc around injection are similar regardless of scale. The upstream interaction reaches only to the steps in all cases.

Figures 4.7 and 4.8 show the temperature and H_2O mass fraction contours plots, respectively. It is seen that the recirculation region ahead of the jet convects hydrogen upstream. Water is rapidly produced by combustion near the injection and diffuses in the leeward. Again the scaled models capture the qualitative characteristics of the flow.

Velocity vectors and streamlines are shown in Figs. 4.9 and 4.10. These figures show clearly the recirculation zones created by the steps and the jet injection. The results are similar for all geometric scales.

4.2 Two-Dimensional - Full-Height Domain

Numerical results for a scaling investigation of a two-dimensional simplified dual-mode scramjet combustor configuration (Fig. 4.11) with significant upstream interaction were obtained using a coarse unstructured grid consisting of 30,000 triangular cells, shown in Figure 4.12. The geometry was simplified to have one upper and one lower jet (slot diameter was calculated to maintain the fuel to air ratio of the original three-dimensional combustor). To encourage upstream interaction a lower total pressure and static pressure for the freestream vitiated air was used. The boundary conditions are given in Table 4.2. Comparisons are made between symmetric results (at early iterations) and asymmetric results (much more iterations). While convergence was decent (residuals $O[10^{-3}]$), these results cannot be considered a steady state "solution," due to the periodic nature of the results.

The Mach number contour plots for the asymmetric results are given in Fig. 4.13. Main characteristics of the flow are well developed and are quite similar for each scaled model. Hydrogen injection expands from sonic and then recompresses forming the Mach disk. The bow shock is formed as the supersonic air interacts with the subsonic injectant. Leeward of the Mach disk a recompression shock is observed.

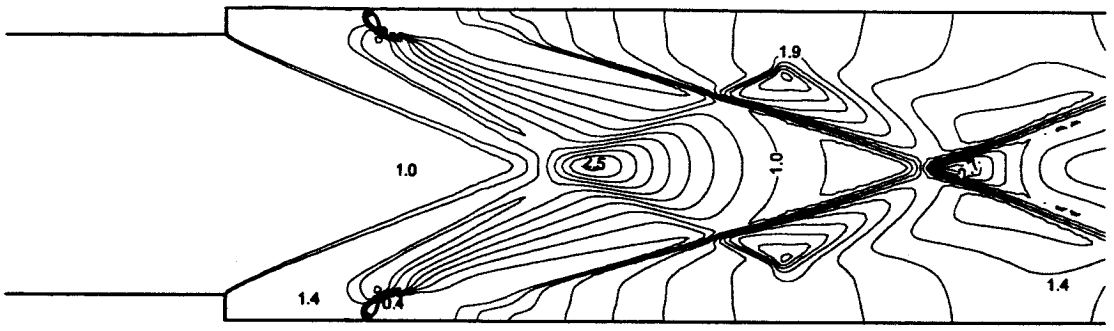

a. 1/4 Scale

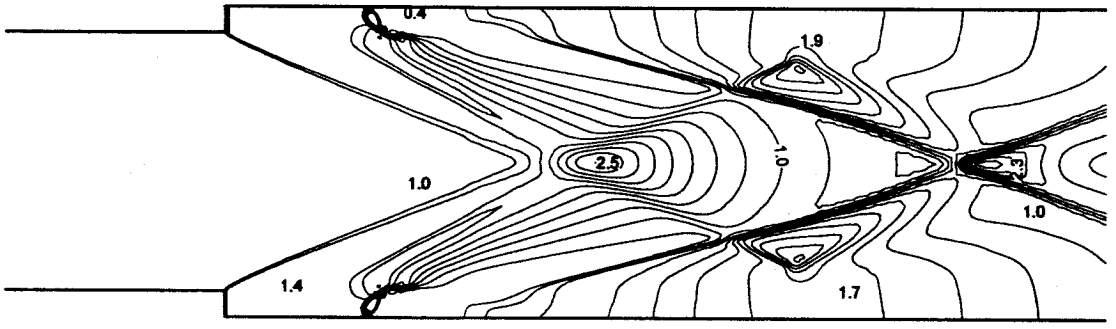

b. 1/2 Scale

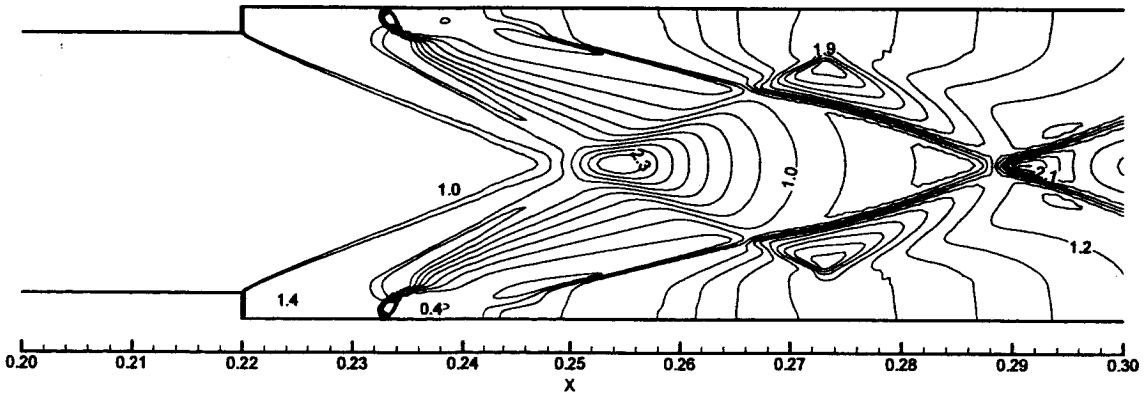

c. Full scale

Figure 4.6 Pressure contours.

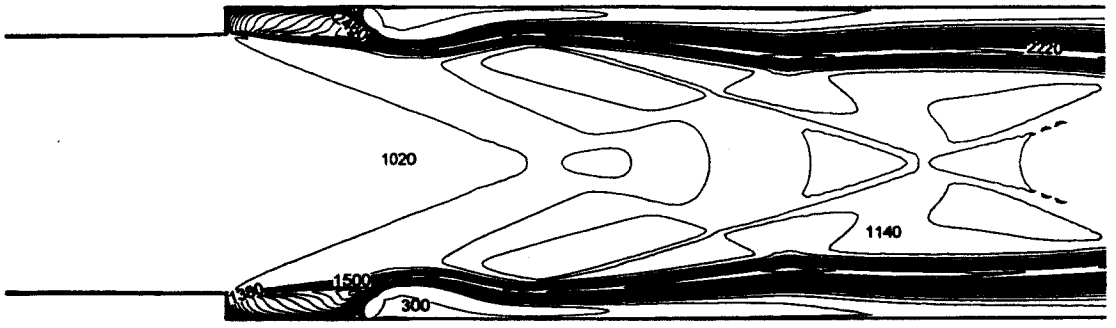

a. 1/4 Scale

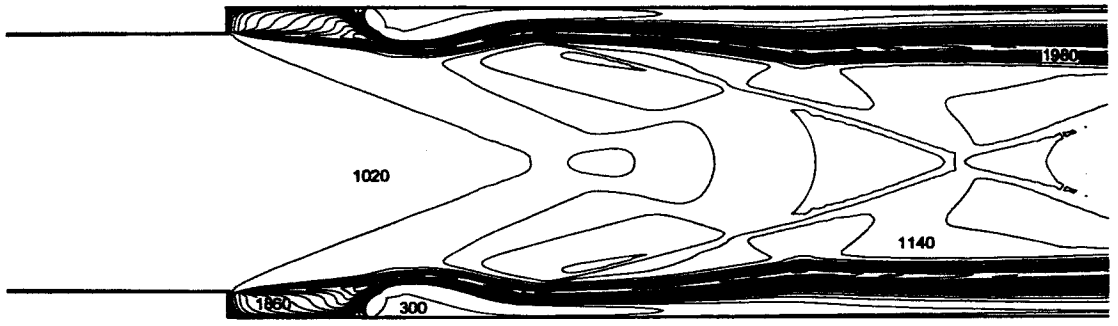

b. 1/2 Scale

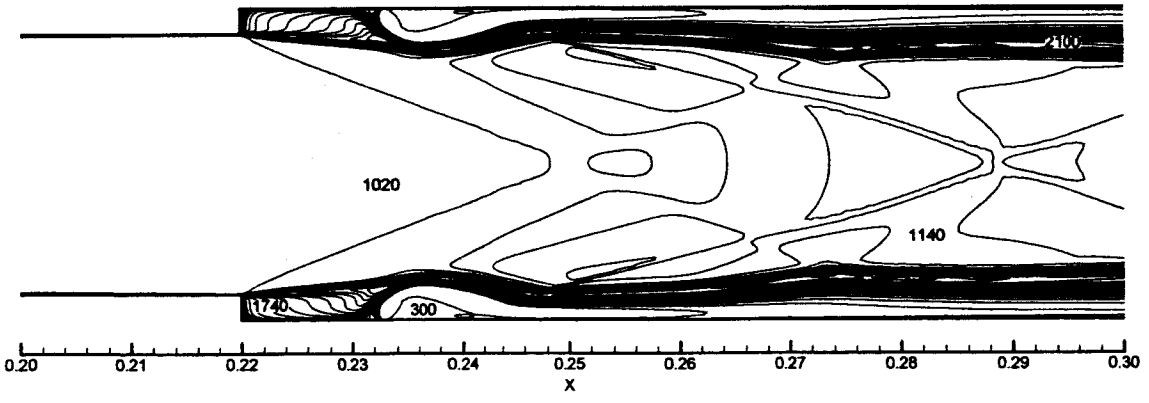

c. Full scale

Figure 4.7 Temperature contours.

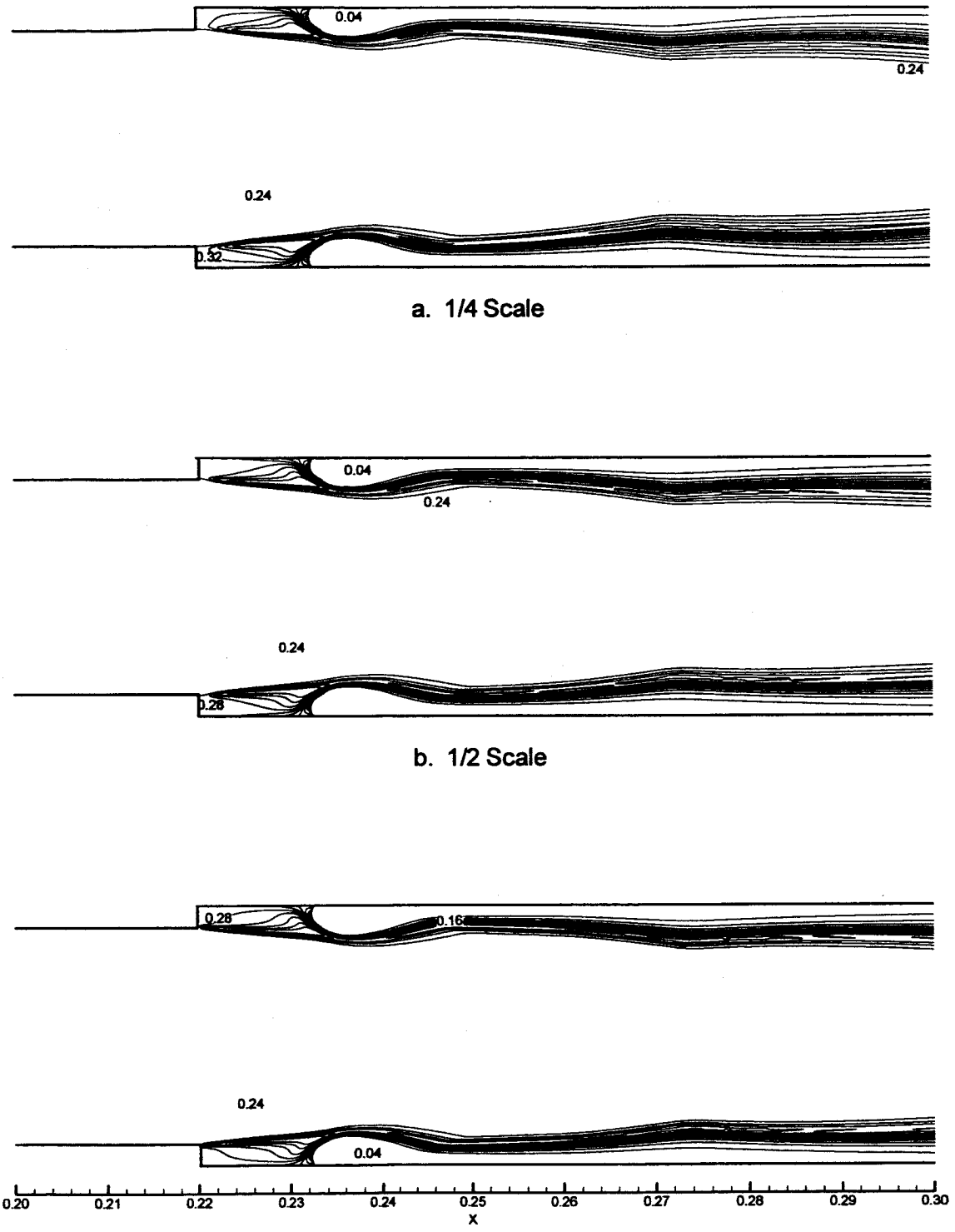

Figure 4.8 H_2O mole fraction contours.

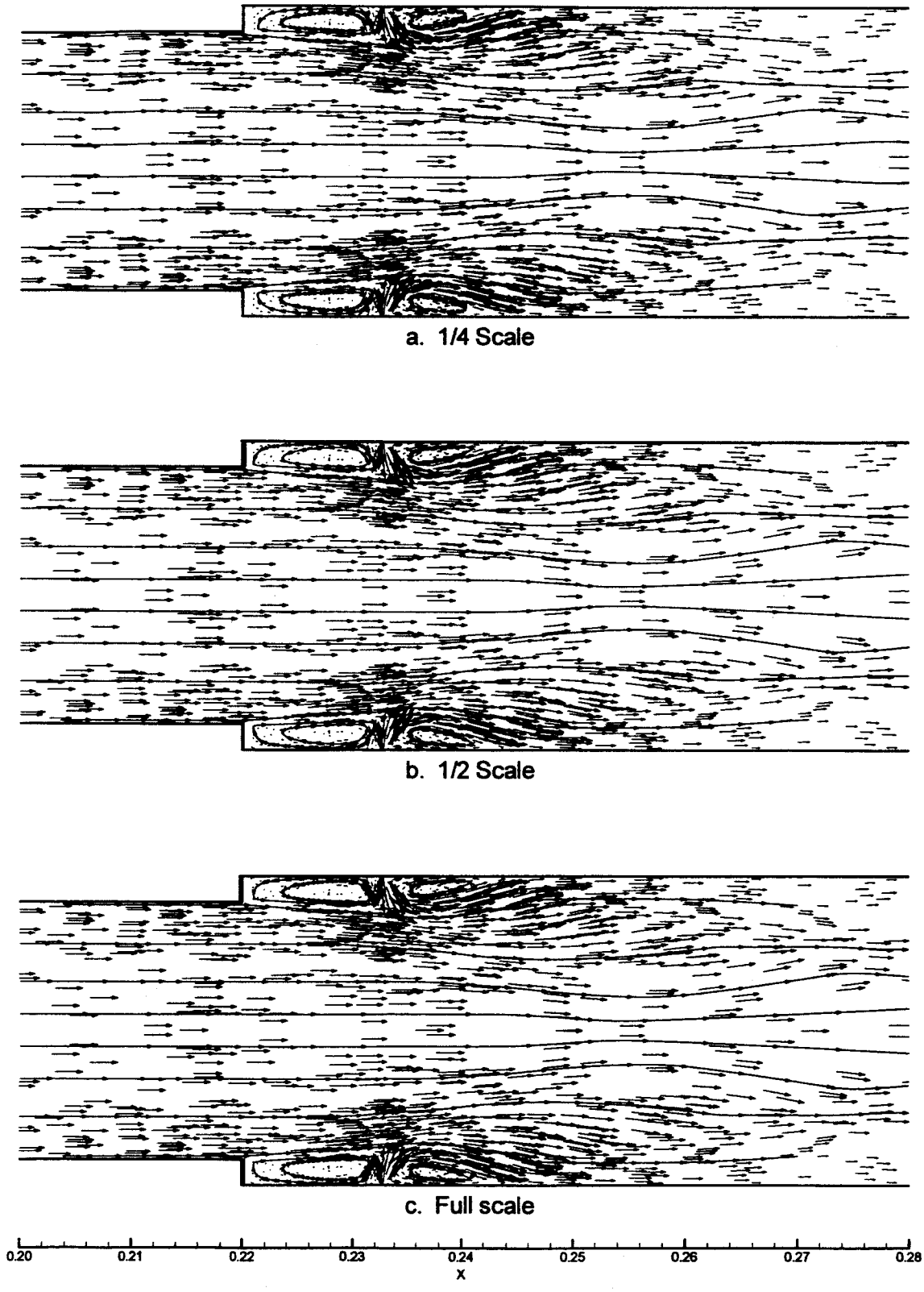

Figure 4.9 Velocity vectors and streamlines.

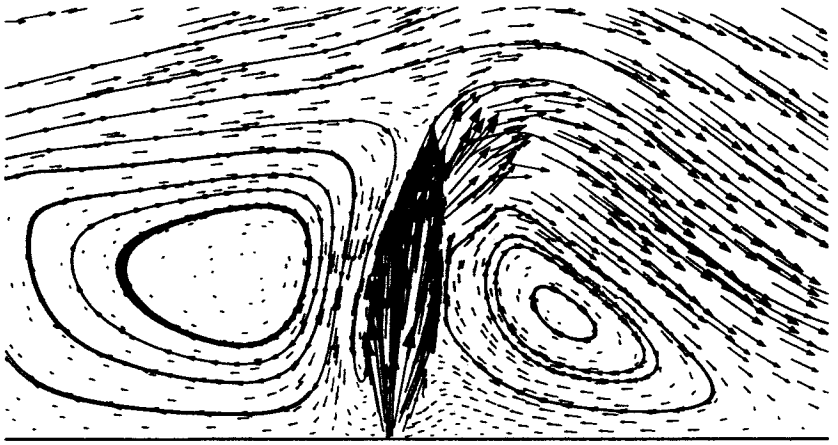

a. 1/4 Scale

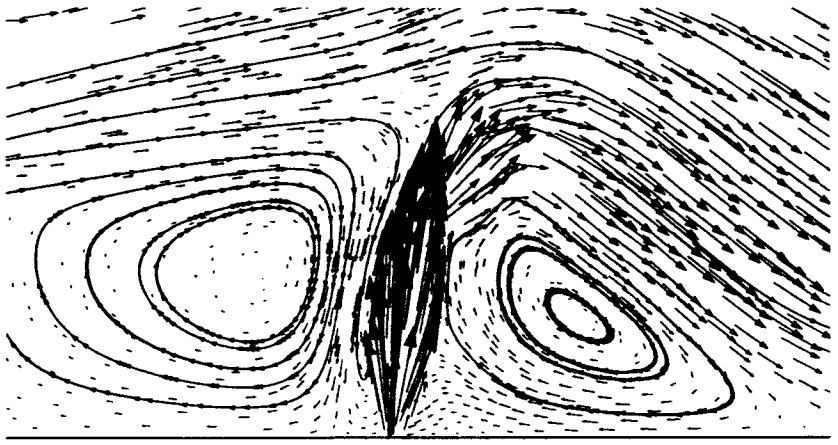

b. 1/2 Scale

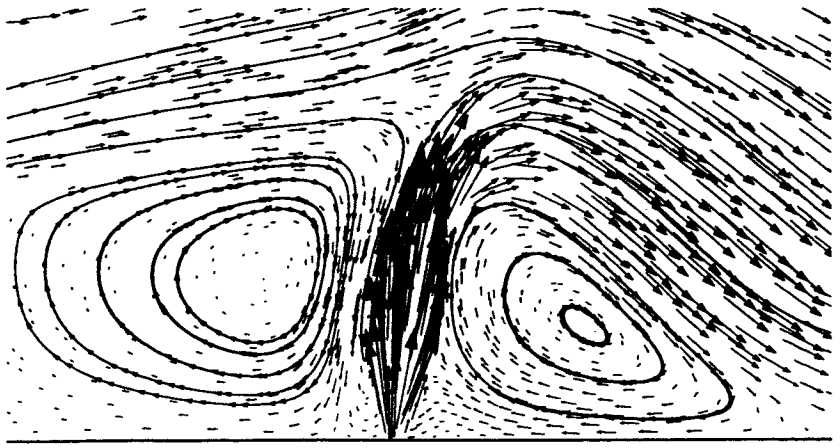

c. Full scale

Figure 4.10 Velocity vectors and streamlines at injectant location.

Table 4.2 Boundary conditions for full-height domain

	Free-stream Viatiated Air	Jet Injection
M	2.5	1.0
Pt (atm)	5	6.64
Ps (atm)	0.275	3.51
Tt (K)	2000	280
Ts (K)	1055	233
Velocity (m/s)	1654	1160

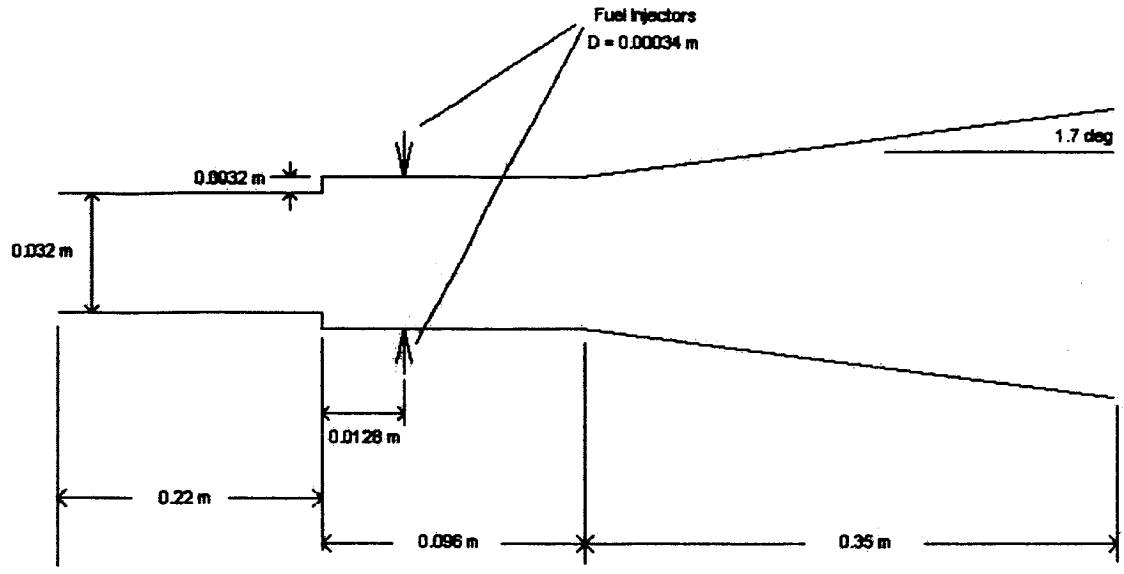

Figure 4.11 Schematic for full-height combustion chamber model.

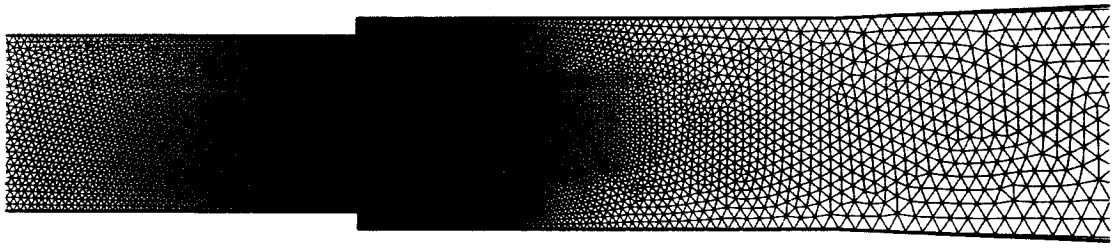

Figure 4.12 Unstructured grid.

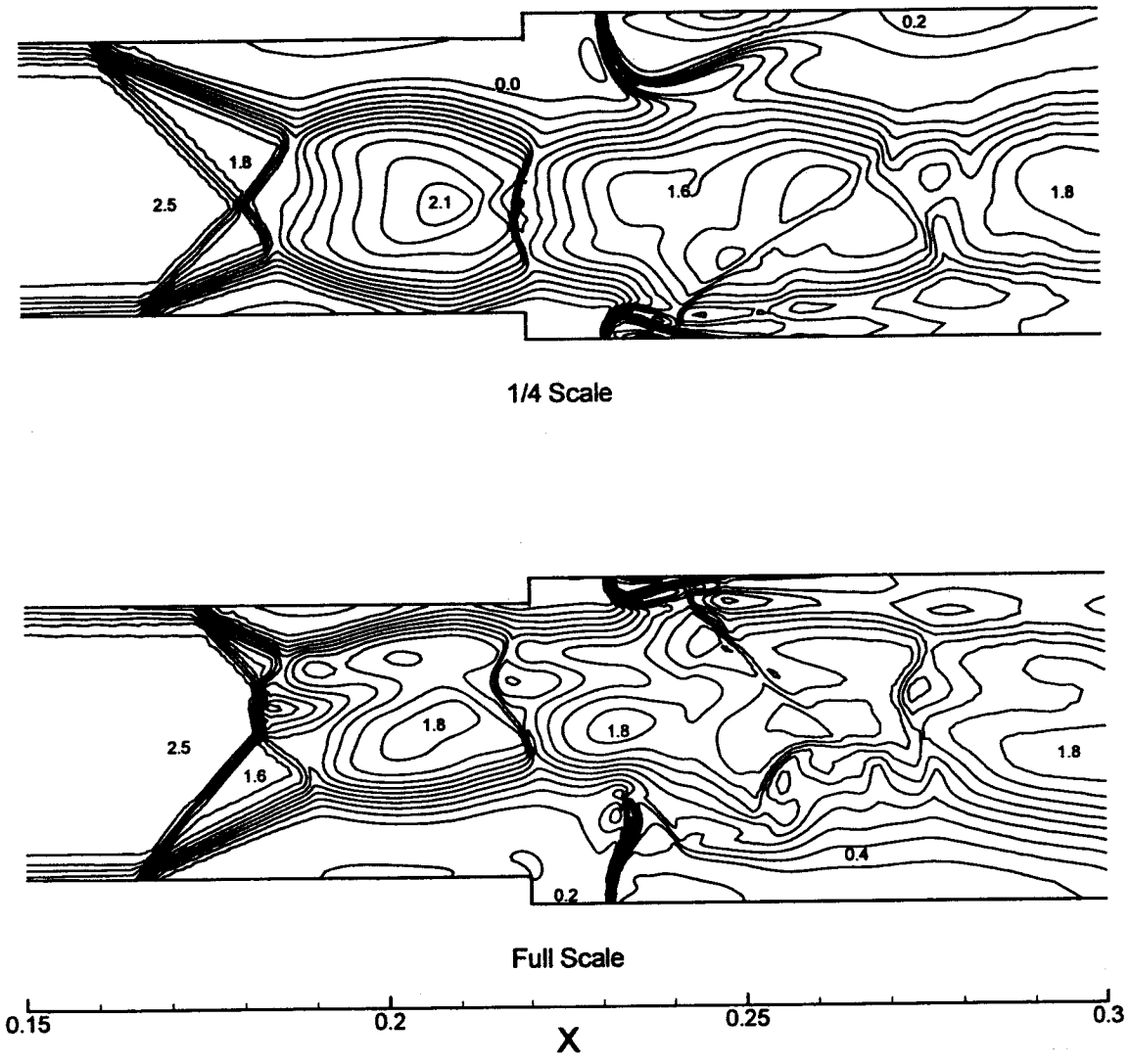

Figure 4.13 Mach number contours.

Figure 4.14 compares the Mach number contours of each model around the injection. Each model has similar features including the injectant height. Figure 4.15 shows a direct comparison of the shock systems (at M = 1.8). The results produced by the subscale models are quite similar.

Static pressure contours are shown in Fig. 4.16, for both symmetric results and asymmetric results. Characteristic flow features, including expansion fan at steps, barrel shock, and Mach disc around injection are similar regardless of scale. The upstream interaction is less than one isolator height for the symmetric results, but extends much further upstream for the asymmetric result.

Figures 4.17 and 4.18 show the temperature and H_2O mass fraction contours plots, respectively, for the asymmetric results. The large recirculation region ahead of the jet carries hydrogen upstream. Water is rapidly produced by combustion near the injection and diffuses leeward. Again, the scaled models capture the qualitative characteristics of the flow.

Velocity vectors and streamlines for symmetric and asymmetric results are shown in Figs. 4.19 and 4.20, respectively. These figures show clearly the recirculation zones created by the steps and the jet injection. The results are similar for all geometric scales.

4.3 Three-Dimensional Jet-to-Jet Symmetric Model

Numerical results for a three-dimensional jet-to-jet geometry are presented and discussed in this section. As shown in Figure 4.21, the computational domain was simplified to encompass half of the upper and half of the lower jet using the symmetry condition. Results presented in this section were obtained using a relatively coarse unstructured hexahedral grid consisting of 86,000 cells. Grid refinement was tested using a finer grid but qualitatively no significant differences in the overall flow structures were observed. Mesh cells were concentrated around the walls, particularly in the region of the steps and jets. The boundary conditions are noted in Table 4.3. The available experimental data is from pressure taps located along the duct centerline.

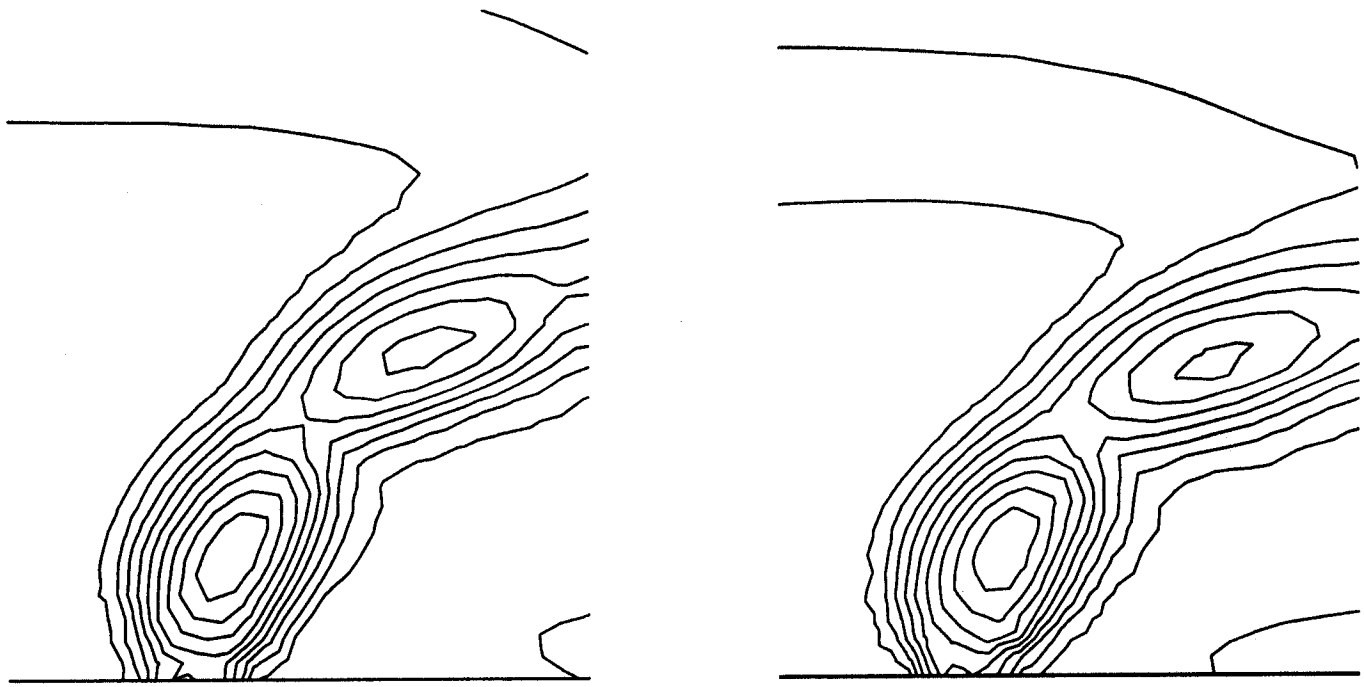

a. 1/4 Scale

b. Full Scale

Figure 4.14 Mach number contours at injection.

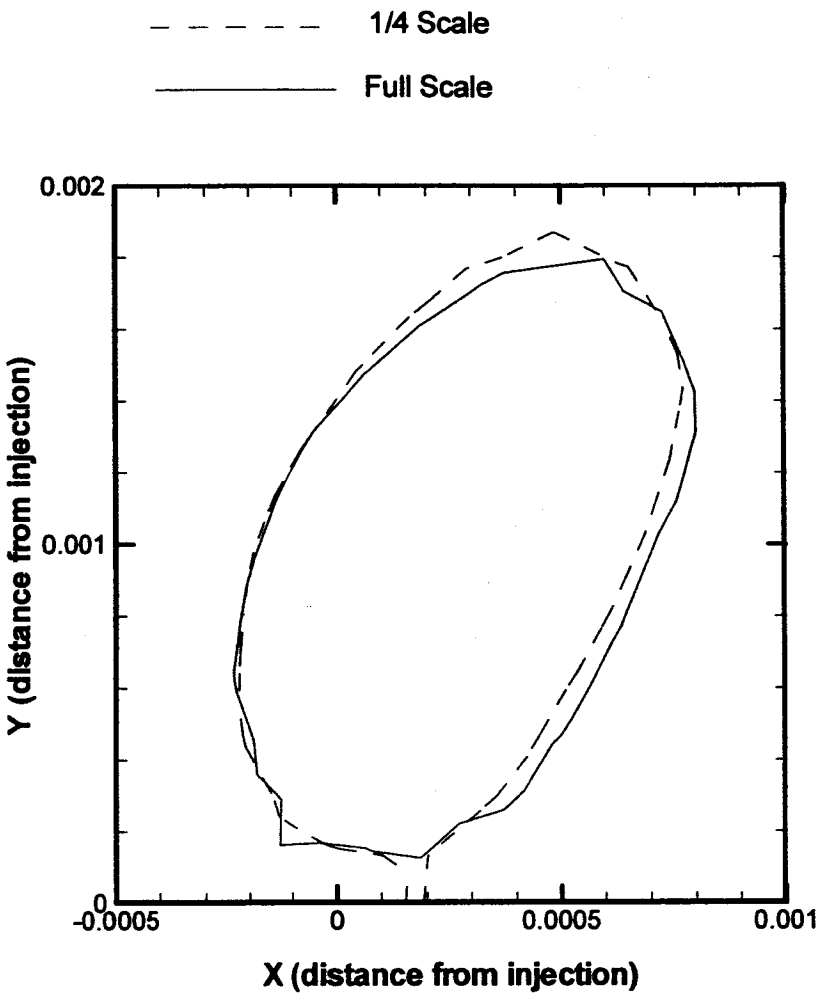

Figure 4.15 Comparison of shock system.

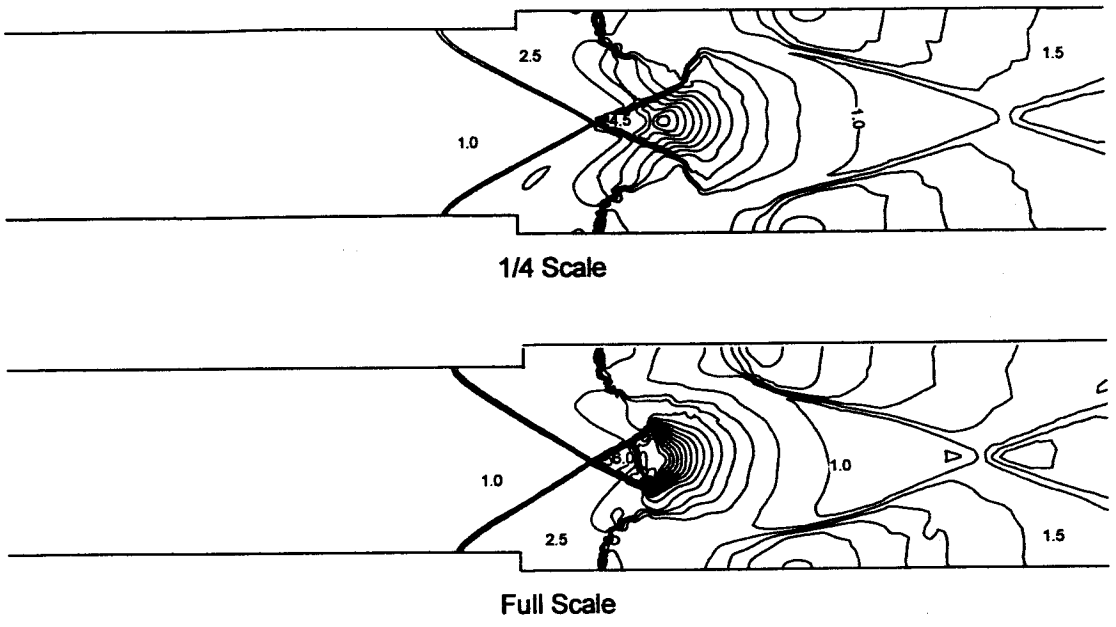

a. Symmetric Results

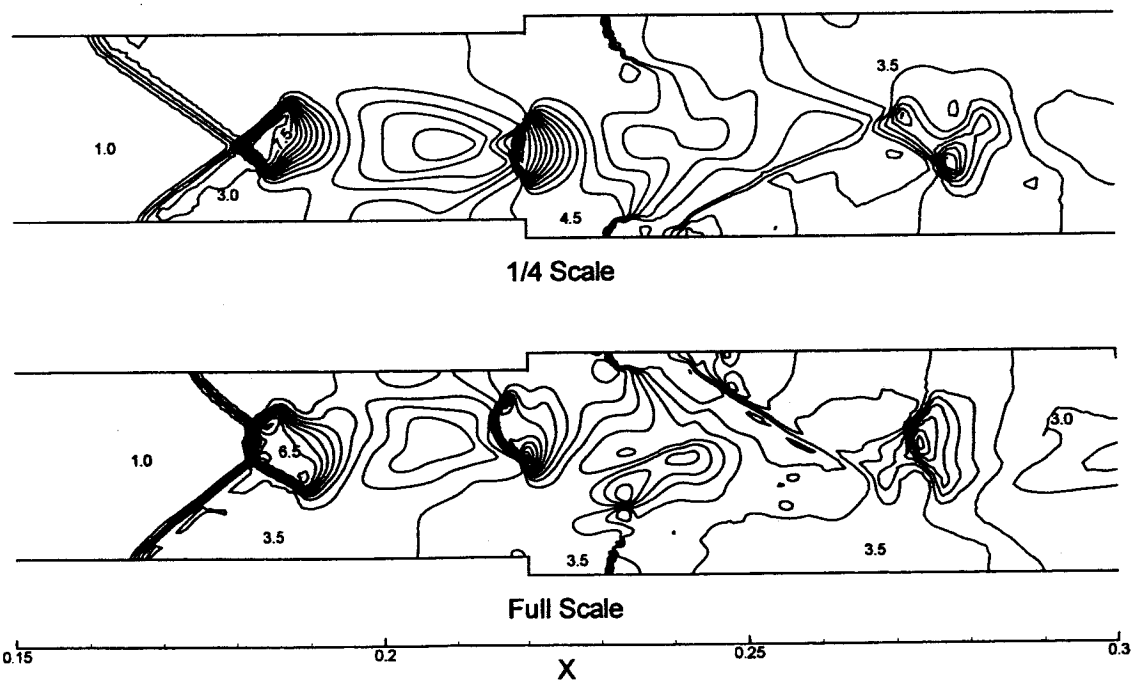

b. Asymmetric Results

Figure 4.16 Normalized pressure contours.

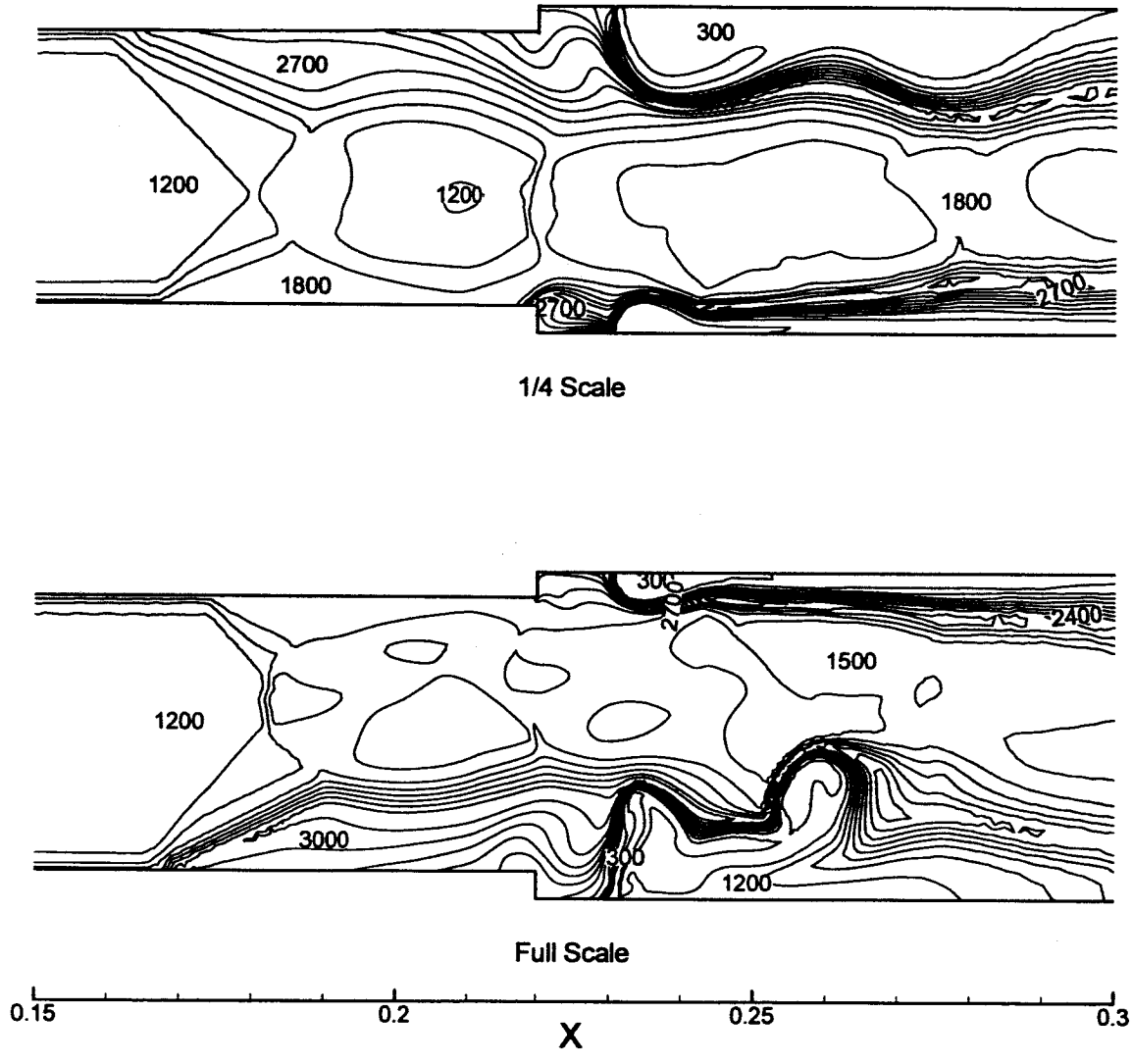

Figure 4.17 Temperature contours.

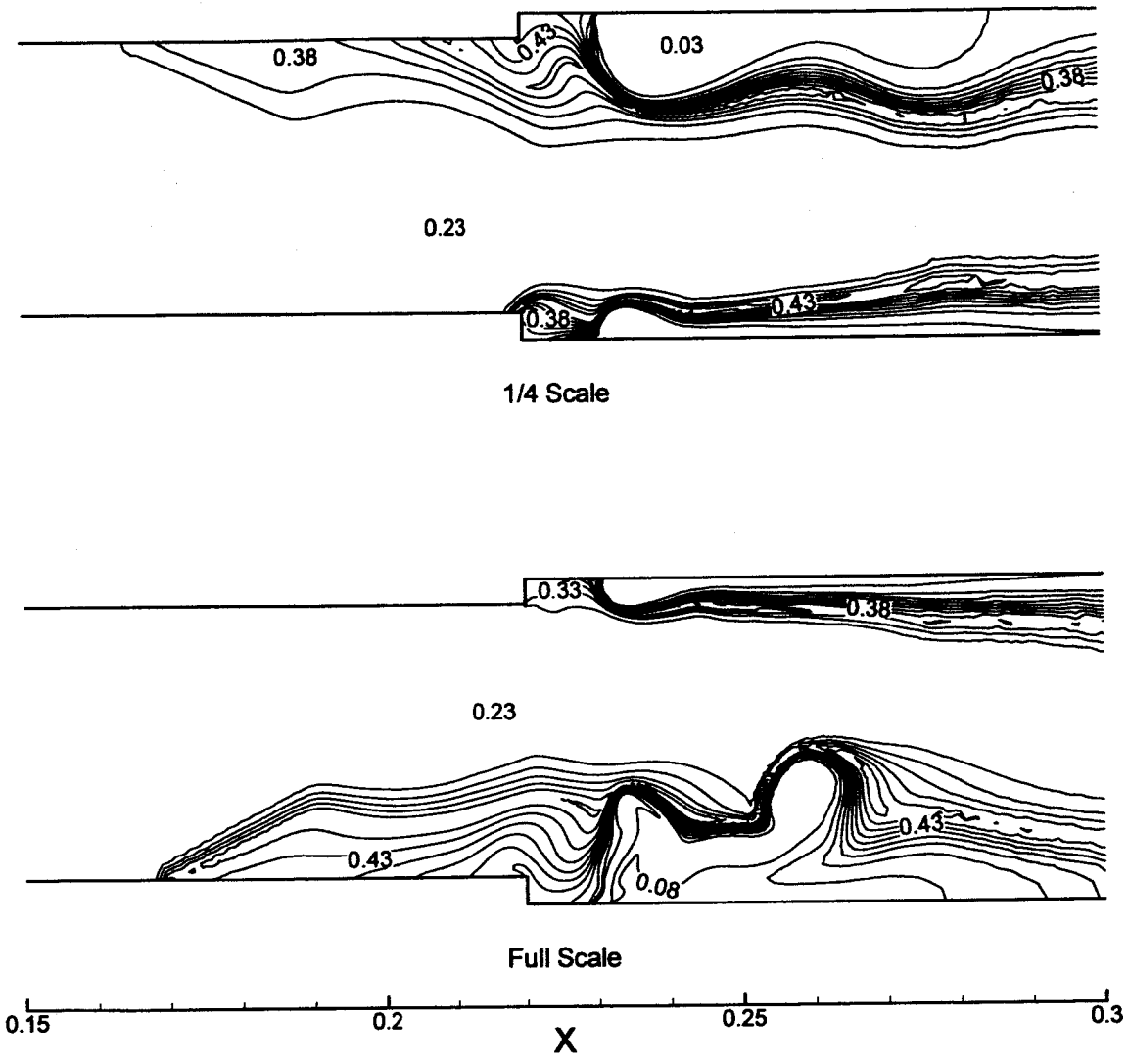

Figure 4.18 H_2O mole fraction contours.

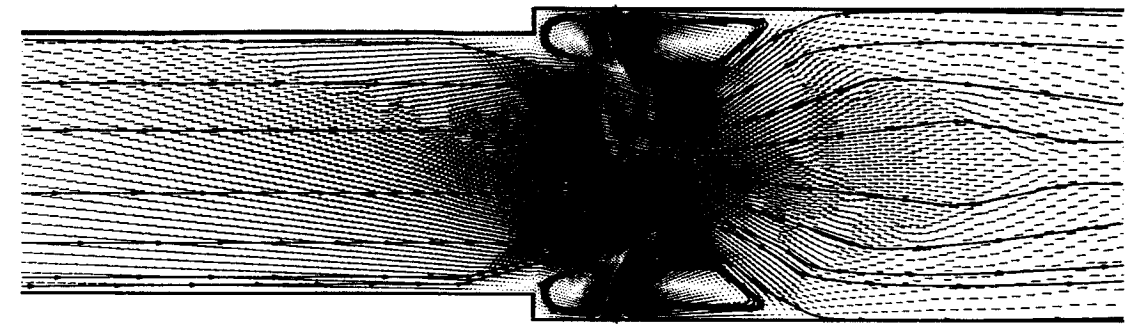

1/4 Scale

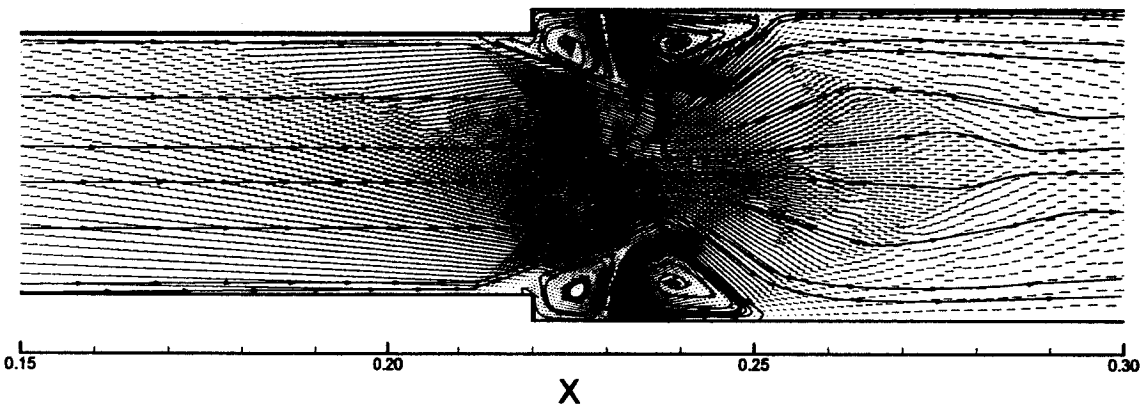

Full Scale

Figure 4.19 Velocity vectors and streamlines for symmetric results.

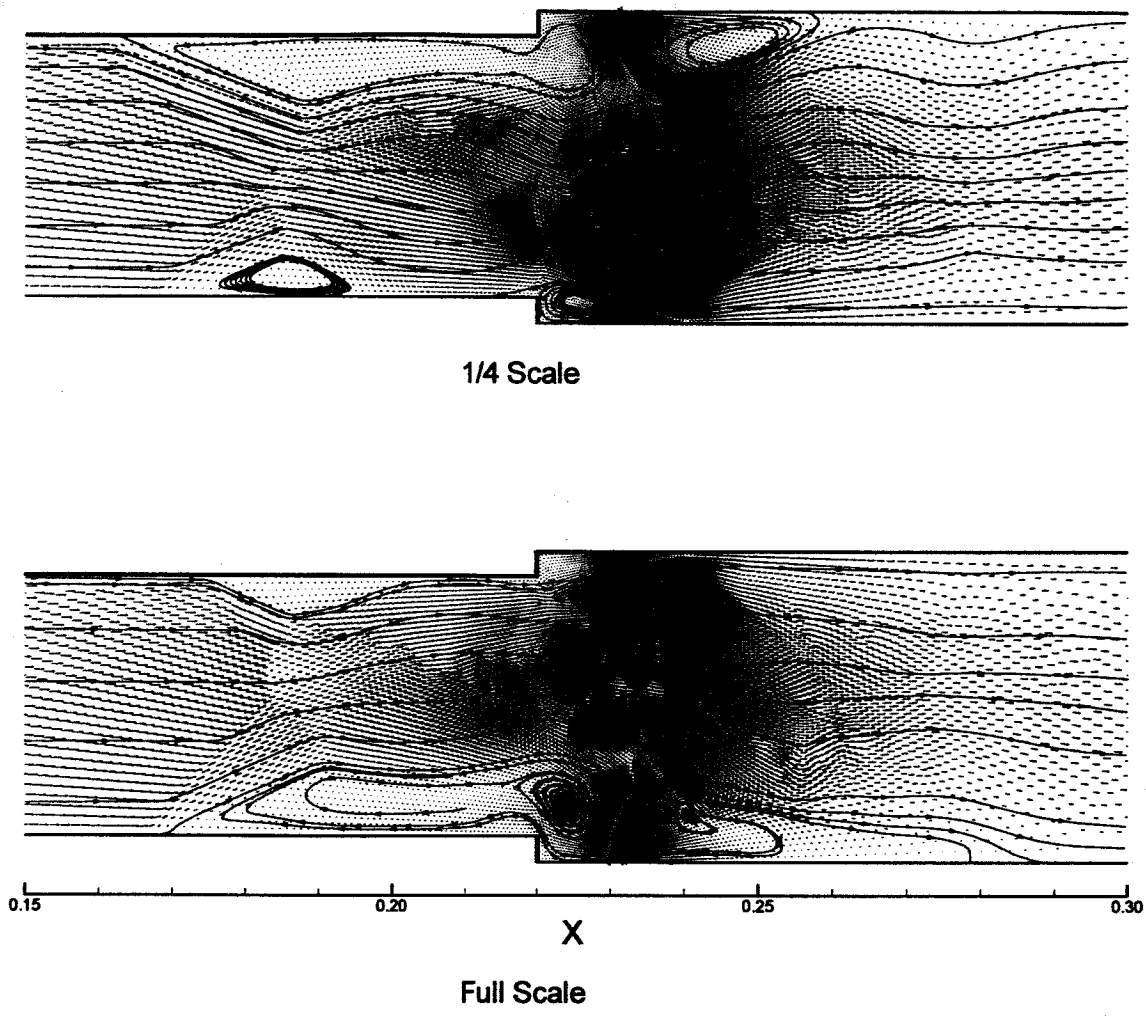

Figure 4.20 Velocity vectors and streamlines for asymmetric results.

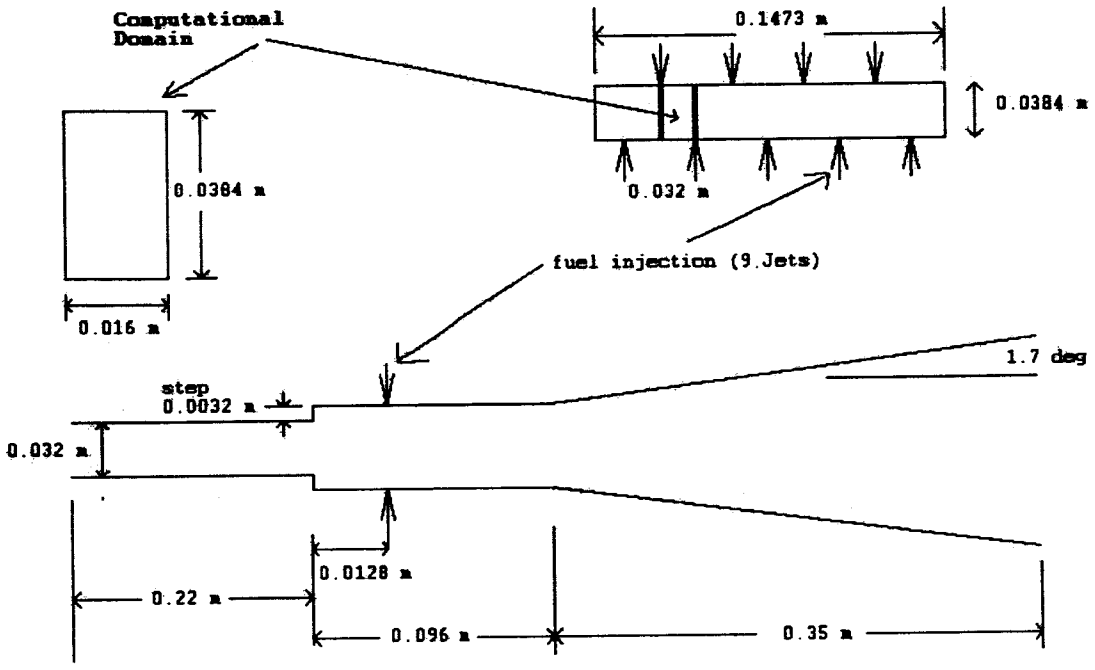

Figure 4.21 Schematic of experimental combustion chamber.

Table 4.3 Boundary conditions for three-dimensional investigation

	Free-stream Viatiated Air	Jet Injection
M	2.5	1.0
Pt (atm)	10	6.64
Ps (atm)	0.55	3.51
Tt (K)	2000	280
Ts (K)	1055	233
Velocity (m/s)	1654	1160

In References 6 and 7, three separate data sets are available for the above conditions. Rodriguez[14] explains the uncertainty in the data. For consistency, this study compares the results to the same data set as analyzed in Reference 14.

A simplified ¼ scale three-dimensional combustor model was used to reduce the physical distance for the upstream interaction to traverse against the main flow. Specifically, a convergence-acceleration technique to reduce the computational time and minimize resources requirement was examined. A comparison was made between the asymmetric results. The ¼ scale and full scale cases reported a symmetric flowfield at earlier iterations. It is assumed that for further iterations the large upstream separation region will oscillate between each wall. Numerical results from the present study are not fully converged solutions. While the residuals are O [10^{-3}], the solution appears to be transient. The results shown are at intermediate steps.

The Mach number contour plots, given in Figure 4.22, are shown at the centerline between the upper and lower fuel jets. The pressure rise due to the heat released by combustion is so large that shock waves are generated in the upstream of the steps and the core flow is decelerated almost to subsonic and accelerated again to supersonic in the expansion region. Both cases report significant upstream interaction; however, the extent of the upstream interaction is different. The resulting flow is asymmetric and the extent of the upstream interaction is more than three isolator heights. This figure shows that a large separation bubble occurs on the lower wall, and the supersonic core flow is displaced to the upper flow region. In fact, at the injector station, the lower half of the combustor is subsonic, while the upper half is predominantly supersonic. This will certainly be expected to impact the fuel penetration and mixing. Finally, at about one isolator height downstream of the step, the subsonic pockets end and the core flow begins to expand with supersonic flow filling the duct.

Although the flow characteristics, separated flow and core flow, are similar for both full scale and ¼ scale models, the degree of upstream interaction is larger for the ¼ scale solution. Fewer iterations are needed to obtain intermediate ¼ scale results. These results may provide initial conditions to start the full-scale analysis, and can lead to significant reduction in the computer time required to obtain a converged solution. This

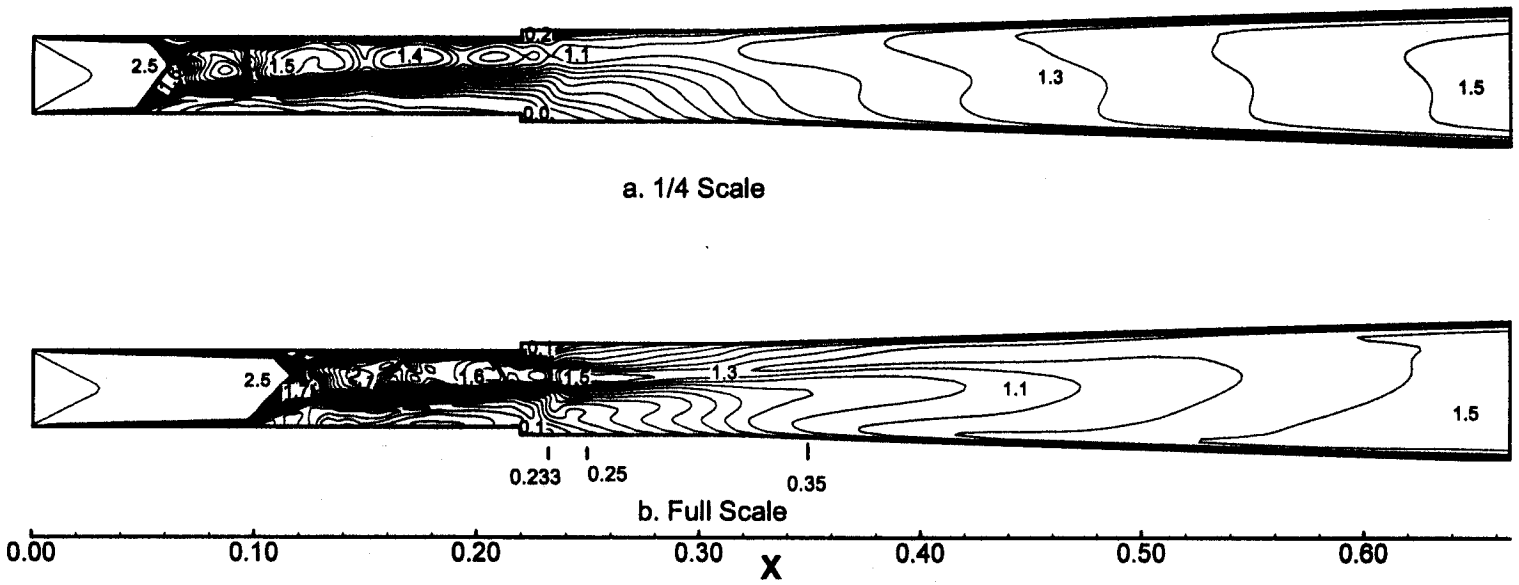

Figure 4.22 Mach number contours at centerline between jets.

acceleration approach does not require a fully converged solution, as the sub-scale model over-predicts the interaction.

Lower wall static pressure distribution along the centerline between upper and lower jets is compared in Figure 4.23. These results show fairly good agreement with experimental results of Refs. 7 and 8. The extent of the upstream interaction is over-predicted when the ¼ scale is used and is close to the experimental values when the full scale is used. The peak wall pressure is slightly under-predicted using the full scale and over-predicted using the ¼ scale model. The impact of the shock-train on the upper wall is also apparent. The solutions show that most of the important features are well resolved. Discrepancies in the amount of upstream interaction are noted. This may be due to the fact that the boundary conditions are assumed to be uniform and the amount of separated flow is dependent on the local boundary layer momentum thickness; starting with uniform flow may affect the results. It should also be noted that more detailed measurements are required to determine the initial shock strength/pressure rise.

Velocity vectors plot and streamlines are shown in Fig. 4.24. As expected, the ¼ scale model predicts larger upstream interactions. This figure shows clearly the asymmetries of flow with much upstream interaction and larger circulation bubble at the lower wall. It is also apparent that the separation bubble is rapidly closed in the combustion region, due to the constant high pressure.

In Fig. 4.25 the static pressure contours for the plane located along centerline of the jets is shown. Note that the peak pressure occurs just downstream of the fuel injectors for both full scale and ¼ scale cases. After this peak pressure the pressure distribution becomes more uniform, top to bottom. This is also the point at which the low-subsonic bubble is dissipated and the very low supersonic core flow expands to fill the duct. Clearly, the characteristic equal wall pressures downstream of the "thermal throat" are apparent in this figure.

Figures 4.26 and 4.27 show the H_2O mass fraction and the temperature contours at the centerline between the fuel jets. As expected, combustion products are transported upstream on the lower wall, which has the larger recirculation region, while on the

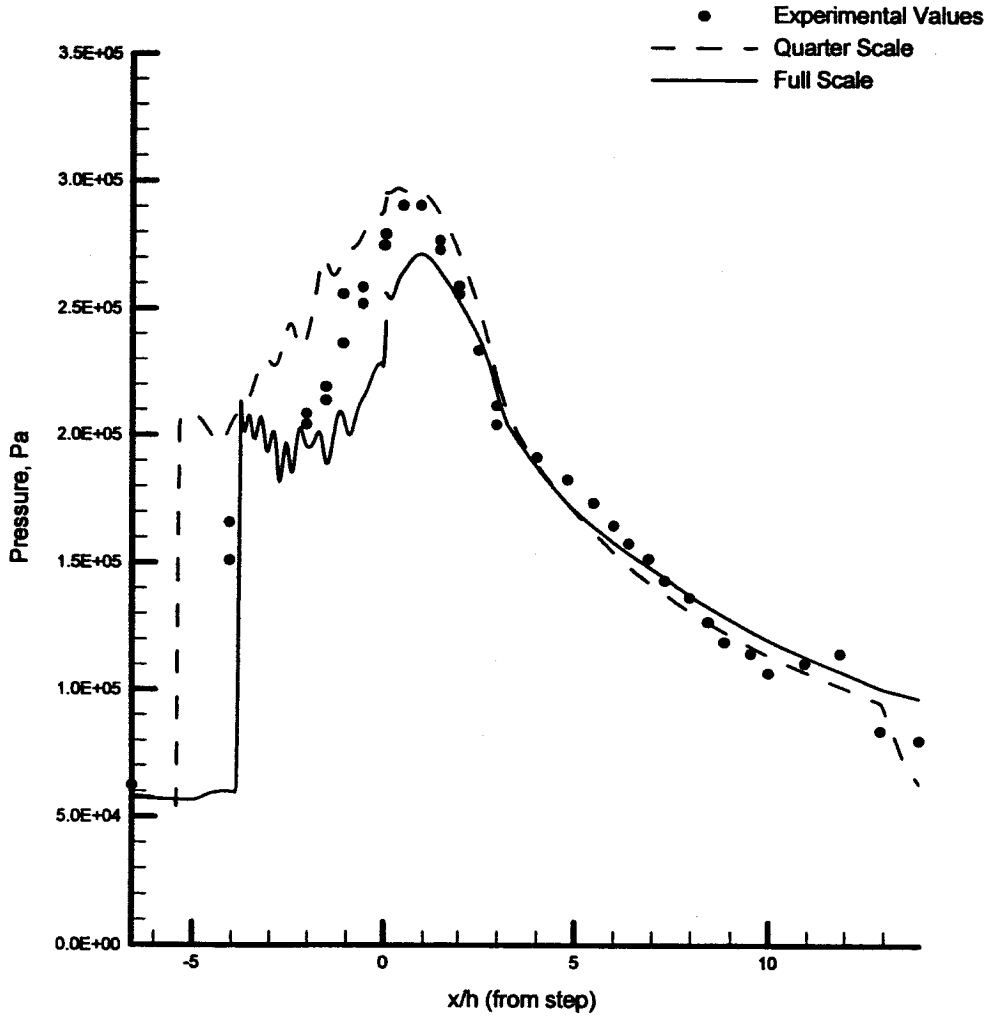

Figure 4.23 Wall static pressure distribution.

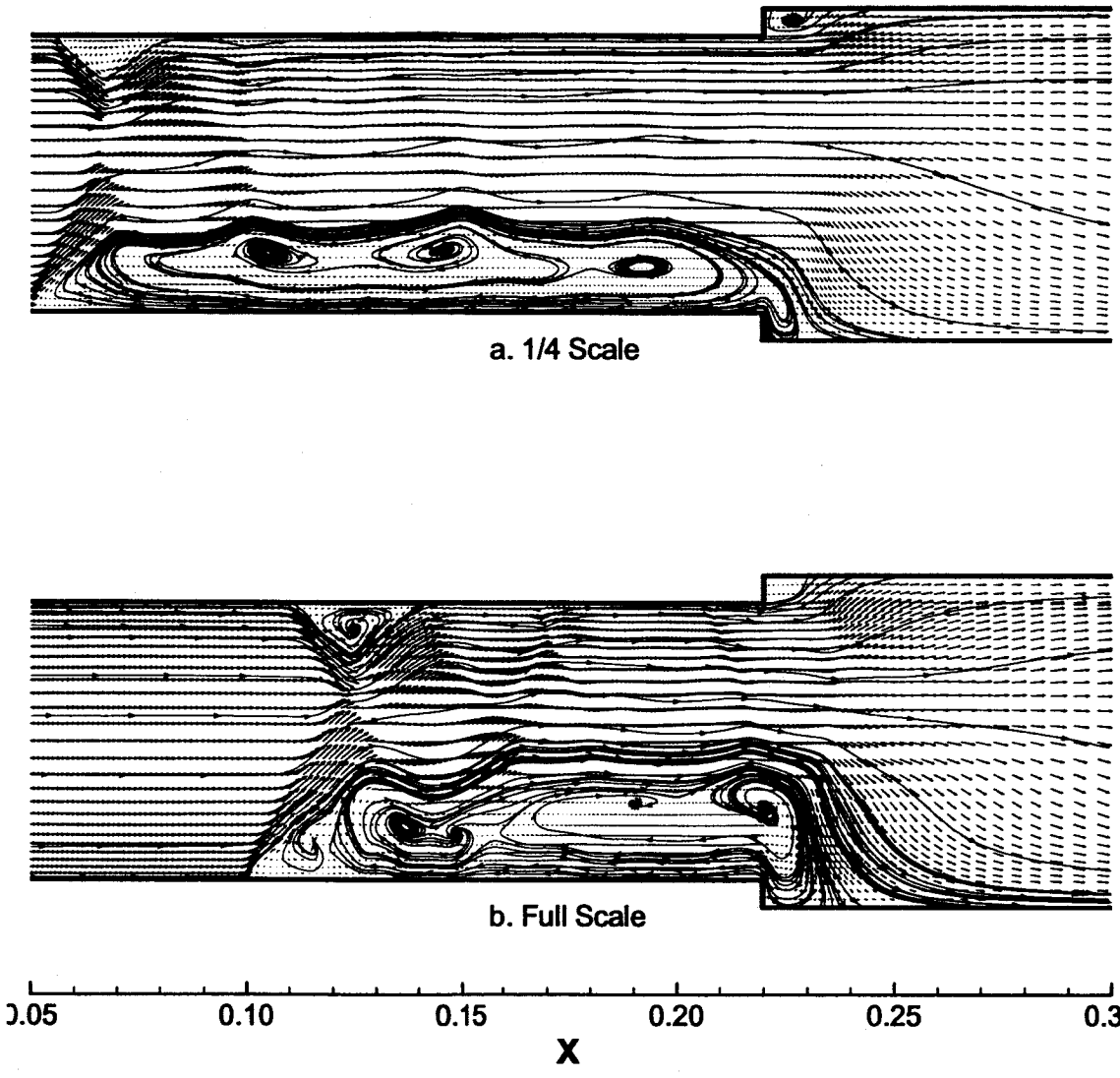

Figure 4.24 Velocity vectors and streamlines.

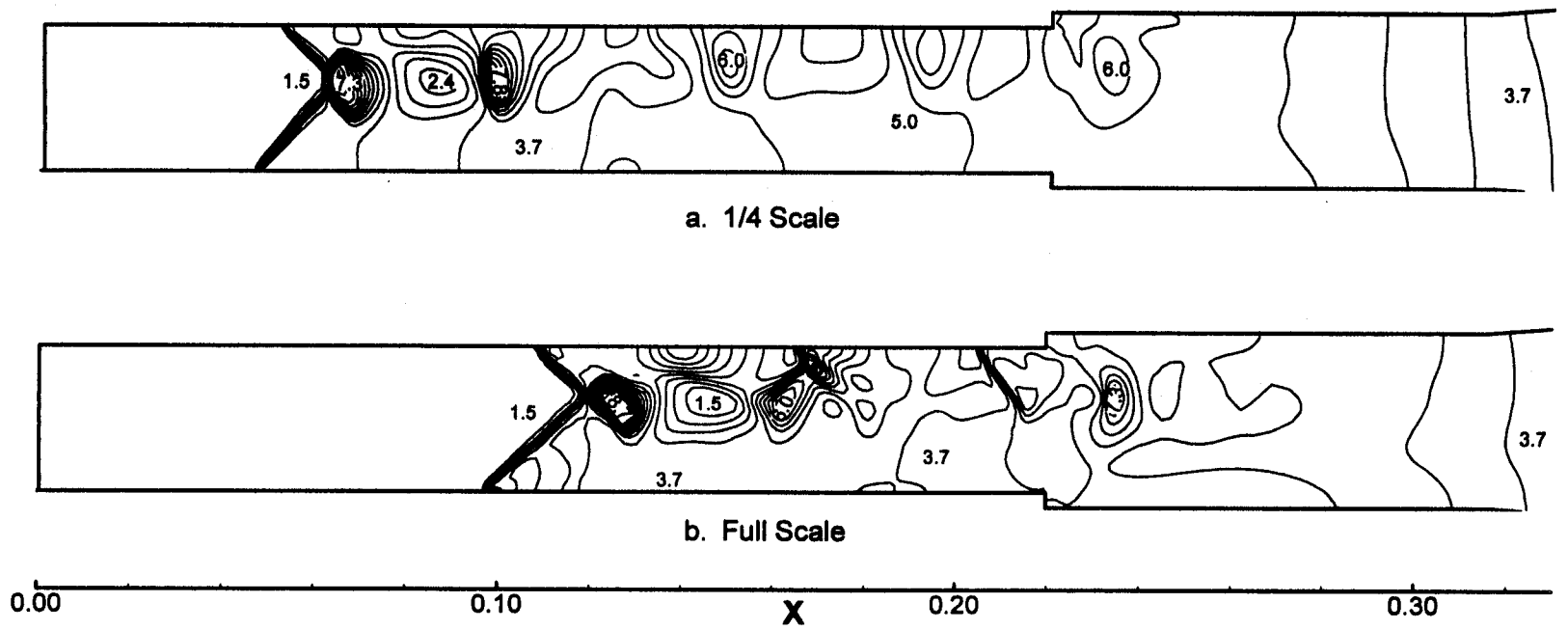

Figure 4.25 Static pressure contours at centerline.

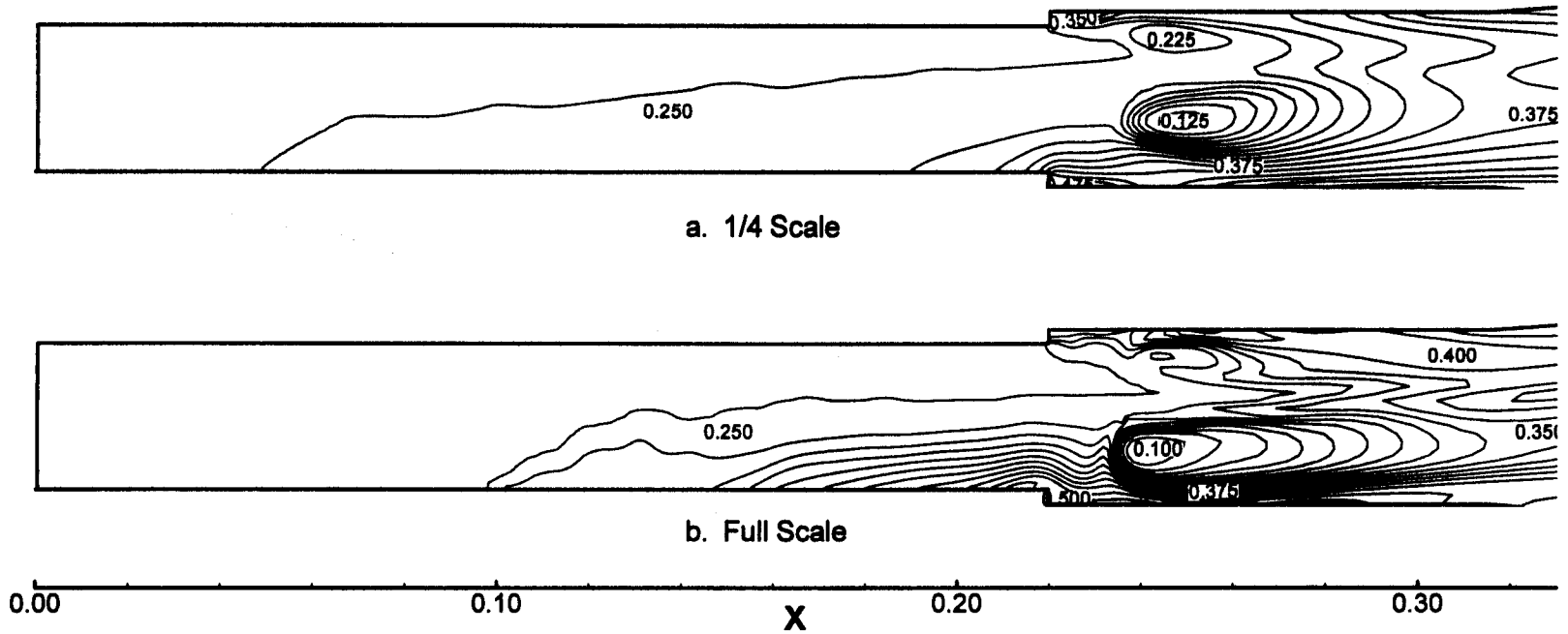

Figure 4.26 H_2O mass fraction contours.

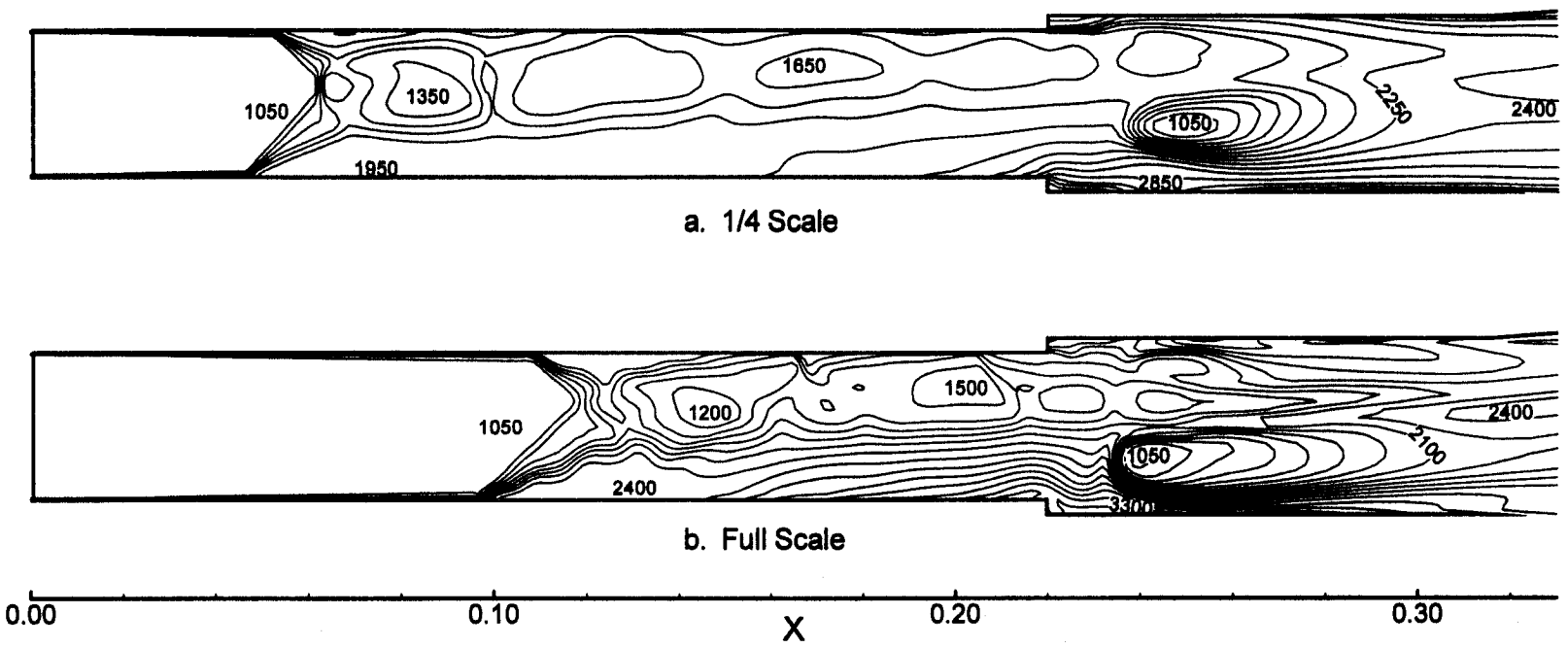

Figure 4.27 Static temperature contours (K).

upper wall no upstream transport occurs due to the proximity of supersonic core flow. However, compared with the full-scale model, the ¼ scale model produces more H_2O mass fraction upstream in the injector region. This is consistent with the larger amount of upstream interaction predicted by the sub-scale model. Static temperature is dependent of the local Mach number and combustion. As expected, the temperature is higher for the lower half of the isolator due to both effects. Temperature is also very high in the recirculation region behind the steps, which are effective flame holders.

Cross flow contours of the injectant mole fraction at three axial locations downstream of the step are shown in Fig. 4.28. The longitudinal locations of these planes are shown in Fig. 4.22. Hydrogen from the lower jets seems to penetrate further into the cross flow. The pronounced decrease in the mole fraction distribution near the upper wall downstream of the injection is due to a relatively low level of circulation and weaker vortices created by the asymmetric flow structure upstream of the injectors as shown in Fig. 4.29. This figure compares the cross flow velocity vectors plots at the same three positions downstream of the step. As expected the lower jets penetrate higher. These create significant blockage to the subsonic air flow, as shown in Fig. 4.30, and hence create large recirculation. A revealing feature apparent in both cases is the large size of the lower circulation bubbles and the small upper circulation bubbles. The development of asymmetric flow structure between the top and the bottom regions is not evident in the experimental data. Results obtained from the ¼ scale model are essentially identical to the results from the full-scale model.

Mach number at three locations downstream of the jets are shown in Fig. 4.30. Close to the jets the flow is primarily subsonic. In fact, at the injector station a very small supersonic core exists. This core flow rapidly expands by 0.25 m and 0.35 m. Also apparent is the supersonic core from the "sonic" injectors. Both sub-scale and full scale models show similar results.

A comparison of the solutions shows that most of the important features were well resolved for geometric scaled models. The extent of the upstream interaction is similar in each case. The numerical results for the two-dimensional full-height domain and the three-dimensional jet-to-jet symmetry show asymmetric flow-structures with

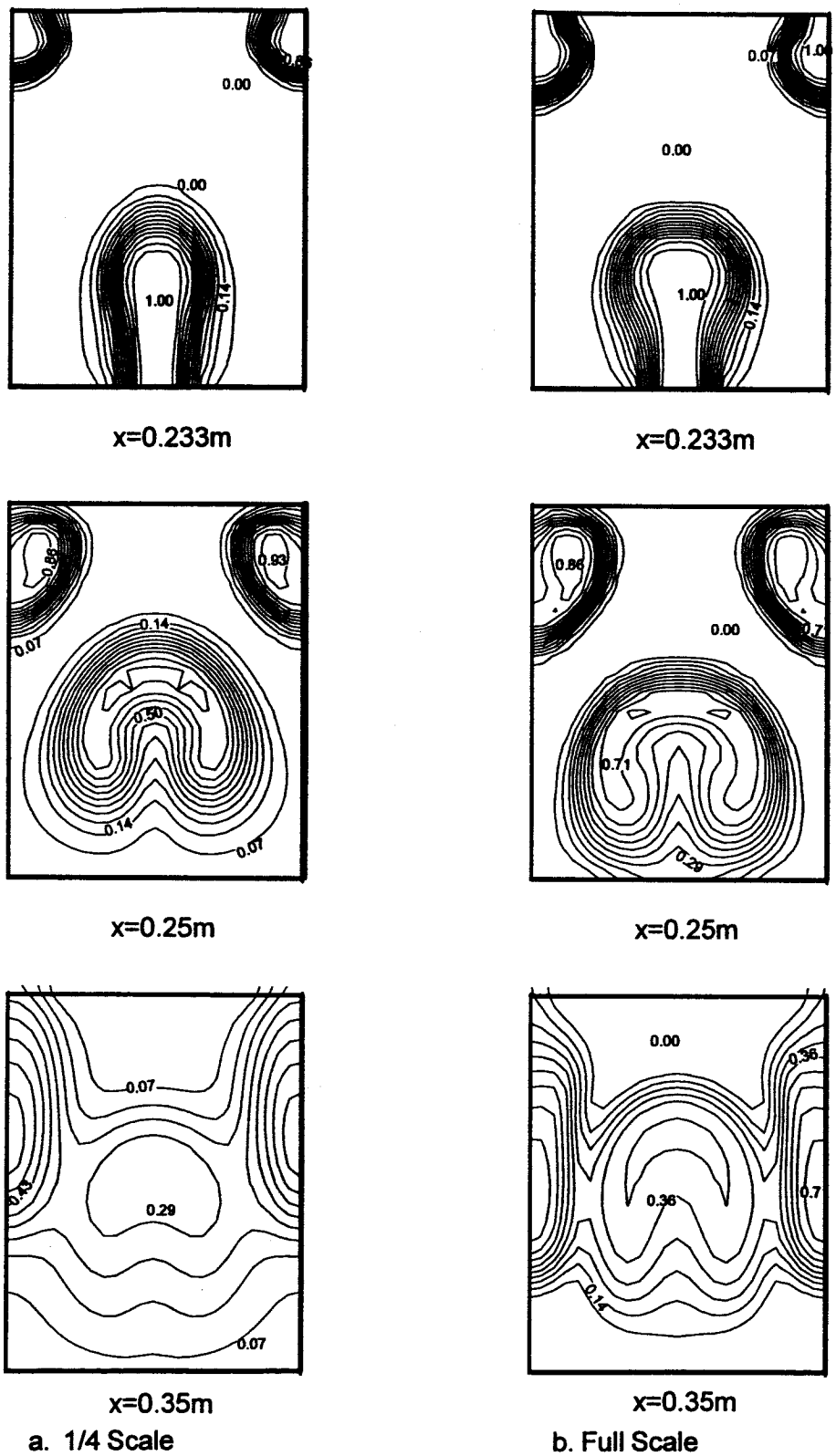

Figure 4.28 Injectant mole fraction contours at 3-axial locations.

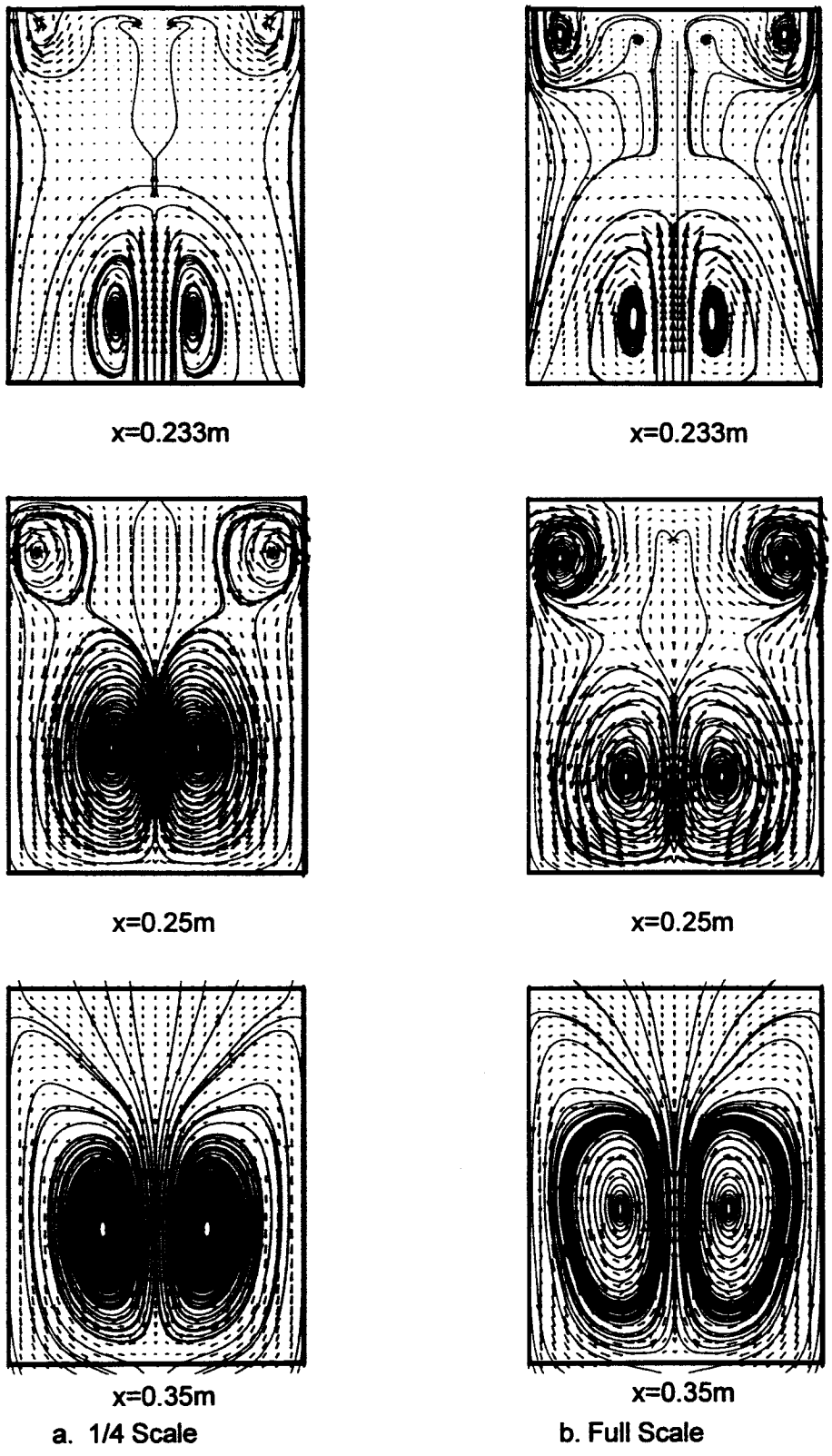

Figure 4.29 Cross-flow velocity vectors at 3-axial locations.

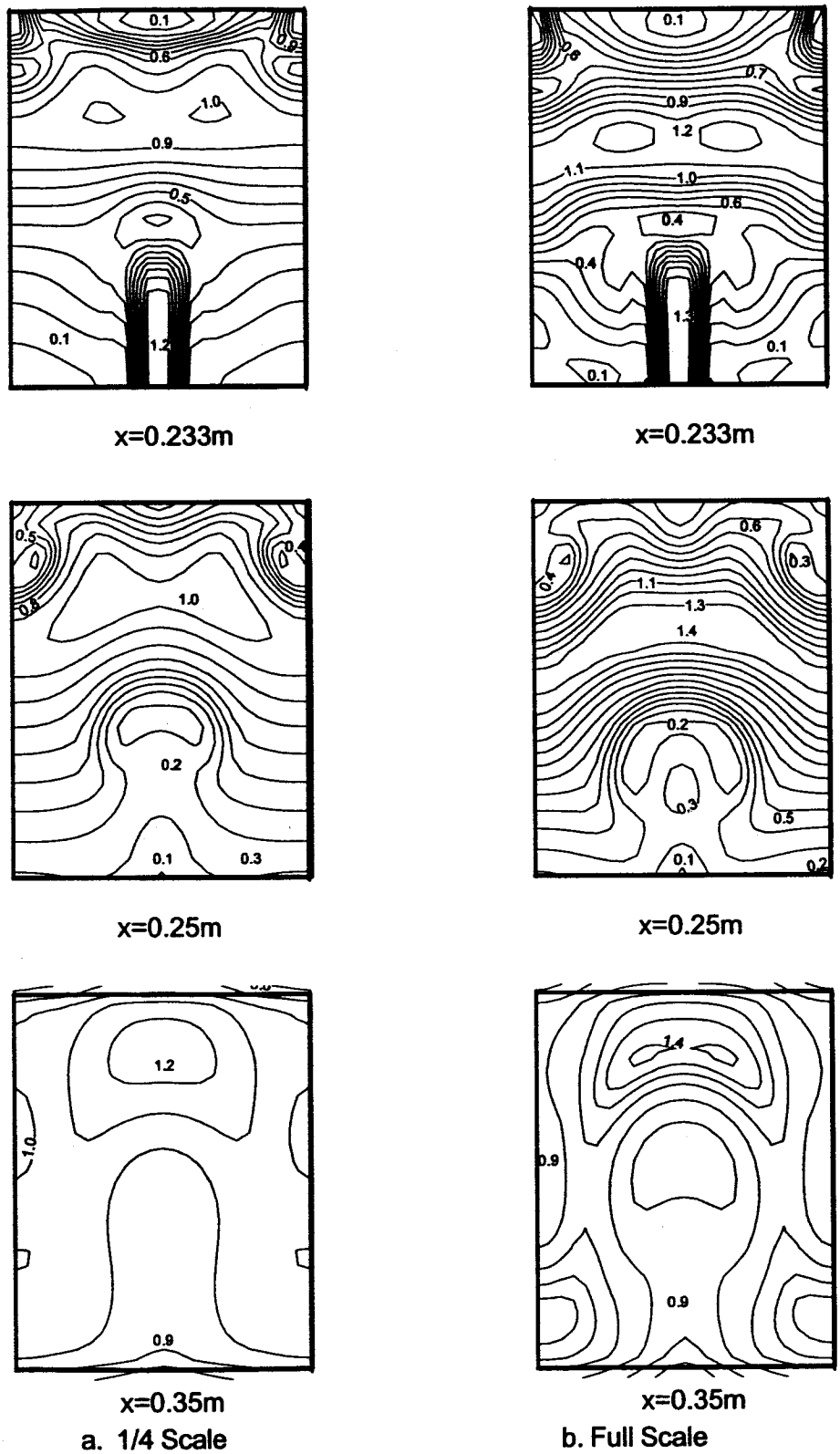

Figure 4.30 Mach number contours at 3-axial locations.

larger separation zone on one wall extending further upstream of the step. The numerical results are remarkably unaffected by geometrical scaling of the computational domain for the conditions employed. Since the large pressure rise due to combustion dominates the flow, it is not surprising that a scaled model captures the flow field well. The results clearly show that the transient development of the upstream interaction region increases significantly and develops rapidly in such a sub-scale model. This study supports the argument that numerical scaling is useful in simulating dual-mode scramjet combustor flow-fields. The scaled results could be interpolated into a full-scale solution to accelerate convergence. Because the upstream interaction moves upstream during development, it is not necessary to have a fully converged solution before passing to the larger scale.

4.4 Breakdown of Symmetric Assumption

Numerical results for a simplified dual-mode scramjet combustor configuration with significant upstream interaction are presented and discussed in this section. In the previous section asymmetric results were observed. In order to understand this asymmetric phenomenon, additional studies were made. The change in the flow field from a symmetric solution to an asymmetric solution is investigated. Numerical results for two-dimensional model and a three-dimensional simplified jet-to-jet geometry are presented and discussed.

4.5 Two-Dimensional - Full-Height Domain

The two-dimensional model was based on the JNAL scramjet combustor. The geometry was simplified to have one upper and one lower jet (slot diameter was calculated to maintain the fuel to air ratio of the original three-dimensional combustor). A schematic of this combustor configuration is shown is Figure 4.11. To encourage upstream interaction a lower total pressure and static pressure for the freestream vitiated air was used. The boundary conditions are given in Table 4.2. Results presented in this section were obtained using a coarse unstructured grid consisting of 30,000 triangular

cells. The computational grid around steps and jet injection is shown in Fig. 4.12.

The Mach number contour plots are given in Fig. 4.31. Figure 4.31a shows well-developed characteristics of the flow. The flow is nearly symmetric with some upstream interaction. Leeward of the Mach disk a recompression shock is observed. Figure 4.31b shows that as the number of iterations increases, the flow still has significant upstream interaction and is relatively symmetric. However, main characteristics of the flow such as the recompression shock are no longer clearly visible. Finally after 49,000 iterations (Fig 4.31c) the solution is asymmetric. There exists a large separated region of subsonic flow on the bottom wall and a very small region on the upper wall. Also, downstream of the jets the solution does not have such clearly defined characteristics. Finally, after more iterations, the flow appears to become symmetric again with little upstream interaction. This result is shown in Fig. 4.31d. Further iterations show the flow pushes upstream again and becomes asymmetric. The asymmetry appears to be random with the larger separation region occurring on either wall. This contour plot also shows the impact of the upstream flow separation on fuel penetration.

Figure 4.32 compares the normalized static pressure contours around the injection at different numbers of iterations. The pressure is normalized by the free-stream static pressure. In Fig. 4.32a, the flow is symmetric with only a little upstream interaction. After many more iterations the flow completely becomes asymmetric, then symmetric again. The pressure in the combustion region appears to be higher for larger upstream interaction, supporting the idea that the pressure rise due to combustion dominates the flow field and is responsible for the upstream interaction. Velocity vectors and streamlines are shown in Fig. 4.33. Upstream recirculation areas as well as recirculation around the jets are clearly visible in these plots.

Figures 4.34 through 4.36 show H_2O mole fraction, H_2 mole fraction and temperature contours plots. In all cases, it is apparent that the recirculation region ahead of the jet convects hydrogen upstream. Here, combustion produces water that is readily dispersed leeward.

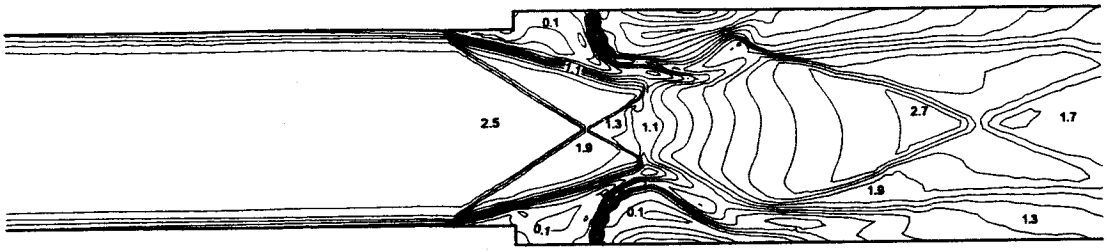

a. 6,000 iterations

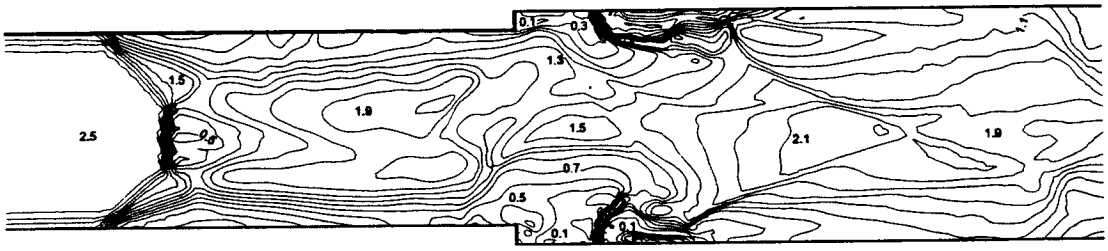

b. 9,700 iterations

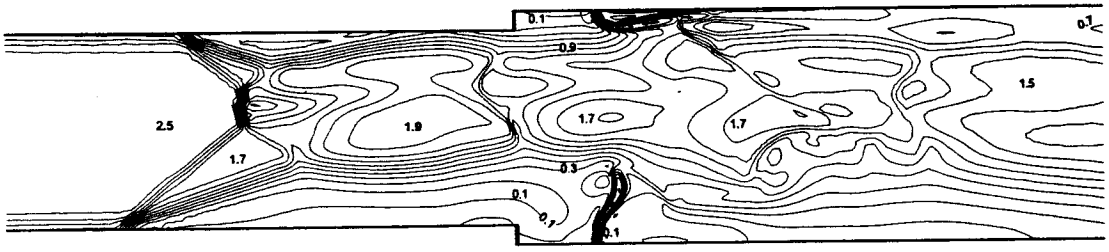

c. 49,000 iterations

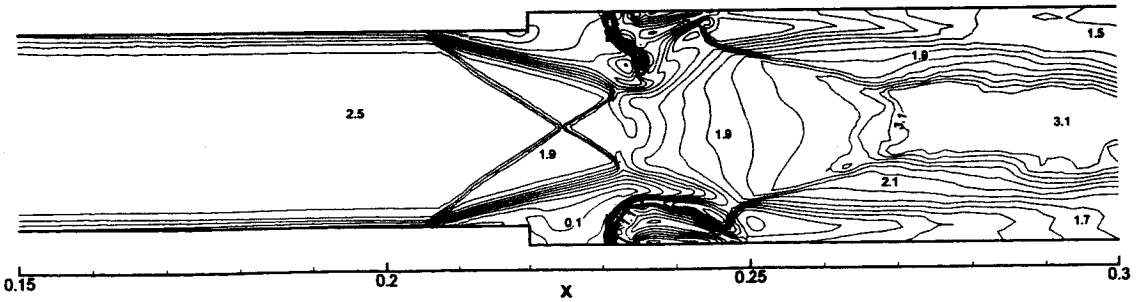

d. 83,000 iterations

Figure 4.31 Mach number contours.

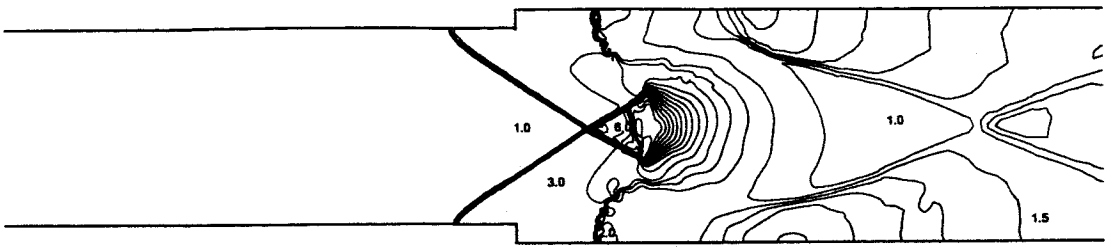

a. 6,000 iterations

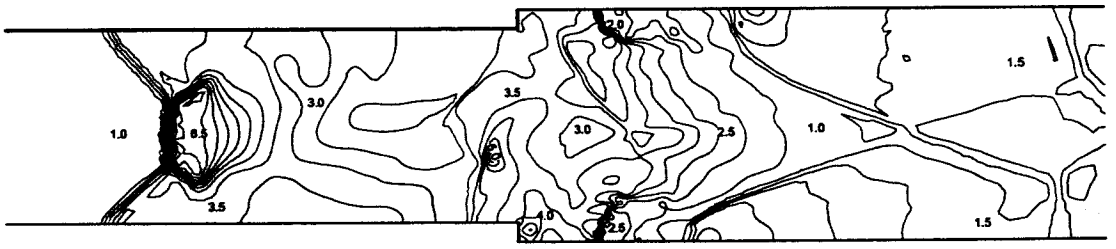

b. 9,700 iterations

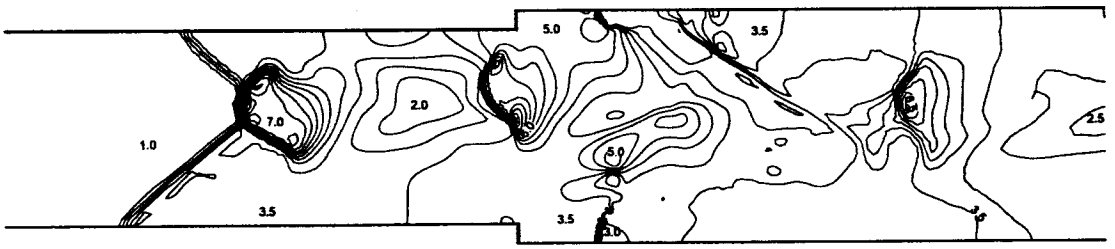

c. 49,000 iterations

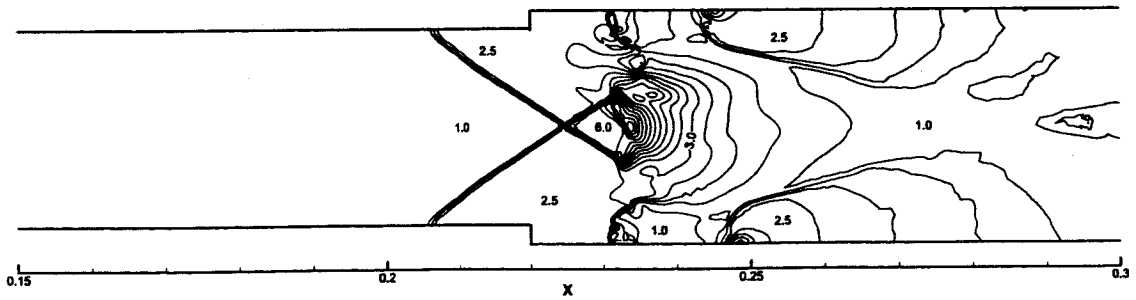

d. 83,000 iterations

Figure 4.32 Pressure contours.

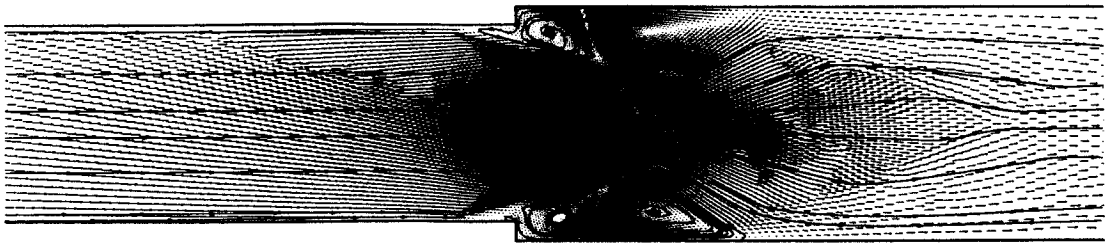

a. 6,000 iterations

b. 9,700 iterations

c. 49,000 iterations

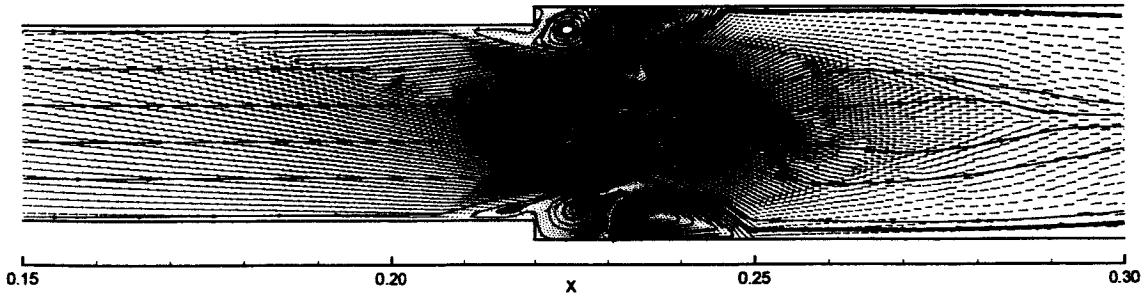

d. 83,000 iterations

Figure 4.33 Velocity vectors and streamlines.

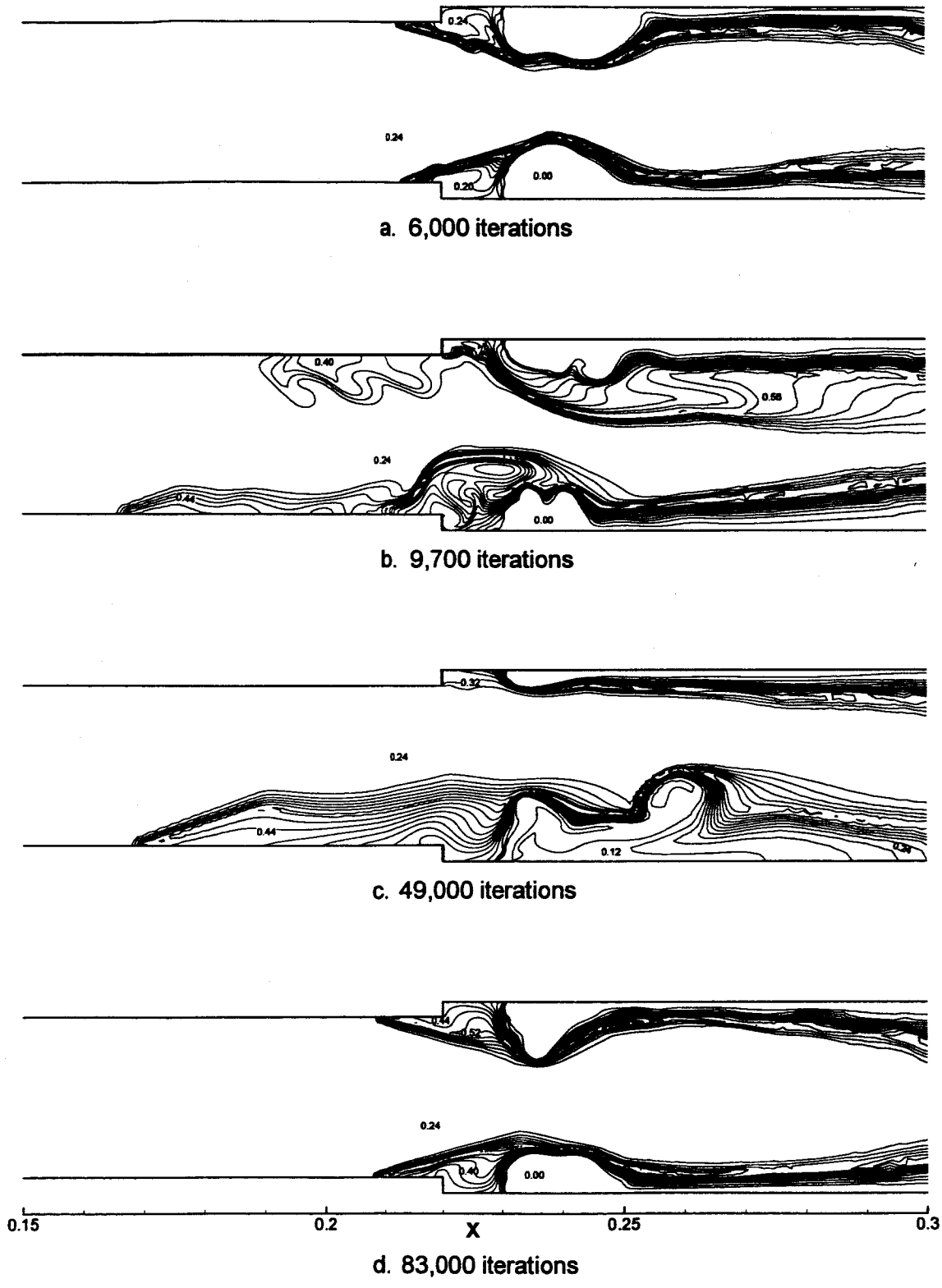

Figure 4.34 H_2O mole fraction contours.

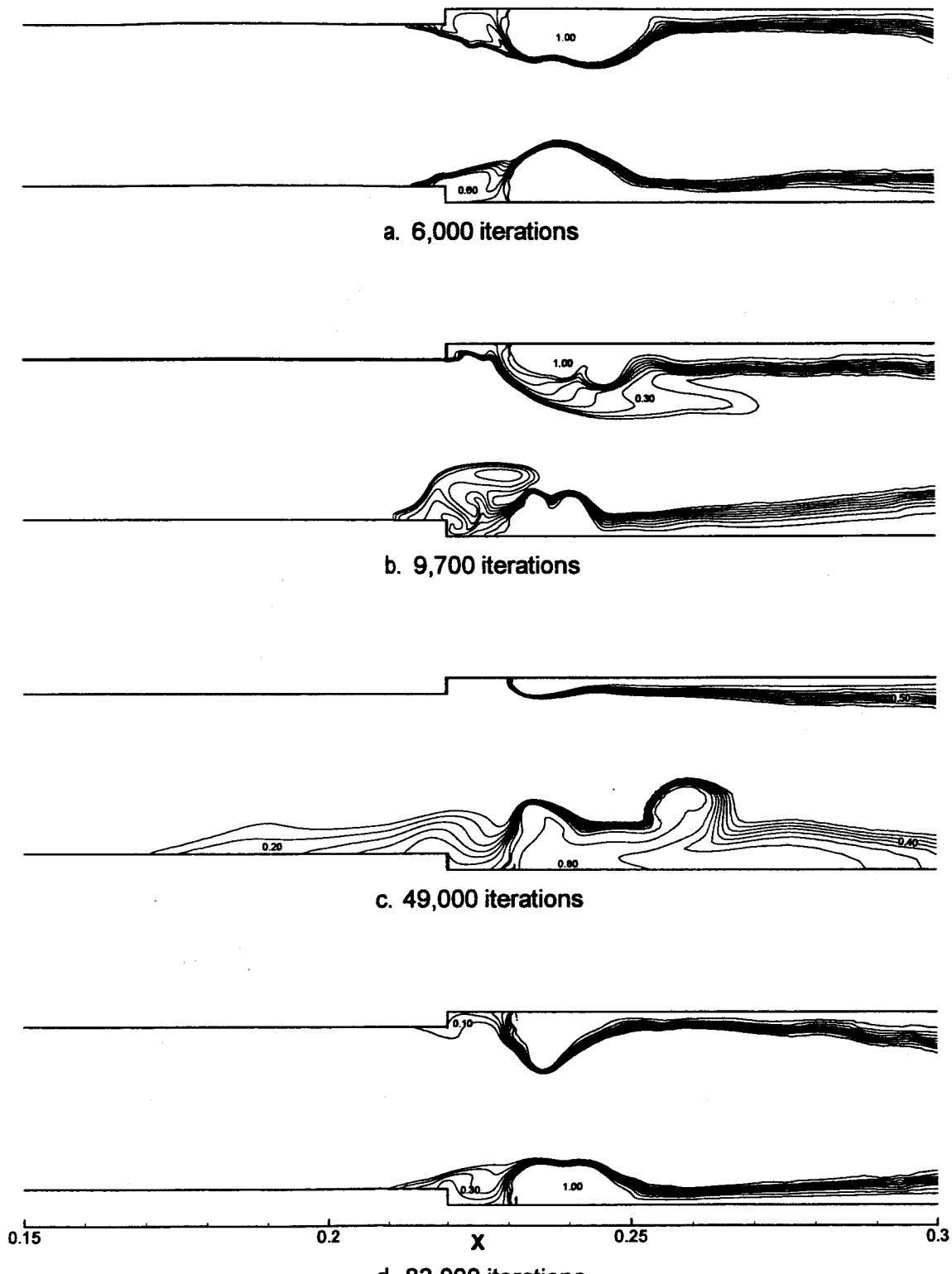

Figure 4.35 H_2 mole fraction contours.

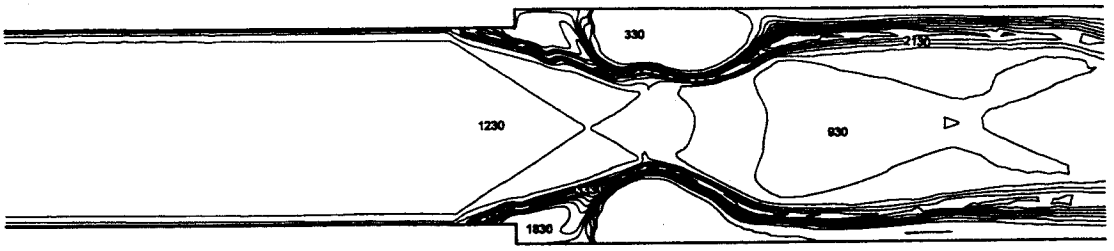

a. 6,000 iterations

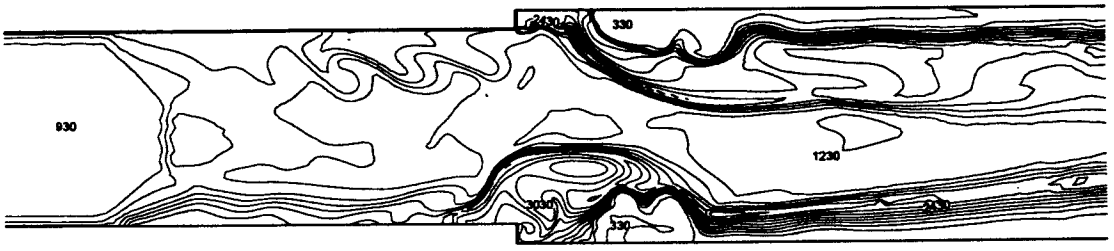

b. 9,700 iterations

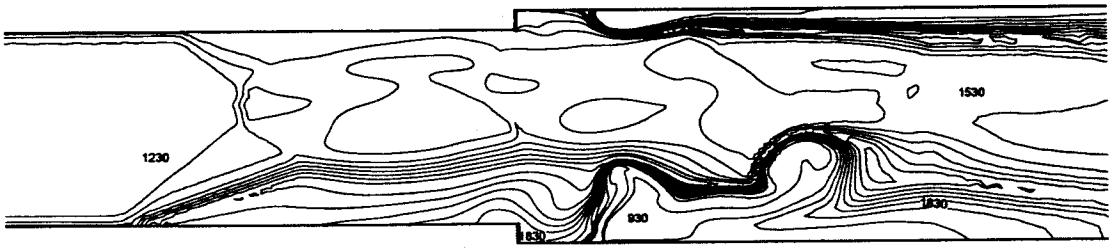

c. 49,000 iterations

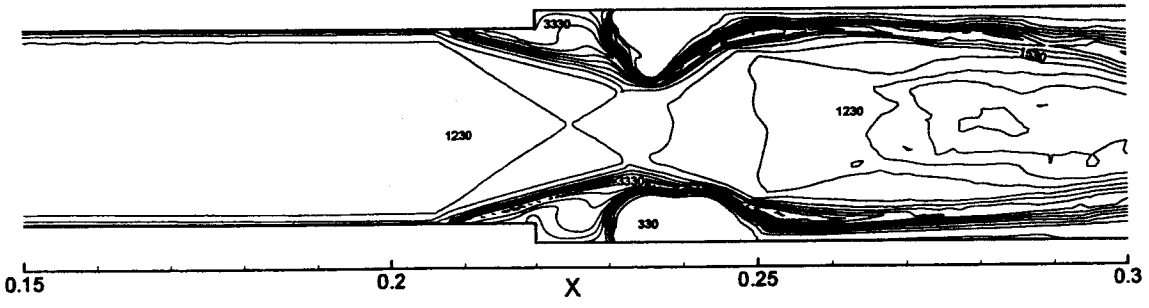

d. 83,000 iterations

Figure 4.36 Temperature contours.

4.6 Three-Dimensional Jet-to-Jet Symmetric Model

As shown in Fig. 4.21, the computational domain was simplified to encompass half of the upper and half of the lower jet using the symmetry condition. Results presented in this section were obtained using a relatively coarse unstructured hexahedral grid consisting of 86,000 cells. Grid refinement was tested using a finer grid but qualitatively no significant differences in the overall flow structures were observed.

Mesh cells were concentrated around the walls, particularly in the region of the steps and jets. Numerical results from the present study are not fully converged solutions. While the residuals are O [10^{-3}], the solution appears to be transient. The results shown are at intermediate steps.

The Mach number contour plots, given in Figs. 4.37 and 4.38, are shown at the lower fuel jet, centerline between the upper and lower fuel jets, and at the upper fuel jet respectively. The contour plots are from 9,600 iterations and 30,000 iterations. The pressure rise due to the heat released by combustion is so large that shock waves are generated upstream of the steps and the core flow is decelerated and then accelerated again to supersonic in the expansion region. The resulting flow is symmetric and the extent of the upstream interaction is about 1.5 isolator heights. Note that for this solution the "supersonic core" flows over both jets, and through the center of the duct on the centerline between the jets. Another interesting phenomena shown here is the appearance of a normal shock in the "core" flow near the injector.

As the flowfield continues to develop, the degree of upstream interaction significantly increases and the resulting flowfield is not symmetric. Figure 4.38 shows that the lower separation region is much larger than the upper one and the overall upstream interaction has dramatically increased. This asymmetrical flow is characterized by the uniform core flow which is uniformly lifted over the solution domain at the injector station. Downstream of the injector station the "core" returns to the symmetric behavior as it expands rapidly downward between the lower jets, continues upward between the upper jets, and remains slightly above the vertical centerline of the solution plane between the fuel injectors.

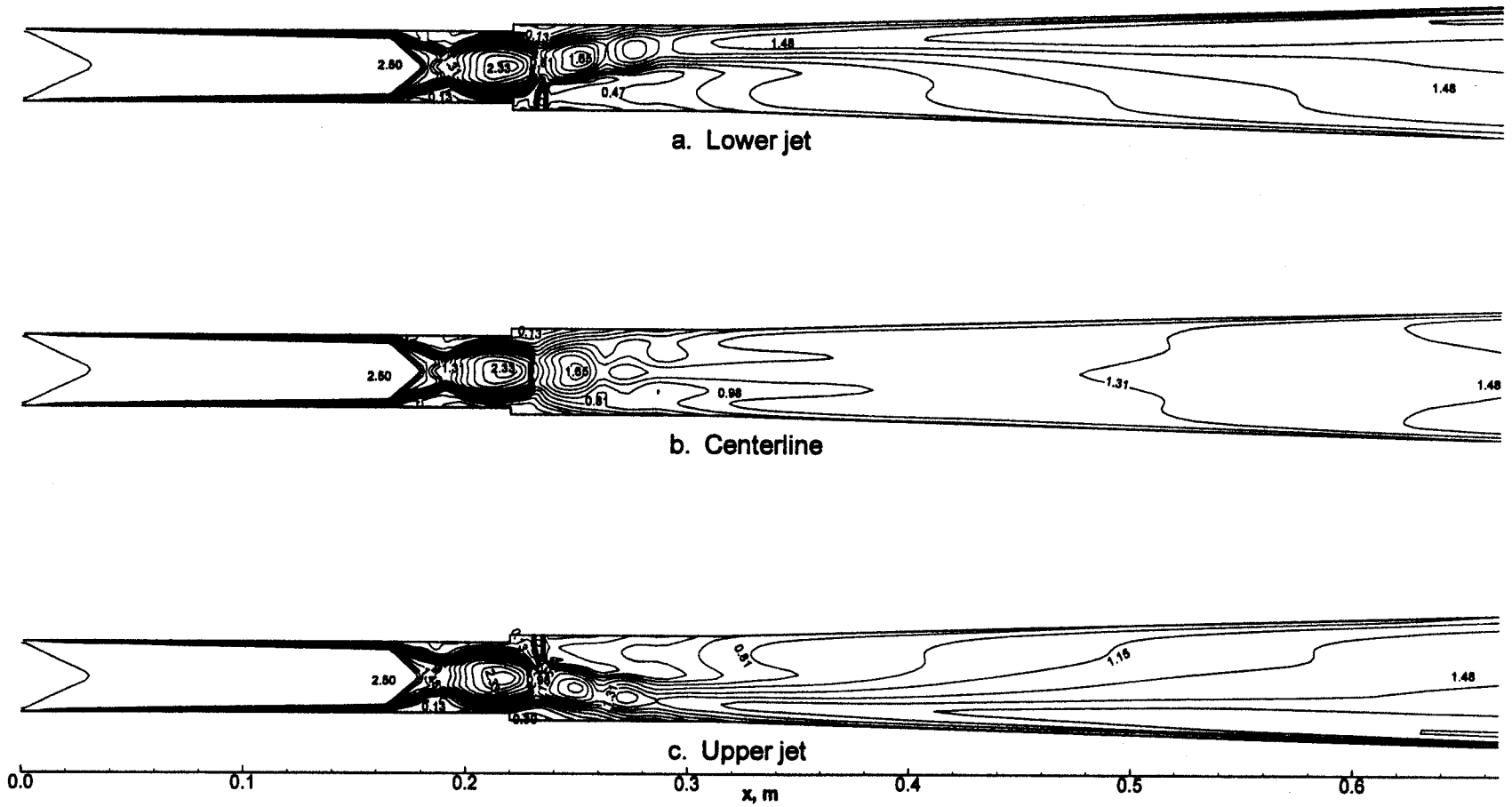

Figure 4.37 Mach number contours after 9,600 iterations. (3-D coarse grid)

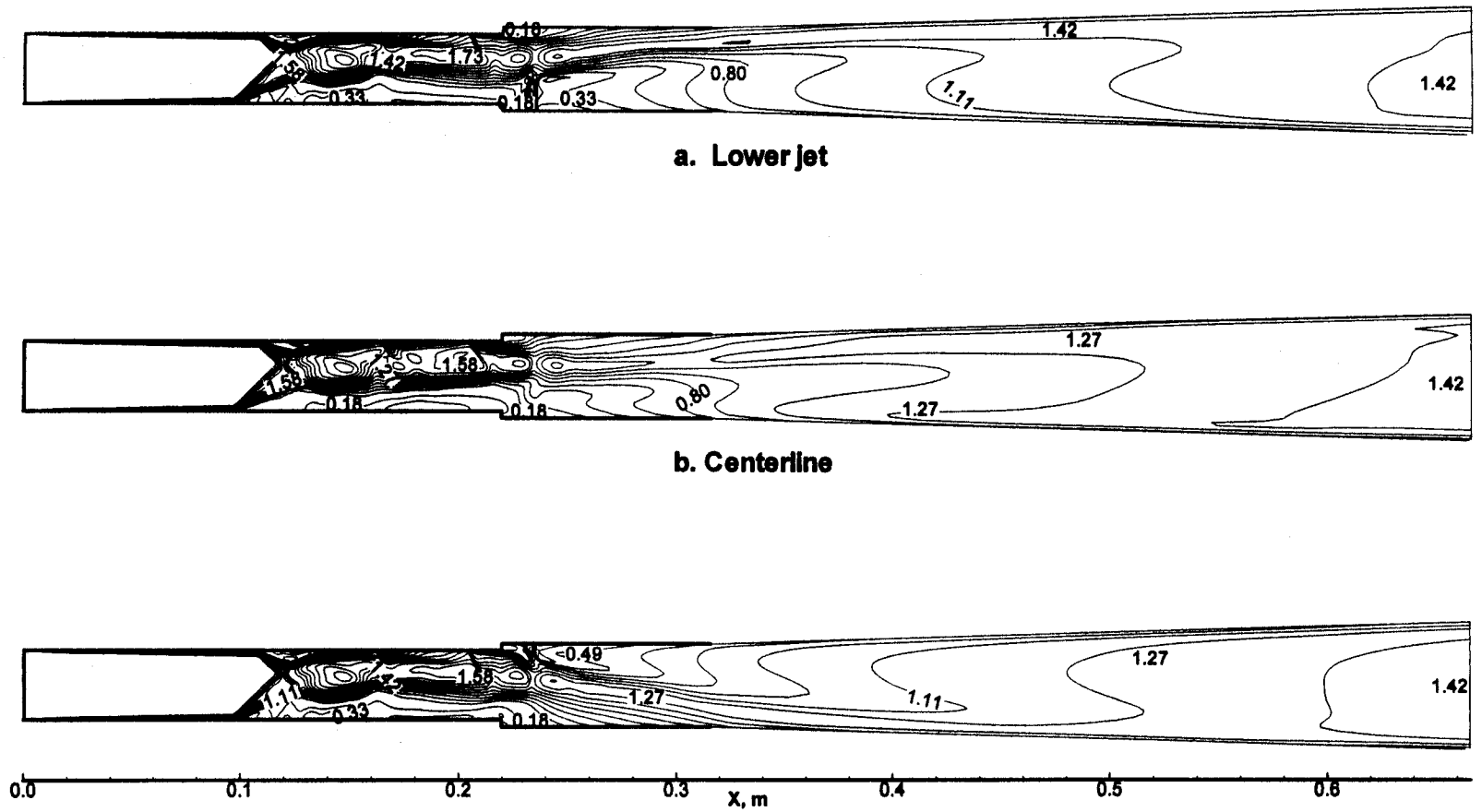

Figure 4.38 Mach number contours after 30,000 iterations.

Wall static pressure distribution along the centerline between upper and lower jets (for asymmetric results both walls and for symmetric results lower wall) is shown in Fig. 4.39. The asymmetric results show fairly good agreement with experimental results of Ref. 13. The lower wall shows a relatively smooth solution, while the upper wall seems to oscillate around the experimental results. A comparison shows that most of the important features were well resolved. The extent of the upstream interaction is close to the experimental values and the peak wall pressure is slightly under-predicted. The impact of the shock-train on the upper wall is also apparent. Some discrepancies are noted due to the facts that a simplified geometry is used, boundary conditions are assumed to be uniform, and a simple 1-step chemistry model is employed. Similar numerical results using a similar computational domain were reported by Ref. 16. The lower wall pressure distribution for the symmetric results reports lower pressure throughout the domain and much less upstream interaction. This finding is consistent with the belief that the pressure increase due to combustion is responsible for the upstream interaction.

Velocity vectors and streamline plots are shown in Fig. 4.40. This figure shows clearly the change in the flow structure from symmetric flow with smaller upstream interaction (at the intermediate step) to asymmetric flow with bigger upstream interaction and larger circulation bubble at lower wall when the flow continues to develop with iterations.

Figures 4.41-4.43 show static pressure, H_2O mass fraction, and temperature contours at the centerline between the fuel jets. It is seen that the recirculation region ahead of the jet convects hydrogen upstream and water is rapidly produced by the combustion near the injection and diffused in the leeward.

Figure 4.44 shows cross flow velocity vector plots at three positions downstream of the step. Close to the jets the flow is primarily subsonic. At the expansion region downstream of the jets the flow is accelerated. A revealing feature in these plots is the increased size of the lower circulation bubbles and the decreased size of the upper circulation bubbles as the flow continues to develop. This can be attributed to the asymmetric flow developed upstream of the injection. As discussed earlier, the

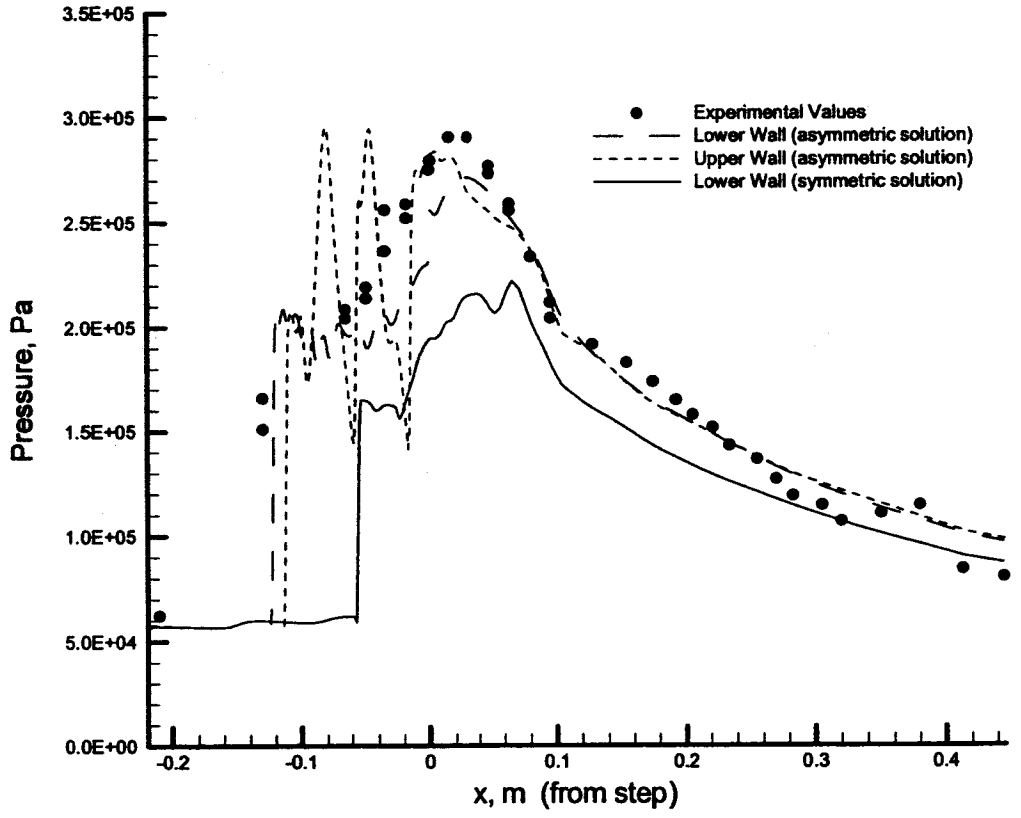

Figure 4.39 Wall static pressure distribution.

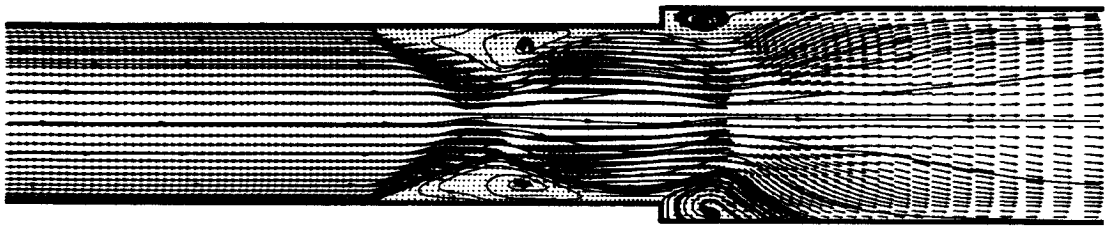

a. Symmetric

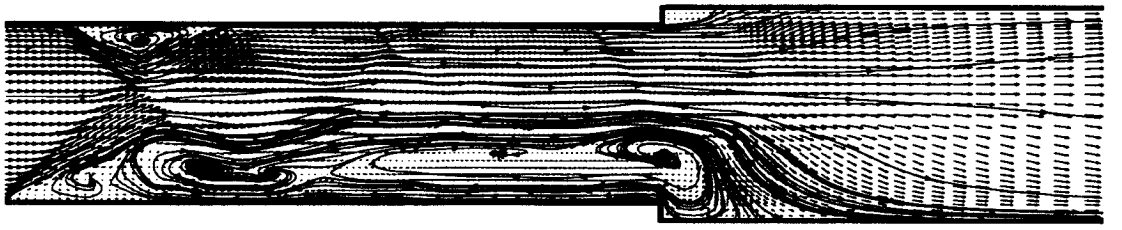

b. Non-symmetric

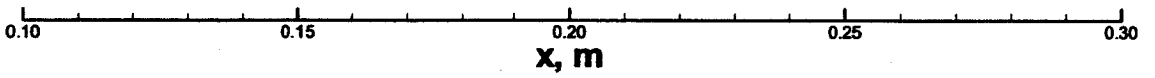

Figure 4.40 Velocity vectors and streamlines.

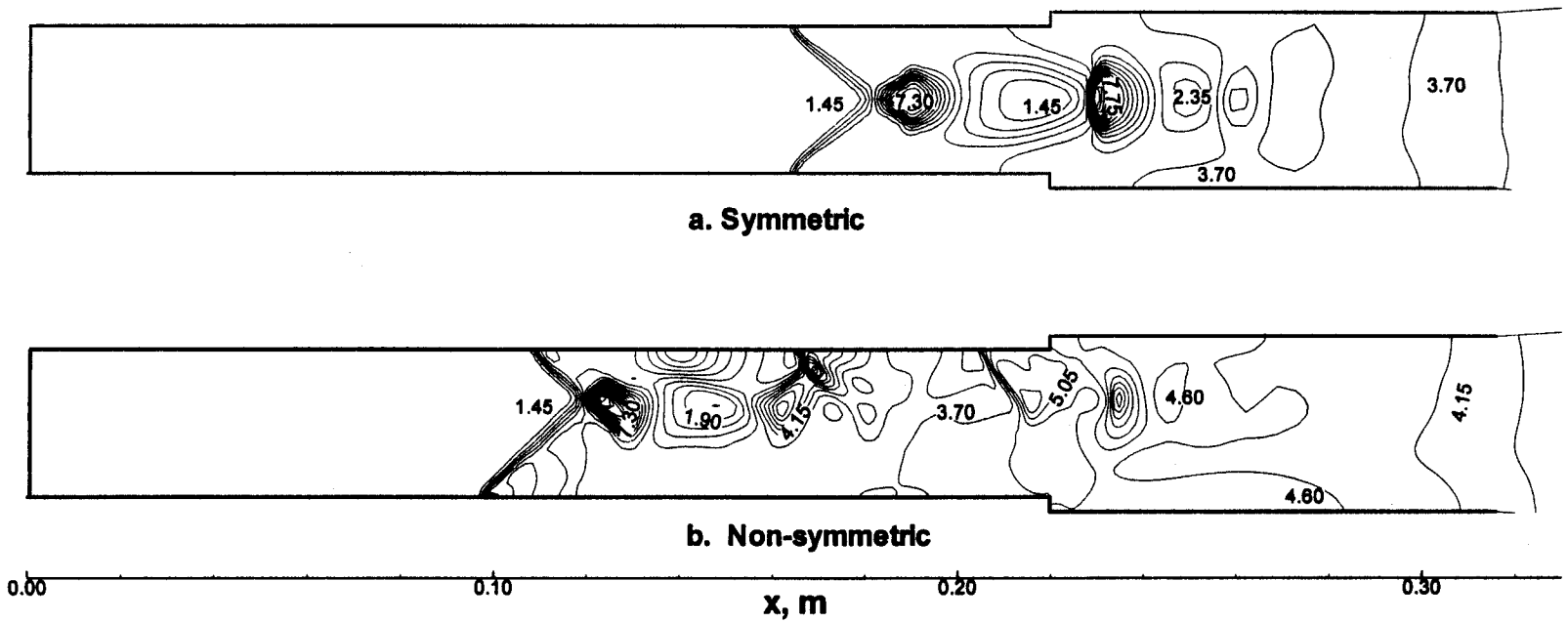

Figure 4.41 Static pressure contours.

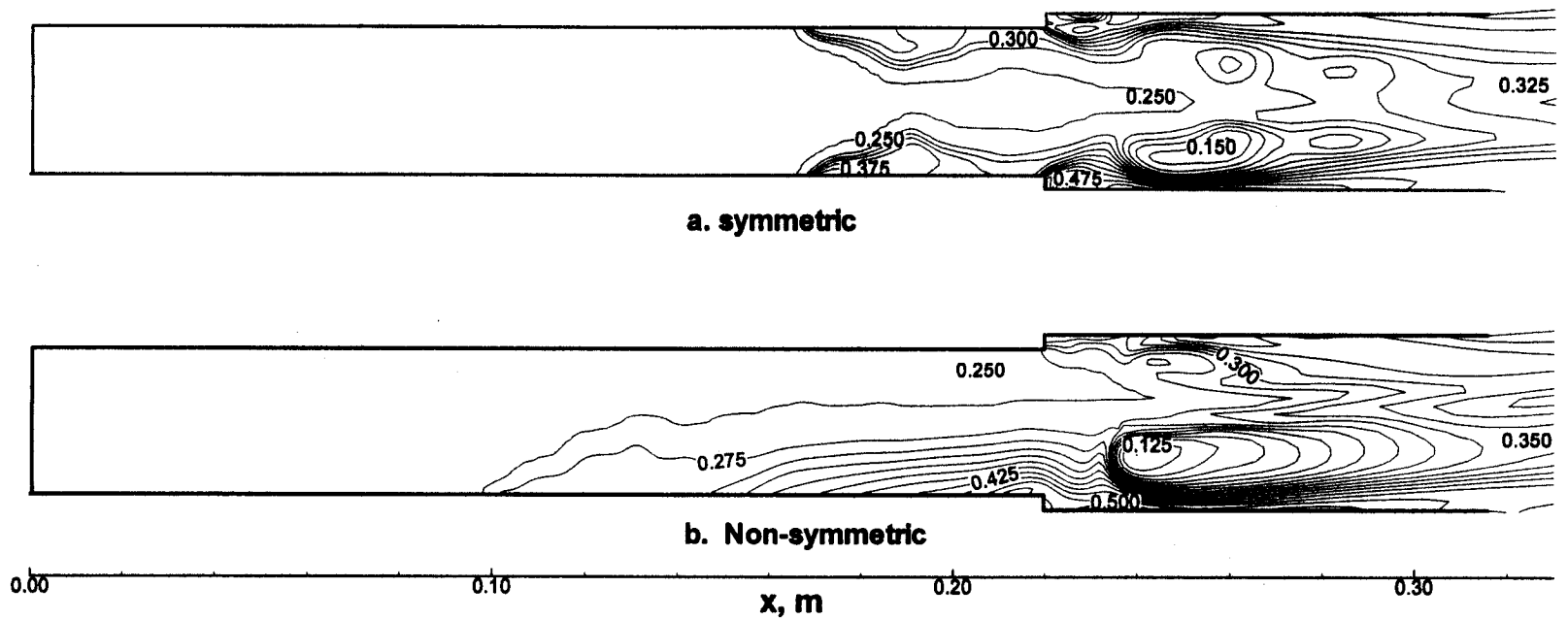

Figure 4.42 H_2O mass fraction contours.

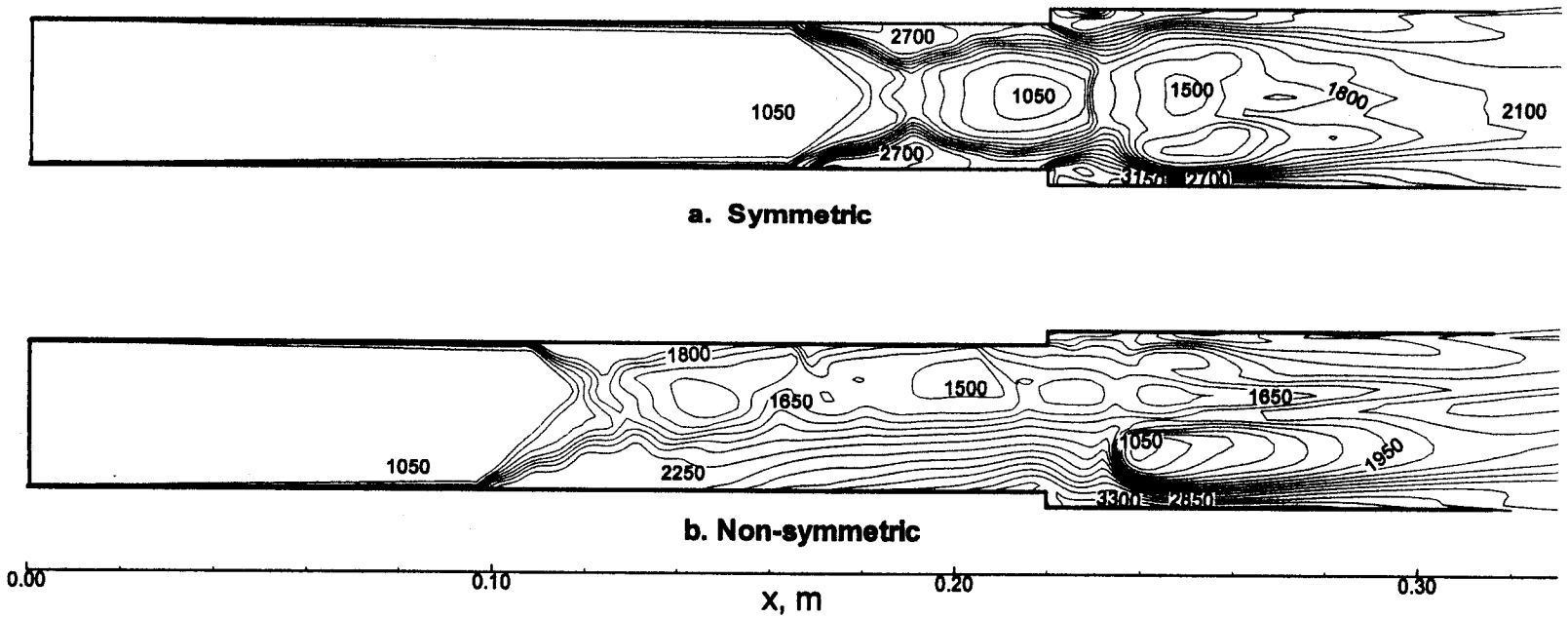

Figure 4.43 Static temperature contours.

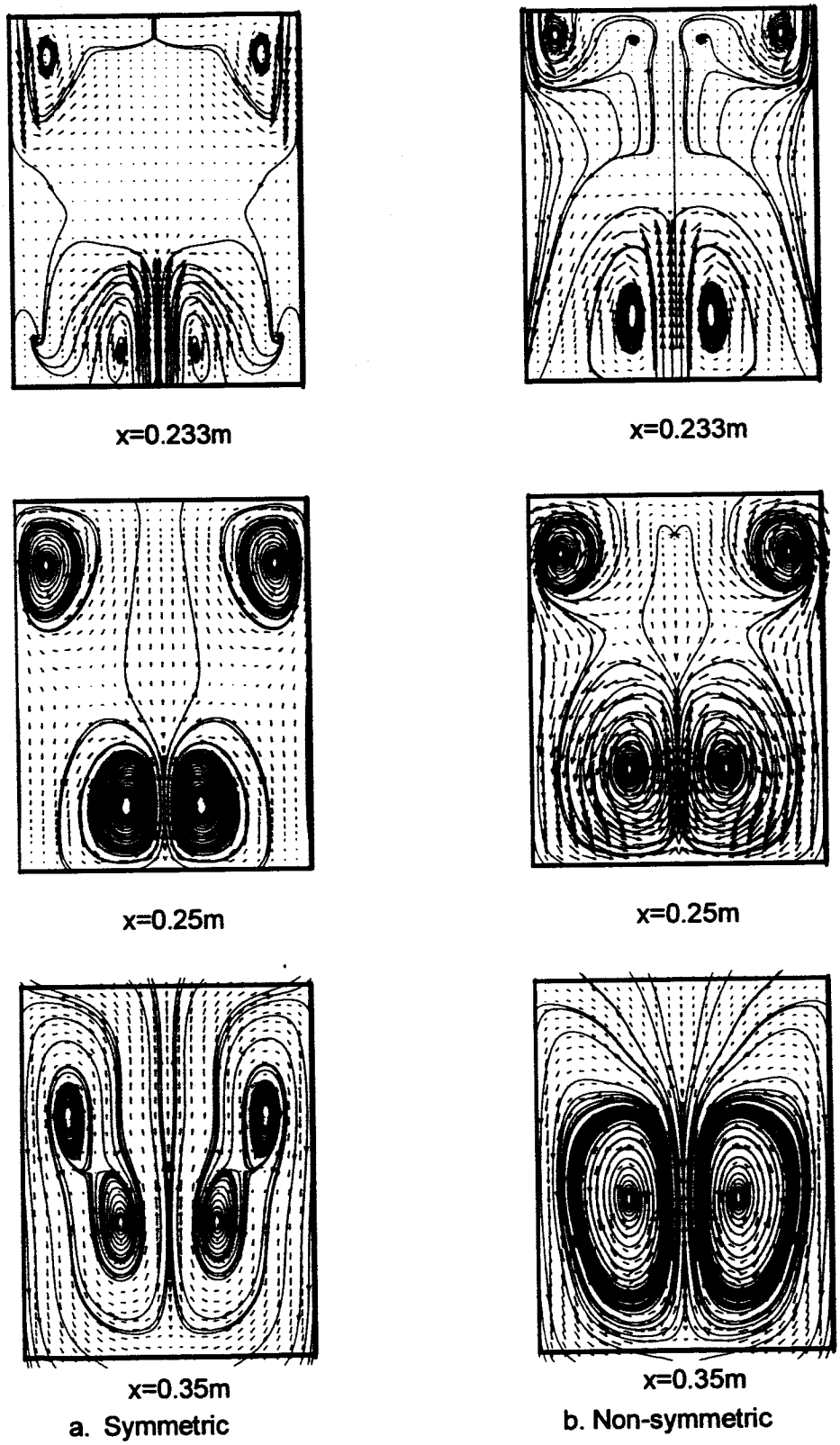

Figure 4.44 Cross-flow velocity vectors at 3-axial locations.

development of asymmetric flow structure between the top and the bottom regions is not evident in the experimental data. Figures 4.45 and 4.46 focus on the flow field downstream of the steps for the asymmetric case, showing velocity vectors with streamlines and vorticity contour plots, respectively. These figures show how the separate vortices merge together to form a large vortex pair and the magnitude of vorticity dissipates further from jet.

Cross flow contours of the injectant mole fraction, H_2O mole fraction, Mach number, and temperature at three locations downstream of the jets are shown in Figs. 4.47 to 4.50. Greater fuel penetration of the lower jet and better mixing in the lower region is apparent when comparing the symmetric and asymmetric results. The pronounced decrease in the mole fraction distribution near the upper wall downstream of the injection is due to a relatively low level of circulation and weaker vortices downstream of the injection.

While investigating geometric scaling of this dual mode combustor, an asymmetric result was found, when a symmetric result was expected. Asymmetry was observed as a large recirculation region upstream present on only one wall. This asymmetric flow structure is not seen in the experimental data. The breakdown of the symmetric assumption became a focus of this numerical study.

A comparison of the intermediate flowfield solutions yields the deterioration of the symmetry assumption, as the extent of upstream interaction increases. The steady state "solutions" appear to be periodic. With further iterations, the large separation bubble oscillates from one wall to the other. Also, note that the static wall pressure distributions oscillate around the experimental results.

Numerous studies have shown that flow in a symmetric sudden expansion duct may be asymmetrical. The cause of this instability is yet unknown. It has been proposed that the asymmetries in the recirculation region downstream of the sudden expansion are related to shear layers and to coherent flow structures embedded in the random velocity fluctuations. In this dual-mode combustor, asymmetries are likely to be caused by the same phenomenon. The initial perturbation may occur downstream and be carried

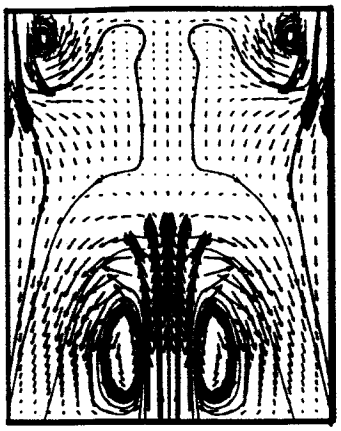

x=0.233m

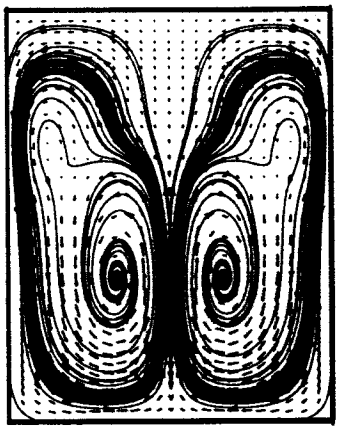

x=0.3m

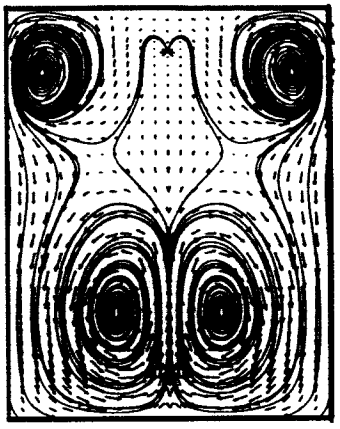

x=0.25m

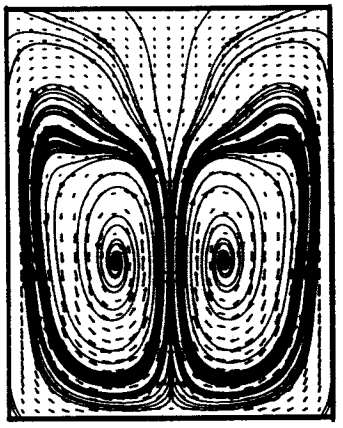

x=0.32m

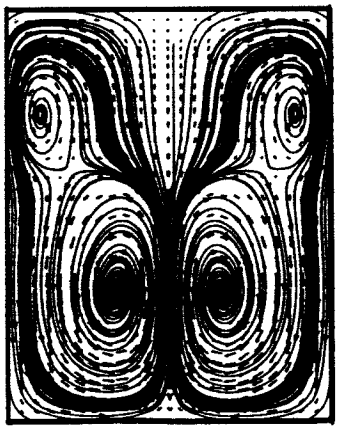

x=0.28m

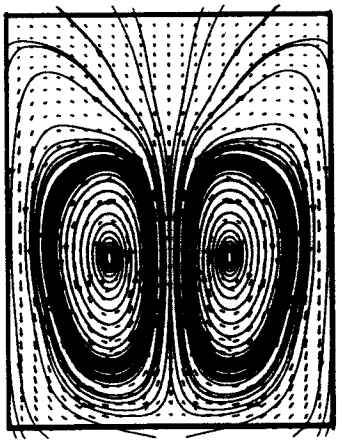

x=0.35m

Figure 4.45 Velocity vectors and streamlines at 6-axial locations.

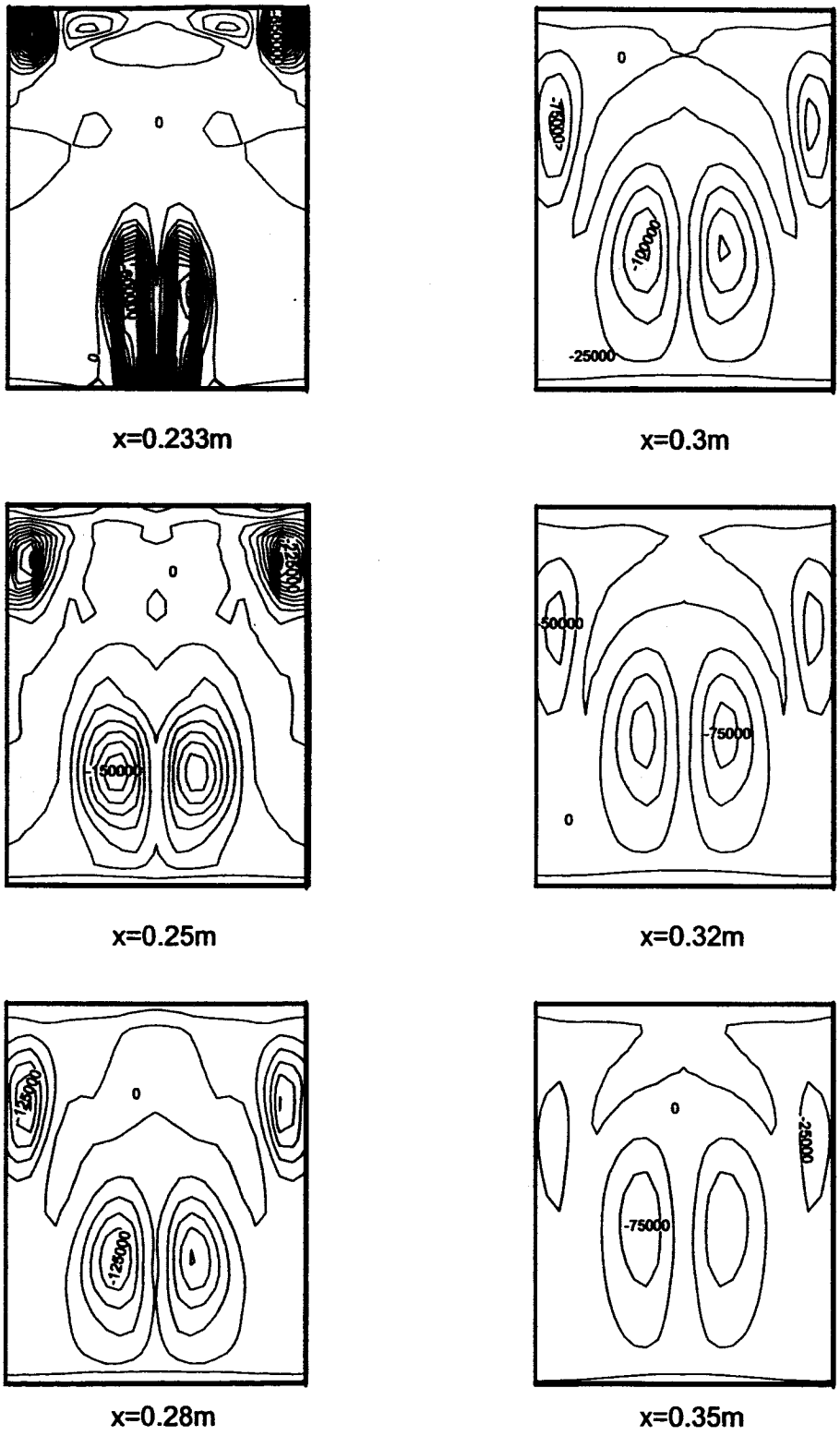

Figure 4.46 Axial vorticity contours at 6-axial locations.

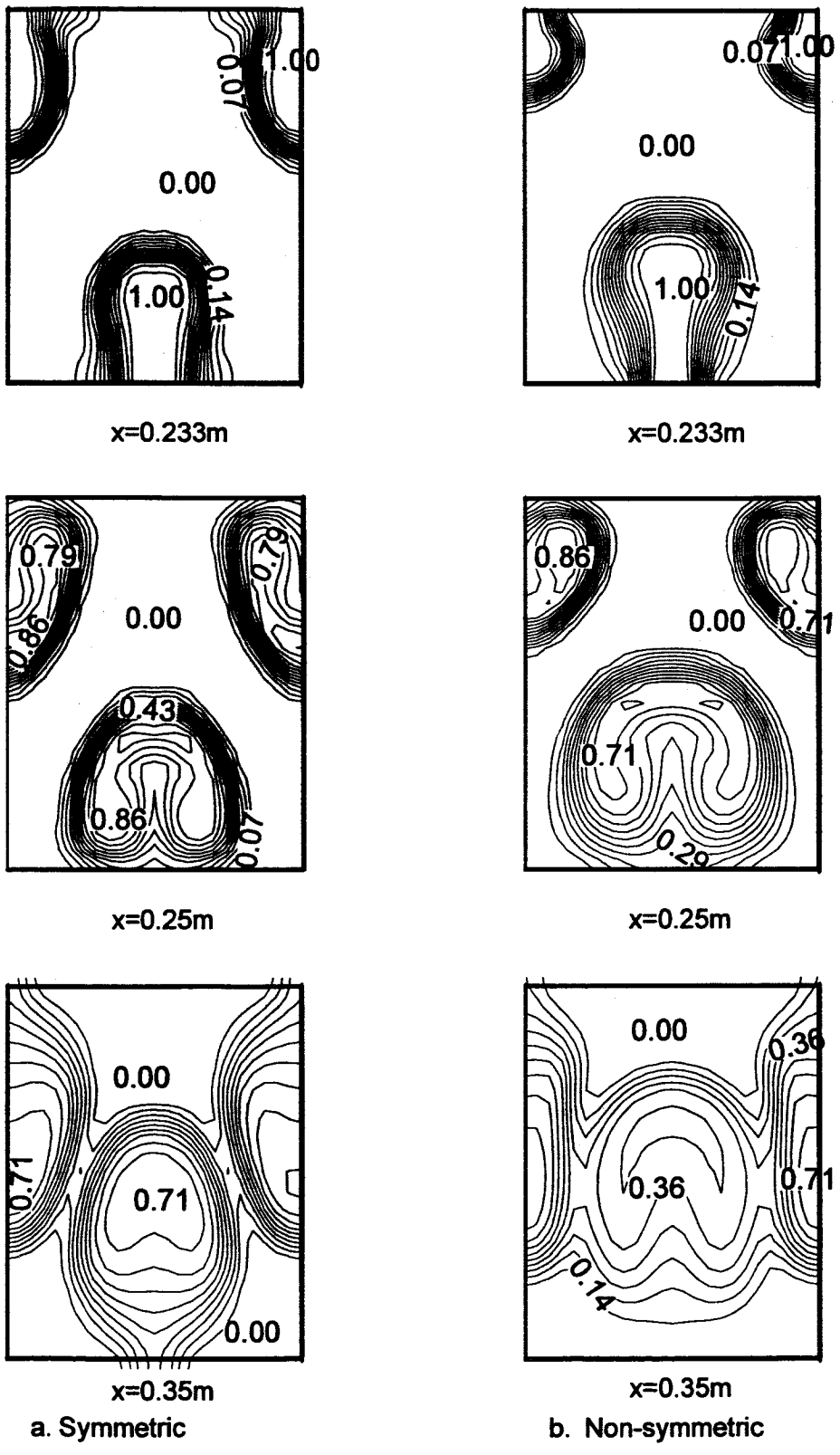

Figure 4.47 Injectant mole fraction contours at 3-axial locations.

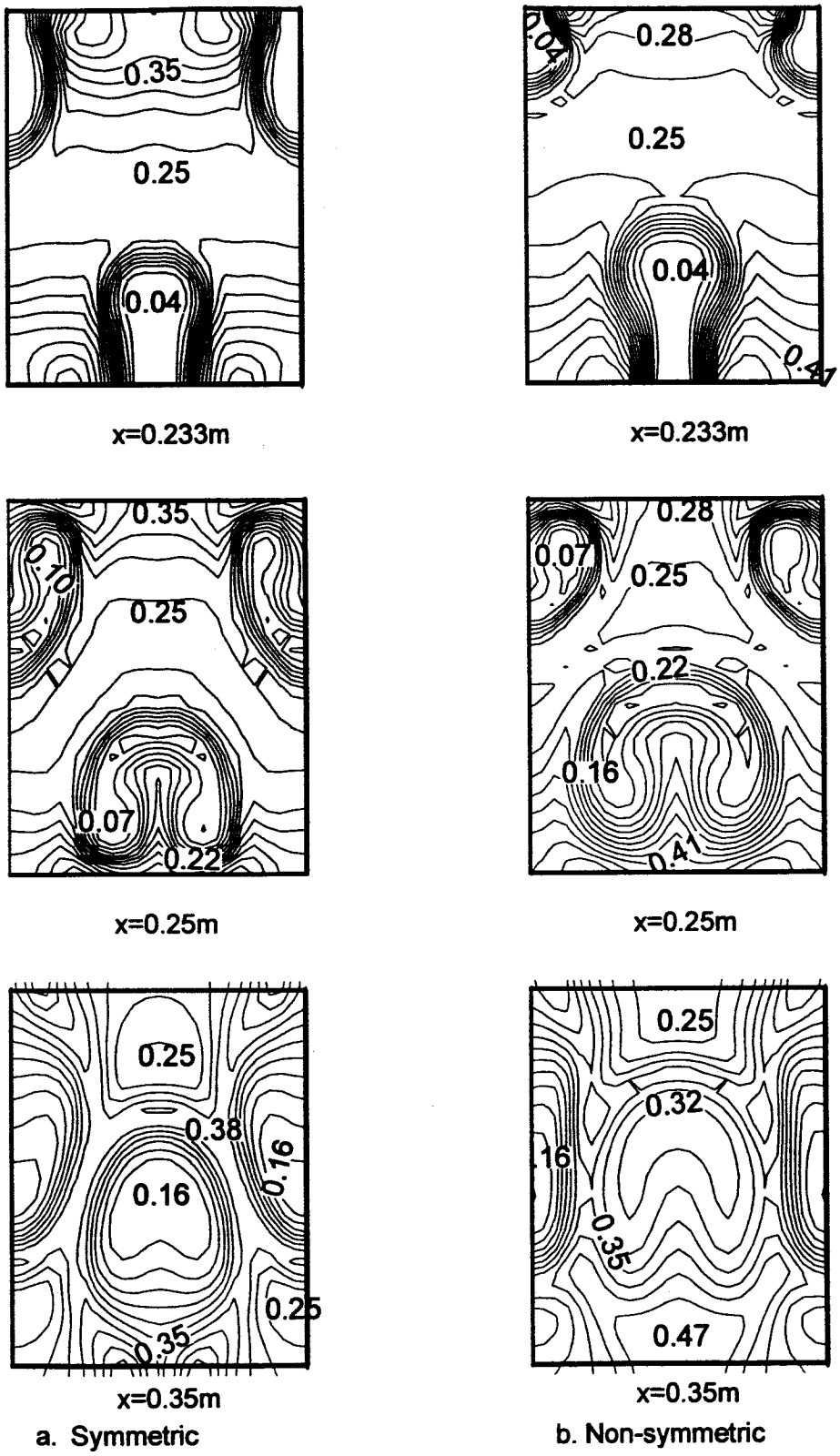

Figure 4.48 H_2O mole fraction contours at 3-axial locations.

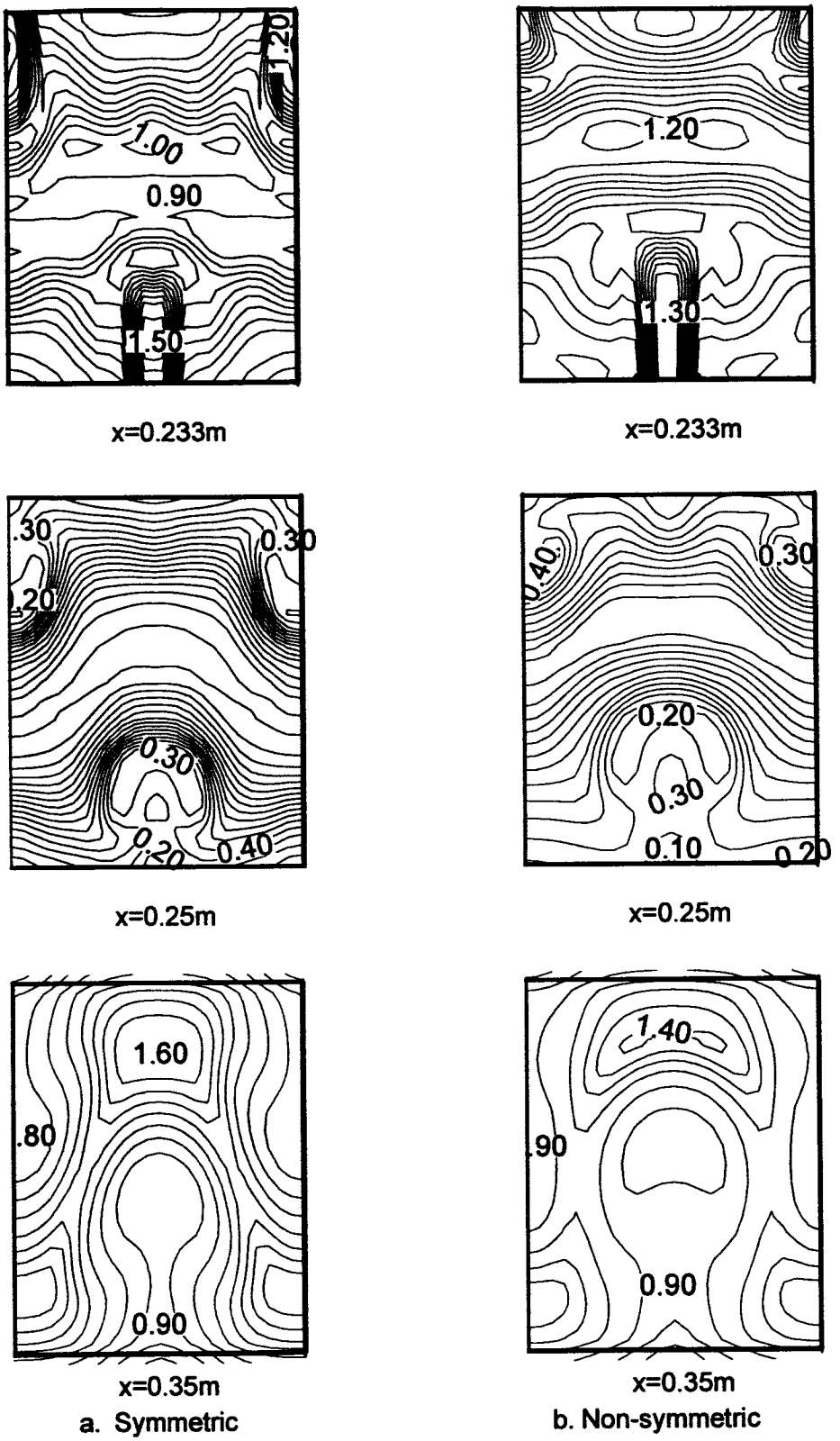

Figure 4.49 Mach number contours at 3-axial locations.

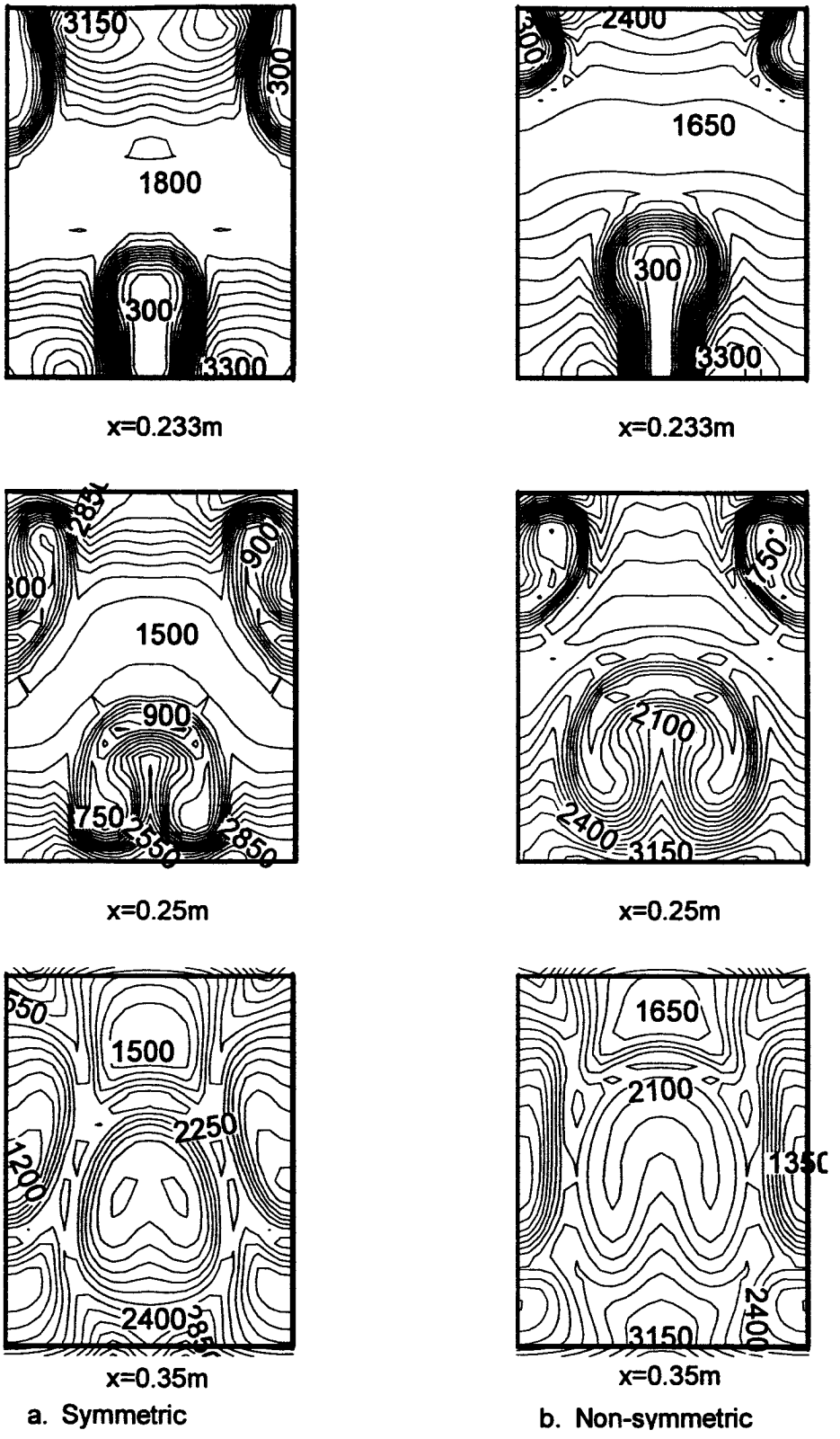

Figure 4.50 Temperature contours at 3-axial locations.

upstream into the isolator region by the recirculation bubble or occur in the upstream separated region.

Many studies have shown that an understanding and accurate model of turbulence are important for both sudden expansion and dual-mode combustion configurations. Especially crucial is the investigation of self-generated turbulence in the recirculation regions. For sudden expansion flow, the self-generated turbulence dominates the flow field. Similarly, the dual mode combustor flowfield is dominated by extensive upstream interaction, or self-generated turbulence.

Large upstream recirculation regions may be responsible for creating a situation where the flow may become asymmetric as well as being the source of the perturbation. It is possible that when the upstream recirculation regions become large, they essentially reduce the duct cross-section to a small fraction of the geometrical cross section. Also, as the interaction extends far upstream, the narrow duct is elongated. With the addition of dual backward facing steps, the appearance of a sudden expansion geometry is created. Therefore, the presence of large upstream recirculation regions is responsible for creating a "sudden expansion" geometry.

Since similar turbulent flows are known to have time dependent results, it seems likely that the asymmetries in this dual-mode combustor case are due to the flow physics, not a numerical error. Although the geometry of the present study does not qualify as a sudden expansion geometry, the flow fields have similar features, especially the presence of such large separation regions. It seems logical that if instabilities can occur in separated regions, they will in this complex dual-mode combustor scenario.

Based on research into asymmetric flow in sudden expansion geometries, the possible mechanism of the breakdown of symmetry can be described below:

1. Heat released during combustion increases chamber pressure forcing the separation region further upstream.

2. As the recirculation region grows, the shape of the velocity profile is changed. In effect, it creates a situation where the cross-sectional area of flow channel is much

smaller than the actual channel. Downstream, either at the steps or downstream of jet injection, this flow is subjected to a large expansion. Numerous studies have observed transient or asymmetric behavior in sudden expansion geometries.

3. The separated shear layers receive positive momentum from the free stream, thereby creating large vortices. The presence of these coherent structures is the source of the instability. This mechanism is currently the focus of numerous experiments and studies.

4. Asymmetry can be observed by the presence of a larger separation region on one wall.

5. As the size and location of the separation regions change, "widening" the flow channel occurs. The perceived aspect and area ratios of the flow decrease. This has a stabilizing effect.

6. Separation regions decrease and the flow field again becomes symmetric.

7. This cycle begins again.

5. CONCLUSIONS AND RECOMMENDATIONS

Computational fluid dynamics results have been presented for an analysis of a two-dimensional and a three-dimensional dual-mode scramjet combustor with significant upstream interaction. This study has been conducted to provide basic understanding of key features of upstream interaction, and to identify physical and numerical issues relating to modeling of dual-mode scramjet configurations. Results were presented for a two-dimensional model with symmetry assumption, a two-dimensional model without symmetry assumption, and a three-dimensional jet-to-jet symmetry assumption model. The following list summarizes some of the information gathered:

1. Results obtained from the sub-scale domain qualitatively recovered the flow physics obtained with the full-scale model.
2. The flow field is not completely dependent on upstream profile. Without an inlet boundary profile, the numerical solution still captures the flow physics. This is not consistent with the usual strong dependence on boundary layer momentum thickness in most isolator models. But is consistent with sudden expansion characteristics and Abbott and Kline's belief that the turbulent characteristics of separation dominate the flow field. Also Matsuo et al.[10] and Mizobuchi et al.[11] conclude that turbulence modeling is the key to accurate simulation of dual mode combustor.
3. For dual-mode systems, a sub-scale solution could be used as an initial condition for a full-scale simulation. This technique could be used in early transients and then interpolated into a full-scale solution process to accelerate convergence.
4. Results show substantial oblique shock train upstream of the fuel injectors. Strong shock-boundary layer interactions create separated regions. These flow characteristics significantly slow the numerical convergence as the length of upstream interaction increases slowly with iterations.
5. As the upstream interaction continues to develop, the symmetric assumption fails to persist when the length of the interaction exceeds the isolator height. The numerical

results show asymmetric flow-structures with larger separation zone at the lower wall extending further upstream of the step. This larger recirculation bubble oscillates between the upper or lower wall.

6. Numerical convergence is not achieved. For continued iterations the asymmetric flow oscillates, from one wall to symmetric result to the opposite wall. This suggests a time dependent solution.
7. The asymmetric flow structure is not shown in the experimental data. Currently, it is unknown if this asymmetric flow-structure is a physical phenomenon or developed due to numerical modeling. However, it seems likely that the experimental results are time averaged. Note that the wall pressure distributions oscillate around the experimental results.
8. Comparisons of the wall static pressure show fair agreement with experimental data with a slight underprediction in peak wall pressure.
9. Extensive numerical analysis is being conducted to understand the breakdown of the symmetry assumption when the upstream interaction increases. This report presents two possibilities. i) It is possible that when the upstream interaction progress far enough, it essentially reduces the duct cross-section to a small fraction of the geometrical cross section. If this occurred, the presence of small backward facing steps would be seen by the flow as a sudden large expansion. It has been shown that the presence of sudden expansions in symmetric ducts can result in asymmetric behavior. This asymmetric perturbation is normally observed in the recirculation region downstream of the steps. With large upstream interaction, the asymmetry would also extend upstream into the isolator region. ii) It is also possible that the asymmetry in the upstream separated region is created much the same as the frequently observed asymmetry in the separated region downstream of a step. This mechanism is not truly understood. Yet, it has been proposed that these asymmetries are related to shear layers and to coherent flow structures embedded in the random velocity fluctuations. With the presence of such large separation regions, extending upstream and downstream of the step, it seems logical that if instabilities can occur in separation regions, they will in this complex scenario.

10. One step in investigating this asymmetric phenomenon is to model a two-dimensional dual-mode scramjet combustor and provide time accurate results. This would help to determine if the flow is periodic. Also a three-dimensional model comprised of an entire half of the domain should be considered using a symmetry boundary to represent the other half. Finally, if the time allowed and the computer capability was allocated, the whole geometry should be considered using both steady and time accurate simulation.

6. REFERENCES

1. Dimotakis, P.E., "Turbulent Free Shear Layer Mixing and Combustion," High Speed Flight Propulsion Systems," Chapter 7, Progress in Astronautics and Aeronautics, Vol. 137, 1991.

2. Cox, S.K., Fuller, R.P., Schetz, J.A., and Walters, R.W., "Vortical Interactions Generated by an Injector Array to Enhance Mixing in Supersonic Flow," AIAA Paper 94-0708, January 1994.

3. Tishkoff, J.M., Drummond, J.P., and Edwards, T., "Future Directions of Supersonic Combustion Research: Air Force/NASA Workshop on Supersonic Combustion," 35th AIAA Aerospace Sciences Meeting and Exhibit, Reno, Nevada, AIAA Paper 97-1017, January 1997.

4. Billig, F.S., Waltrup, P.J., and Stockbridge, R.D., "Integral-Rocket Dual-Combustion Ramjets: A New Propulsion Concept," Journal of Spacecraft, Vol. 17, No.5, Sep-Oct. 1980, pp. 416-424.

5. McDaniel, J.C., Jr., "Combustor Data Bases for Hypersonic Airbreathing Propulsion Systems," AIAA Paper 98-1646, April 1998.

6. Komuro, T., Kudo, K., Masuya, G., Chinzei, N., Murakami, A., and Tani, K., "Experiment on a Rectangular Cross Section Scramjet Combustor" (in Japanese), National Aerospace Lab, NAL TR-1068, Tokyo, Japan, 1990.

7. Murakami, A., Komuro, T., and Kudo, K., "Experiment on a Rectangular Cross Section Scramjet Combustor"(in Japanese), National Aerospace Lab, NAL TR-1220, Tokyo, Japan, 1990.

8. Murakami, A., Komuro, T., and Kudo, K., "Experiment on a Rectangular Cross Section Scramjet Combustor (II) – Effects of Fuel Injector Geometry," (in Japanese), National Aerospace Lab, NAL TR-1220, Tokyo, Japan, 1993.

9. Chinzei, N., Komuro, T., Kudou, K., Murakami, A., Tani, K., Masuya, G., and Wakamatsu, Y., "Effects of Injector Geometry on Scramjet Combustor Performance," AIAA Journal of Propulsion and Power, Vol. 9, No. 1, Jan-Feb 1998, pp.146-152.

10. Matsuo, Y., Mizobuchi, Y., and Ogawa, S., "Parallel Numerical Simulation of Compressible Free Shear Layers in a Scramjet Engine," AIAA Paper 98-0963, January 1998.

11. Mizobuchi, Y., Matsuo, Y., and Ogawa, S., "Numerical Estimation of Turbulence Temperature Fluctuation Effect on Hydrogen-Oxygen Reaction," AIAA Paper 97-0910, January 1997.

12. Riggins, D.W., "The Numerical Investigation of a Dual-Mode Scramjet Combustor," 1998 JANNAF Joint Meetings, December 10, 1998.

13. Rodriguez, C.G., Riggins, D.W., and Bittner, R.D., "Numerical Simulation of Dual-Mode Scramjet Combustor," 1999 JANNAF Joint Meetings, October 18, 1999.

14. Rodriguez, C.G., "Simulation of an Experimental Dual-Mode Scramjet (II): Jet-to-Jet Symmetry," HX Report HX-791, March 2000.

15. Rodriguez, C.G., White, J.A., and Riggins, D.W., "Three-Dimensional Effects in Modeling of Dual-Mode Scramjets," AIAA Paper 2000-3704, July 2000.

16. Rodriguez, C.G., "Asymmetric Effects in Numerical Simulation of Supersonic Flows with Upstream Separated Regions," AIAA Paper 2001-0084, January 2001.

17. Dutton, D.C., and Carroll, B.F., "Numerical and Experimental Investigation of Multiple Shock Wave/Turbulent Boundary Layer Interactions in a Rectangular Duct," Final Technical Report, Report No. UILU-ENG-88-4001, University of Illinois at Urbana-Charmpaign, Urbana, Illinois, January 1988.

18. Mohieldin, T.O., Tiwari, S.N., and Olynciw, M.J., "Asymmetric Flow-Structures in Dual Mode Scramjet Combustors with Significant Upstream Interaction," AIAA Paper 2001-3296, July 2001.

19. Uenishi, K., Rogers, R.C., and Northam, G.B., "Three-Dimensional Numerical Predictions of the Flow Behind a Rearward-Facing Step in a Supersonic Combustor," AIAA Paper 87-1962, July 1987.

20. Matsuo, A., and Mizomoto, M., "Flow Structure of Supersonic Flow Past Backward-Facing Step with Perpendicular Injector," AIAA Paper 98-0939, January 1998.

21. Abbott, D.E., and Kline, S.J., "Experimental Investigation of Subsonic Turbulent Flow over Single and Double Backward Facing Steps," Journal of Basic Engineering, Vol. 84, September 1962, pp.317-325.

22. Durst, F., Melling, A., and Whitelaw, J.H., "Low Reynolds Number Flow over a Plane Symmetric Sudden Expansion," Journal of Fluid Mechanics, Vol. 64, 1974, pp. 111-128.

23. Cherdron, W., Durst, F., and Whitelaw, J.H., "Asymmetric Flows and Instabilities in Symmetric Ducts with Sudden Expansions," Journal of Fluid Mechanics, Vol. 84, 1978, pp. 13-31.

24. Resitvo, A., and Whitelaw, J.H., "Turbulence Characteristics of the Flow Downstream of a Symmetric, Plane Sudden Expansion," Journal of Fluids Engineering, Vol. 100, 1978, pp. 308-310.

25. Cole, D.R., and Glauser, M.N., "Flying Hot-Wire Measurements in an Axisymmetric Sudden Expansion," Experimental Thermal Fluid Science, Vol. 18, pp. 150-167, 1998.

26. Kudela, H., "Viscous Flow Simulation of a Two-Dimensional Channel Flow with Complex Geometry Using the Grid-Partical Vortex Method," ESAIM: Proceedings, Vol. 7, 1999, pp. 215-224.

27. Aloui, F., and Souhar, M., "Experimental Study of Turbulent Asymmetric Flow in a Flat Duct Symmetric Sudden Expansion," Journal of Fluids Engineering, Vol. 122, March 2000, pp. 174-177.

28. Lee, I., and Sung, H.J., "Characteristics of Wall Pressure Fluctuations in Separated Flows over a Backward-Facing Step," Experiments in Fluids, Vol. 30, 2001, pp. 273-282.

29. Sobey, I.J., and Drazin, P.G., "Bifurcations of Two-Dimensional Channel Flows," Journal of Fluid Mechanics, Vol. 171, 1986, pp. 263-287.

30. Fearn, R.M., Mullin, T., and Cliffe, K.A., "Nonlinear Flow Phenomena in a Symmetric Sudden Expansion," Journal of Fluid Mechanics, Vol. 211, 1990, pp. 595-608.

31. Diskin, G.S., and Northam, G.B., "Effects of Scale on Supersonic Combustor Performance," AIAA Paper 87-2164, July 1987.

32. Mohieldin, T.O., Olynciw, M.J., and Tiwari, S.N., "Convergence-Acceleration Technique for Dual-Mode Combustors Simulation," Report HX-845, NASA Langley Research Center, Hampton, VA, October 2000.

33. McDaniel, J.C. and Graves, J., "Laser-Induced-Fluorescence Visualization of Transverse Gaseous Injection in a Nonreacting Supersonic Combustor," Journal of Propulsion and Power, Vol. 4, No. 6, Nov.-Dec. 1988, pp.591-597.

34. Billig, F.S., Orth, R.C., and Lasky, M., "A Unified Analysis of Gaseous Jet Penetration," AIAA Journal, Vol. 9, No. 6, June 1971.

35. Drummond, J.P., "Numerical Investigation of the Perpendicular Injector Flow Field in a Hydrogen Fueled Scramjet," AIAA Paper 79-1482, July 1979.

36. Heister, S.D., and Karagozian, A.R., "Gaseous Jet in Supersonic Crossflow," AIAA Journal, Vol. 28, No. 5, May 1990, pp. 819-827.

37. GAMBIT. Vers. 1.3.0. Computer Software. Fluent Inc., 1988-2001. IBM PC-WINNT System 4.0, CD-ROM.

38. FLUENT/UNS AND RAMPANT 4.2 User's Guide., Lebanon, NH: Fluent Incorporated, 1997.

39. Spaid, F.W., and Zukoski, E.E., "A Study of the Interaction of Gaseous Jets from Transverse Slots with Supersonic External Flows," AIAA Journal, Vol. 6, February 1968, pp. 205-212.

40. Hosangadi, A., Cavallo, P.A., Arunajatesan, S., Ungewitter, R., and Lee, R.A., "Aero-Propulsive Jet Interaction Simulations Using Hybrid Unstructured Meshes," AIAA Paper 99-2119, June 1999.

41. Rodriguez, C.G., "Two-Dimensional, Compressible-Flow Test-Cases for Validation of the VULCAN Flow-Solver," NASA Report HX-763, Hyper-X Program Office, November 1999.